Title
Improving Access to Safe Water in West Bengal, India: From Arsenic and Bacteria Removal to Household Behavior Change

Author
Delaire, Caroline

Publication Date
2016

Peer reviewed|Thesis/dissertation

Improving Access to Safe Water in West Bengal, India: From Arsenic and Bacteria Removal to Household Behavior Change

By

Caroline Delaire

A dissertation submitted in partial satisfaction of the

requirements for the degree of

Doctor of Philosophy

in

Engineering – Civil and Environmental Engineering

in the

Graduate Division

of the

University of California, Berkeley

Committee in charge:

Professor Ashok Gadgil, Chair
Professor Kara Nelson
Professor Isha Ray

Spring 2016

Abstract

Improving Access to Safe Water in West Bengal, India:
From Arsenic and Bacteria Removal to Household Behavior Change

by

Caroline Delaire

Doctor of Philosophy in Civil and Environmental Engineering

University of California, Berkeley

Professor Ashok Gadgil, Chair

Millions of people in rural West Bengal, India, are exposed to groundwater containing toxic concentrations of arsenic, unpleasant levels of iron and non-negligible fecal contamination. Before publicly-provided piped water becomes widely available, a promising approach to address this unacceptable situation is to treat groundwater in small decentralized plants that sustain themselves by selling water to households at an affordable price. This approach hinges on two hypotheses: first, that groundwater can be treated for all contaminants –arsenic, iron, and microorganisms– at very low-cost and with locally available materials and labor; second, that a large fraction of households –ideally all households– will purchase treated water. This dissertation examines these two hypotheses in detail. First, it analyzes the concurrent removal of arsenic and bacteria from contaminated groundwater using iron electrocoagulation (Fe-EC), a simple and robust process suitable for operation in resource-limited settings. Second, it investigates household water practices and drivers of behavior change in rural West Bengal.

Fe-EC relies on the dissolution of an Fe(0) anode to produce strong oxidants and Fe(III) precipitates with a high sorption affinity for arsenic. Building on previous work, a computational model is used to investigate the combined effects of pH and operating conditions (Fe dosage rate and O_2 recharge rate) on arsenic removal by Fe-EC. A relationship is established between the impact of operating conditions and the process limiting arsenic removal (As(III) oxidation versus As(V) adsorption), which depends on the pH and the O_2 concentration. The robustness of the trends predicted by the model, which operates at constant pH, is evaluated against lab experiments reproducing more realistic conditions where pH increases during treatment –as a result of groundwater equilibrating with atmospheric CO_2. The results provide a nuanced understanding of the levers that an operator might use to optimize Fe-EC performance in a range of groundwaters under economic constraints.

Bacteria attenuation by Fe-EC is investigated in detail using a series of laboratory experiments. After showing that Fe-EC can attenuate bacteria in synthetic Bengal groundwater without detriment to arsenic remediation, the impact of operating parameters (Fe dosage and dosage rate), groundwater composition (pH, HCO_3^-, Ca, Mg, Si, P, and natural organic matter (NOM)), and bacteria type are systematically investigated, with a focus on elucidating the mechanisms of bacteria attenuation. The results show that attenuation is primarily due to bacteria

encapsulation in Fe(III) flocs and removal by gravitational settling, while inactivation by germicidal reactive oxidants remains limited in the presence of HCO_3^- and at pH>7. Fe(III) precipitates are found to adhere to the surface of bacterial cells, primarily through interactions with bacterial phosphate groups, resulting in bacteria enmeshment in precipitate flocs. The effect of major groundwater ions is interpreted in light of this mechanism: Ca and Mg reduce attenuation by complexing bacterial phosphate groups; Si and NOM, which do not strongly compete with phosphate groups for sorption to Fe(III) precipitates, do not affect attenuation; by contrast, P decreases attenuation significantly, except in the presence of bivalent cations, which can bridge between P sorbed to precipitates and bacterial phosphate groups. Finally, Fe-EC is shown to be equally effective towards Gram-positive and Gram-negative bacteria, smooth and rough alike, likely due to the universal presence of phosphate moieties on bacterial cell walls. Altogether, results show that Fe-EC can effectively remove all types of bacterial contamination from a range of groundwaters.

Results of a 501-household survey about water practices in the arsenic-affected district of Murshidabad, in West Bengal, India, are presented. 53% of the surveyed population was found to use alternatives to shallow groundwater including domestic filters, water purchased from small private entrepreneurs, government tubewells, and municipal piped water. The analysis shows that following socioeconomic status, risk perception of gastric illness and dissatisfaction with iron are the primary predictors of the use of alternatives, prevailing over arsenic risk perception. This finding indicates that households react to readily noticeable water problems more than to an invisible contaminant with long-term effects. The factors affecting the choice amongst available alternatives are investigated. The results show that purchased water does not currently provide universal access and that it only reduces, but does not eliminate, arsenic ingestion. Overall, the findings suggest that the provision of treated water through small independent entrepreneurs can be an interim, but partial, solution to the arsenic crisis until piped water becomes widespread in rural West Bengal.

A mes parents, qui m'ont transmis le goût de l'effort,
de l'aventure, et de la découverte

Table of Contents

List of Tables

List of Figures

List of Abbreviations

ATR-FTIR	Attenuated Total Reflectance Fourier-Transform Infrared Spectroscopy
BGS	British Geological Survey
CFU	Colony forming units
DOC	Dissolved organic carbon
EAWAG	Swiss Federal Institute of Aquatic Science and Technology
ECAR	Electro-Chemical Arsenic Removal
E. coli	*Escherichia coli*
EPS	Extracellular polymeric substances
Fe-EC	Iron electrocoagulation
FH	Ferrihydrite
GI	Gastro-intestinal
ICP-OES	Inductively coupled plasma optical emission spectrometry
IEP	Iso-electric point
INR	Indian rupee
KJ	"Kena jol" (literally "purchased water" in Bangla)
LPS	Lipopolysaccharides
MCL	Maximum contaminant level
NGO	Non-governmental organization
NRDWP	National Rural Drinking Water Program
NOM	Natural organic matter
PC	Principal component
PCA	Principal component analysis
PHED	Public Health Engineering Department
SES	Socioeconomic status
SGW	Synthetic Bengal groundwater
SSIP	Small-scale independent providers
TEM	Transmission electron microscopy
UC	University of California
WHO	World Health Organization
XAS	X-ray absorption spectroscopy
XRF	X-ray fluorescence

Acknowledgements

I want to express my sincere gratitude to the people who have helped me progress through my PhD research. Specifically, I am extremely grateful to Berkeley professors Ashok Gadgil, Kara Nelson, Isha Ray, and David Sedlak for inspiring me to get my PhD and for being role models ever since; to Susan Amrose and Case van Genuchten for their mentorship and trust during this journey; to James Hake, Pavitra Sharma, Minghui Zhang, and James Britt Abrahamson for their significant contribution to this work; to Taimur Khan, Mostafigur Rahman, Murshid Alom, and Kamal Hassan, my survey enumerators, for their infinite dedication and patience in the field; to Joyashree Roy and Abhijit Das for trusting me and giving me the opportunity to conduct field work in West Bengal, which has been a life-changing experience; to Andrew Torkelson, Andrea Silverman, Samantha Beardsley, Jannis Wenk, Denise Schichnes, Reena Zalpouri, Aidan Ceccheti, John Wertz, Akshay Shrivastava, Debanjan Mukherjee, Rupsa Bhowmick, Alasdair Cohen, Angela Harris, Zachary Burt, and Jaclyn Leaver for their precious help in diverse steps of experimental design, data collection, data analysis, and writing; to my labmates Katya Cherukumilli, Siva Bandaru, and Sara Glade, who gave me so much support; to my brother Simon, my dear friend Soazig Kaam, and all my family for their confidence in my ability to accomplish this task and for encouraging me in difficult times; and to Louis-Alexandre Couston for being a source of happiness and strength every day.

Finally, I want to acknowledge and thank my multiple funding sources, without which none of this research would have been possible: the American Association for University Women (International Fellowship), Dow and the Center for Sustainable Business at Berkeley (Sustainability Innovation Student Challenge Award), the Civil and Environmental Engineering Department at Berkeley (multiple non-resident tuition waivers), USAID and the Development Impact Lab at Berkeley, and the Andrew and Virginia Rudd Family Foundation. Finally, my work at the Lawrence Berkeley National Lab Molecular Foundry was supported by the Office of Basic Energy Sciences of the U.S. Department of Energy under Contract No. DE-AC02-05CH11231.

CHAPTER 1. Introduction

1. ARSENIC IN GROUNDWATER: A GLOBAL OVERVIEW

1.1. Worldwide occurrences and causes of arsenic contamination

Arsenic contamination of groundwater is a worldwide problem that affects an estimated 150 million people[1]. Arsenic concentrations above the World Health Organization (WHO) recommended maximum contaminant level (MCL) of 10 µg/L have been found in more than 70 countries on six continents[1,2], as shown in Figure 1-1. Countries with the largest exposed populations are Bangladesh, India, China, the United States, Myanmar, Pakistan, Argentina, Vietnam, Nepal, Cambodia, Hungary, Chile, and Mexico.

Figure 1-1: Map of the population estimated to be exposed to arsenic concentrations > 10 µg/L (WHO MCL) in drinking water, by country. From Ravenscroft et al., 2009[1].

In the majority of cases, arsenic contamination of groundwater is geogenic: arsenic is naturally present in aquifer rocks and sediments and is released by specific biogeochemical processes. Three major mechanisms of arsenic mobilization have been identified: reductive dissolution of arsenic-bearing iron oxide minerals (e.g., China, eastern Europe, South Asia); arsenic desorption under high-pH arid conditions (e.g., Latin America); and mining-induced oxidation of arsenopyrite (e.g., Ghana, Thailand)[2]. The first mechanism is characteristic of anoxic and organics-rich aquifers, in which microbiological activity creates reducing conditions that result in the dissolution of Fe oxides. There is evidence that anthropogenic activities increasing the influx of biologically-degradable organic carbon into groundwater (e.g. construction of perennial ponds) may exacerbate this process[3,4], but this is not consensual[5]. While arsenic mobilization requires a geochemical trigger, it leads to groundwater contamination only when aquifer flushing is low,

which is often the case in low-lying areas such as deltas. Based on these geological, hydrologic, and biogeochemical factors, scientists at the Swiss Aquatic Research Institute (EAWAG) have developed predictive models of arsenic contamination, which are in good agreement with measured contamination[6,7]. Example probability maps are shown in Figure 1-2. Because the factors described above are highly variable with space, depth, and time, it is worth noting that arsenic concentrations in affected regions can be substantially different from one groundwater well to another, and from one season to another[8,9].

1.2. Health effects of chronic arsenic ingestion

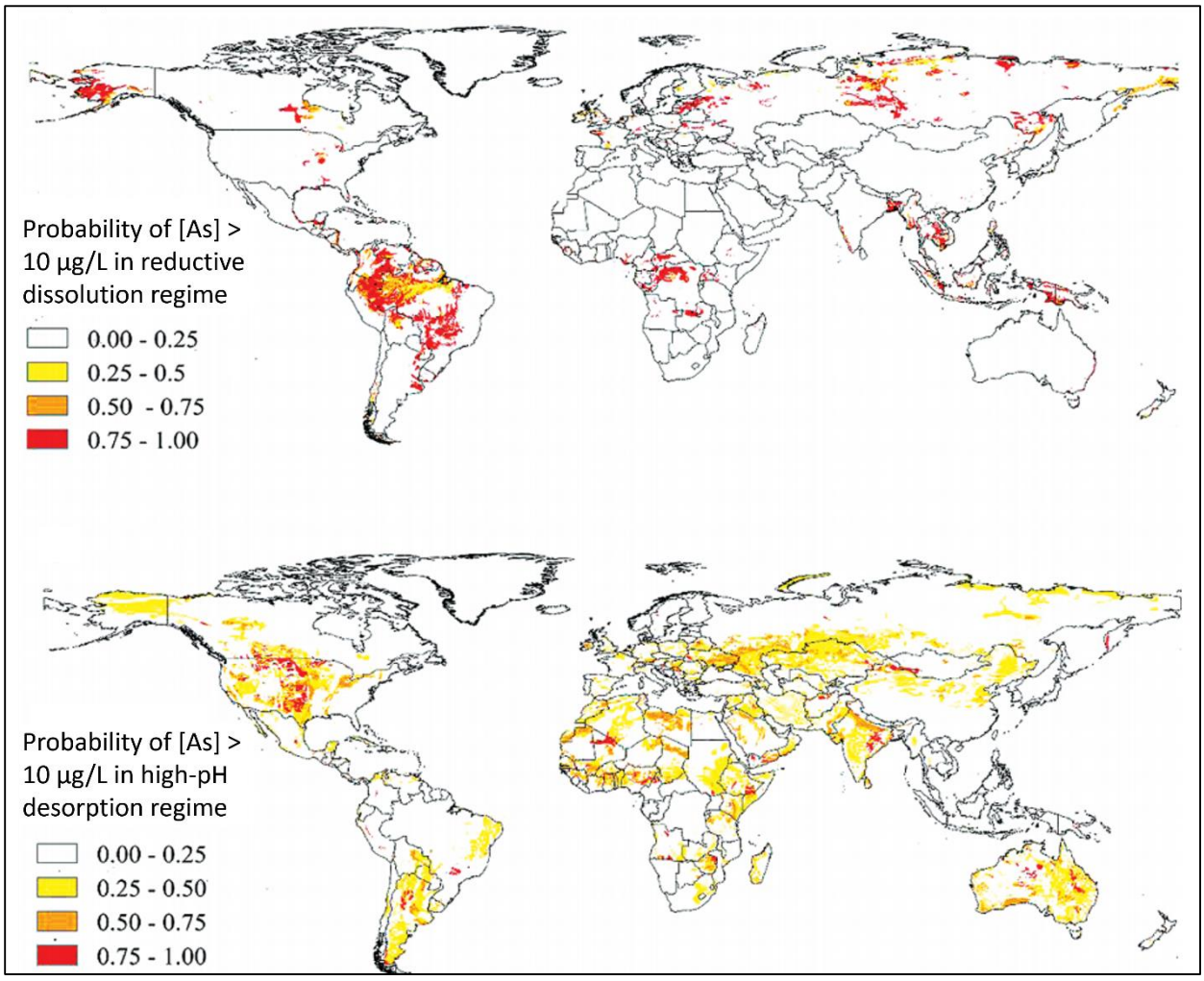

Figure 1-2: Probability of arsenic contamination of groundwater according to EAWAG's predictive models for the two main processes of arsenic mobilization: reductive dissolution (top panel) and high-pH desorption (bottom panel). From Amini et al., 2008[6].

The cumulative ingestion of arsenic can lead to a range of diseases, from keratosis and melanosis, which are characterized by skin lesions and pigmentation, to cardiovascular and respiratory problems, gangrene, various types of cancers (kidney, liver, lung, bladder, and skin), and impaired cognitive functions[1,10]. Prenatal exposure to arsenic has been associated with

drowning of young children in Bangladesh, possibly due to low neurodevelopment[11]. Poor nutrition and lack of dietary diversity likely exacerbate the health impacts of arsenic ingestion[12,13]. There is currently no cure for chronic arsenic poisoning[1]. Treatment of symptoms is possible, but is not available in all arsenic-affected regions. Multiple studies have documented the dire economic, societal, and psychological consequences of arsenic poisoning in low-income populations[1,14,15].

1.3. Focus on South Asia

Amongst arsenic-affected regions, South Asia is the most worrisome due to the size of the population at risk. Not only is South Asia one of the most densely populated areas in the world, but it is also a region where rural populations heavily rely on groundwater for drinking and cooking. Table 1-1 lists the percentages of the population using groundwater as the primary water source in Bangladesh, four Indian States, Nepal, Vietnam, Myanmar and Cambodia, as well as estimates of the population exposed to arsenic. With over 60 million people at risk, the arsenic crisis in South Asia has rightly been called "the largest poisoning of a population in history"[16].

Table 1-1: Scale of the arsenic problem in South Asia: (1) percent of rural and total population using groundwater tubewells as the primary source of drinking water. *Source: WHO/UNICEF Joint Monitoring Programme country files[17], and 2011 Census of India for Indian states[18]. (2) Estimated population at risk of drinking arsenic-contaminated groundwater. **Source: 2005 World Bank report[19], except for Indian states for which the population at risk was estimated as the product of the population of affected districts by the proportion of contaminated wells reported in Chakraborti et al., 2009[20] and Chakraborti et al., 2013[21]. Some Indian North Eastern Hill states, such as Assam and Manipur, are arsenic-affected as well[21], but no robust estimate was available for population at risk.

Country	**% of population using tubewells as the primary drinking water source***		**Population at risk (estimated to drink water with > 50 µg/L As)****
	rural	**total**	
Bangladesh	95.8	85.5	35,000,000
India			
-West Bengal	80.0	66.8	9,400,000 (4,200,000 in [20])
-Bihar	91.3	89.6	4,900,000
-Uttar Pradesh	74.2	67.8	2,300,000
-Jharkhand	50.6	47.3	130,000
Nepal	46.6	43.4	550,000
Vietnam	22.6	18.6	10,000,000
Myanmar	10.1	8.7	3,400,000
Cambodia	33.4	29.5	320,000

2. THE ARSENIC PROBLEM IN RURAL WEST BENGAL, INDIA

2.1. History and persistence of the problem

Until recent decades, the main –if not the only– sources of drinking water in rural Bengal were rivers, ponds, and shallow dug wells. In the 1970s, UNICEF initiated a massive well drilling campaign in the region, in partnership with the West Bengal and Bangladesh governments, as part of an effort to reduce child mortality caused by diarrheal diseases[22–24]. Groundwater was indeed microbiologically safer than surface water (e.g., [25]), which contained microbial pathogens responsible for the high incidence of cholera and other diarrheal illnesses[26,27]. The installation of handpump tubewells, which were relatively cheap, accelerated through the 1990s, with contributions from non-governmental organizations (NGOs) and private citizens[19]. Today, over 10 million tubewells have been sunk in the region[24], and groundwater has become the primary source of drinking water for 80% and 96% of the population in rural West Bengal and Bangladesh, respectively (Table 1-1).

Even though instances of arsenic in groundwater had been reported in north-central India as early as 1976, international institutions and governments failed to test shallow aquifers in rural Bengal prior to installing these millions of tubewells. Arsenic contamination of groundwater in the region was first discovered in 1983 by a dermatologist, Dr. K. C. Saha, but it was not extensively documented until the 1990s, when the efforts of Dr. D. Chakraborti, an environmental chemist from Jadavpur University in Kolkata, led to public recognition of the massive scale of the problem[1,28].

Over 20 years later, why does the arsenic crisis still persist? In West Bengal, the state and central governments have spent over 8.76 billion INR (~ 130 million USD, estimate from 2007) on various arsenic mitigation efforts including the installation of arsenic removal plants and safe deep tubewells, as well as the deployment of piped water supply schemes[14]. These efforts have been described as largely technology-focused, and have overlooked crucial aspects such as incentivizing proper maintenance and creating demand for arsenic-safe water[14]. As a result, the vast majority of household- and community-based technologies have failed to provide arsenic-safe water within the first year of their installation, or have been abandoned[14,29]. Furthermore, most arsenic mitigation efforts in West Bengal have neglected financial sustainability, explaining in part their failure to address the crisis durably and at scale[14]. Finally, scholars have denounced the lack of political commitment to solving the arsenic crisis[28,30].

The public provision of piped water, which seems to be the most preferred alternative to tubewells in the region[31–33], has been progressing steadily, but slowly. According to reports by the Public Health Engineering Department (PHED), piped water coverage in rural West Bengal has increased from close to 0% in 1980 to 48.1 % in 2015[34]. However, this figure is not consistent with the 2011 Census of India, which indicates that piped water is the primary drinking water source for only 11.4% of rural households[18]. This discrepancy suggests that the fraction of the population actually having convenient access to piped water is significantly lower than estimated by PHED. Possible reasons may be that public taps are located too far and/or that the infrastructure is

deteriorated or in disrepair. Overall, it is clear that full piped water coverage will take several decades (35 years assuming that the –optimistic– progress reported by PHED can be sustained).

2.2. Important characteristics of groundwater

Handpump tubewells are the primary source of drinking water for 80% of the 13.8 million households in rural West Bengal[18]. They are often located within or near premises (85% of rural households live within 200 m of their drinking water source), and they generally provide water in sufficient quantities for household activities (85% of rural households get sufficient quantities of water year-round)[35]. Compared to surface water sources, which are more often away from premises and may not be available year-round (similar to rainwater), tubewells have obvious advantages that explain their popularity.

Tubewells are an "improved" source of drinking water by UNICEF/WHO standards, because they are considered to provide water free of microbiological contamination. However, this classification does not reflect the poor quality of shallow groundwater in West Bengal. In addition to toxic levels of arsenic[20], groundwater contains high concentrations of iron[14,36] and non-negligible fecal contamination[37–41]. Iron, which is mobilized by the same geochemical reducing conditions as arsenic, gives a metallic taste and an orange color to water, and might lead to adverse health outcomes[42] such as gastrointestinal disorders[43] and colon cancer[44]. Fecal contamination is likely due to the sustained prevalence of open defecation (40-51%)[18,35] and the close proximity of latrines to tubewells, which are not always adequately sealed[37,39,41]. Fecal contamination can cause diarrheal illnesses even at low levels (e.g., viruses)[45]. Overall, it is important to emphasize that arsenic, which has long-term health effects and no taste, color, or odor, often co-occurs with more tangible contaminants that can cause immediate dissatisfaction (iron) and illness (microbial pathogens). The multi-faceted nature of groundwater contamination in Bengal has important implications for raising awareness about arsenic, developing adequate treatment technologies, and creating demand for arsenic-safe water.

2.3. Long- and mid-term approaches to safe water provision

In the long-term, the solution to the arsenic problem arguably lies in the public provision of piped water. Efforts to achieve this objective are underway[34], and researchers are investigating household willingness to pay for this service[15,31], as user payments could help recover costs. However, as explained earlier, full coverage of piped water supply in rural West Bengal will take many decades, and several generations will risk suffering because of contaminated groundwater if no interim solution is proposed.

In the mid-term, a possible approach is to produce safe drinking water in decentralized small-scale groundwater treatment plants that sustain themselves by selling water to households at an affordable price. This approach is attractive for several reasons. First, it does not rely on household or community-led water treatment, which have failed repeatedly, in part due to the lack of user-friendliness and maintenance of water treatment technologies[14,29,32]. Rather, this approach leverages the entrepreneurship of small-scale independent providers (SSIPs), who can more easily

have access to training, supply chains, maintenance services, and water quality monitoring. Second, this approach has a direct mechanism of cost-recovery and provides a financial incentive to operators, which is critical to ensure durable operation and scale-up.

This mid-term vision hinges on three major hypotheses. The first one is that groundwater can be treated for all contaminants of concern –arsenic, iron, and microbial pathogens– at very low cost. The second hypothesis is that such treatment can be performed in West Bengal villages, with locally available consumables and labor. And the third hypothesis is that a substantial fraction of households –ideally all households– will purchase treated water. Building on previous work by the Gadgil Lab, which developed a technology called Electro-Chemical Arsenic Remediation (ECAR), my PhD research contributes to investigating these hypotheses.

When I started my PhD, the Gadgil Lab had shown that ECAR could effectively remove arsenic from groundwater and a 600-L pilot reactor was about to be tested in the field[46,47]. In addition, the processes of arsenic removal had been extensively documented[48–50]. Finally, the ECAR technology was suitable for decentralized operation in rural Bengal and scalable[51]. Over the past four years, I have attempted to make a multi-disciplinary contribution to this work, by: (1) improving and applying a computational-model to predict the impact of operating conditions on ECAR performance; (2) investigating bacteria attenuation with ECAR to understand its mechanisms and the impact of groundwater chemistry; and (3) conducting a household survey in rural West Bengal to identify the factors driving the use of alternatives to groundwater, including water purchased from SSIPs. My motivation has been to better understand how ECAR, and more broadly the mid-term vision described above, can help improve access to safe water in rural West Bengal, India.

3. DISSERTATION OUTLINE

The rest of my dissertation is organized in five chapters.

Chapter 2 focuses on arsenic removal from groundwater by iron electrocoagulation (Fe-EC), the treatment process at the heart of ECAR, which relies on the dissolution of an Fe(0) anode to produce reactive oxidants and Fe(III) precipitates with a high sorption affinity for arsenic. This chapter establishes a relationship between the impact of operating conditions and the process limiting arsenic removal (As(III) oxidation versus As(V) adsorption), which depends on the pH and the O_2 concentration. It provides a nuanced understanding of the levers that an operator might use to optimize Fe-EC performance in a range of groundwaters under economic constraints.

Chapters 3 and 4 focus on bacteria attenuation by Fe-EC. These chapters demonstrate that Fe-EC can effectively remove all types of bacterial contamination from a range of groundwaters. They elucidate the respective contributions of inactivation and removal via enmeshment in Fe(III) flocs, and provide an in-depth investigation of the molecular processes governing removal. These chapters also analyze the effect of solution composition –pH, HCO_3^-, Ca, Mg, Si, P, and natural organic matter (NOM)– on bacteria attenuation by Fe-EC, which is crucial to predict its performance in different groundwaters.

Chapter 5 brings a social science perspective and focuses on household water practices in rural low-income and arsenic-affected communities in West Bengal. This chapter uses data from a 501-household survey in Murshidabad district to investigate what motivates households to use alternatives to shallow groundwater, when such alternatives are available. It assesses the relative importance of co-occurring groundwater contaminants in shaping household decisions. This chapter also critically analyses the potential for safe water provision through SSIPs, and provides results that can inform arsenic mitigation efforts in West Bengal.

Chapter 6 concludes this dissertation by summarizing the main findings and relating them to the initial motivation of decentralized groundwater treatment by independent entrepreneurs. This chapter also outlines remaining research questions about the science and implementation of ECAR, as well as about the role of public policies in the context of water provision through SSIPs. It ends with a personal reflection about multi-disciplinary research.

CHAPTER 2. Predicting the impact of operating conditions on arsenic removal by Fe-EC.

1. INTRODUCTION

Millions of people worldwide are exposed to arsenic present in groundwater supplies[1,2,21]. In areas where no safer reliable and abundant source of drinking water exists, removing arsenic from contaminated groundwater is critical to protect public health. Fe-EC is a very promising arsenic removal technology because it is highly effective, it relies on consumables that are available in low-income rural areas, it does not involve hazardous chemicals and it produces minimal amounts of sludge[46–48]. In Fe-EC, a small voltage is applied between two Fe(0) (mild-steel) electrodes, leading to the electrolytic dissolution of the anode into aqueous Fe(II). In the presence of dissolved O_2, Fe(II) oxidizes to Fe(III) which is very insoluble at circumneutral pH and precipitates to form Fe(III) (oxyhydr)oxide precipitates with a strong adsorption affinity for arsenic[48,50]. In addition, reactive intermediates produced upon the oxidation of Fe(II) by O_2, such as Fe(IV), oxidize As(III) to As(V), which is more amenable to adsorption[49,52]. Operating Fe-EC involves three consecutive steps: electrolysis, post-electrolysis mixing to ensure full oxidation of aqueous Fe(II), and settling to separate arsenic-laden precipitates by gravity. Fe-EC is most suitable to be operated at the community-scale[47,53], as opposed to the household-scale like other Fe-based arsenic removal technologies[54]. Fe-EC has been shown to effectively remove arsenic to below the World Health Organization (WHO) maximum contaminant limit (MCL) of 10 µg/L during a 3-month field trial in rural West Bengal, India[47]. The scale-up and success of this technology now hinges on the ability to maximize its performance under economic constraints in groundwaters with a range of chemical compositions.

The performance of Fe-EC is governed both by the chemical characteristics of groundwater and by operating conditions. For example, the amount of Fe required to remove a given concentration of arsenic to below the WHO MCL highly depends on solution pH, which affects the kinetics of As(III) oxidation[49] and the affinity of Fe(III) (oxyhydr)oxides for oxyanions[55,56]. Groundwater oxyanions (P, Si) and bivalent cations (Ca, Mg) also affect arsenic removal by respectively competing for adsorption sites on EC precipitates[49,57] and enhancing arsenic uptake[57]. Operating conditions have ambivalent effects on the performance of Fe-EC. Increasing the Fe dosage rate allows to decrease the duration of treatment and therefore to reduce the costs associated with electricity use for mixing. However, it also leads to the accumulation of Fe(II), which competes with As(III) for reactive intermediates, and can thus increase the amount Fe required to treat groundwater[49]. Inversely, enhancing aeration may increase energetic costs but may improve arsenic removal by limiting the accumulation of Fe(II). Optimal operating conditions that minimize the cost of treatment are expected to depend on groundwater characteristics, especially on pH, which controls key arsenic removal processes in Fe-EC. Based on 155 tubewell samples collected in Bangladesh by the British Geological Survey (BGS), the pH of arsenic-contaminated groundwater can vary substantially between 6.4 and 8.4[36]. Therefore, understanding how operating

conditions, such as the Fe dosage rate and the O_2 recharge rate, affect arsenic removal at different pHs is crucial to guide decision making.

In this study, we investigated the combined effects of pH, Fe dosage rate and O_2 recharge rate on arsenic removal by Fe-EC. We improved upon a computational model of Fe-EC previously developed by *Li et al.*[49] to predict arsenic removal in a range of groundwater and operating conditions. Specifically, we extended Li's model, which had been developed at pH 7.1, to a realistic pH range (6.6 to 8.1) and incorporated O_2 kinetics. Using the new model, we first identified the process limiting arsenic removal (As(III) oxidation versus As(V) adsorption) at different pHs. Second, we investigated the effect of Fe dosage rate on arsenic removal in different pH and O_2 recharge scenarios. Finally, we assessed the robustness of the trends predicted by the model, which operates at constant pH, against lab experiments reproducing more realistic conditions where pH increases during Fe-EC as a result of groundwater equilibrating with atmospheric CO_2. Our results provide a nuanced understanding of the impact of operating conditions on arsenic removal by Fe-EC and can inform decisions regarding the operation of this technology in a range of groundwaters.

2. METHODS

2.1. Arsenic Removal Experiments

The list of experiments conducted for this chapter is given in Tables 2-1 and 2-2. The majority of experiments were conducted in synthetic Bengal groundwater (SGW), which is intended to mimic arsenic-contaminated groundwater in the Bengal Basin. The composition of SGW (Table 2-1) was derived from the sampling of 3534 tubewells in Bangladesh by the British Geological Survey in 2001[36,58]. Fe-EC experiments were conducted by applying a galvanostatic current between two Fe(0) electrodes (98% Fe, 0.5 mm thick, 0.5 cm apart, 1 cm x 8 cm, submerged surface area of ~1.5 cm^2) immersed in 200 mL SGW. Electrodes were cleaned with sand paper before each experiment to remove rust deposits. Operating conditions were selected based on previous studies to avoid the anodic production of chlorine or oxygen[46,48,49]. Current densities of 2-20 mA/cm^2 were applied, corresponding to Fe dosage rates of 0.93-9.3 C/L/min according to Faraday's law. The electrolysis time was adjusted to achieve the desired Fe dosage (from 7.2 to 72.4 ppm). After electrolysis (or $FeSO_4$ dosage in some experiments, see Table 2-2), the solution was mixed in open air until full Fe(II) oxidation. Two types of experiments were conducted (Tables 2-1 and 2-2): constant-pH experiments to calibrate the computational model (pH 6.6, 7.0, 7.5 and 8.1), and drift-pH experiments to reproduce realistic field conditions (initial pH of 6.0, 7.0 and 8.0). In constant-pH experiments, the solution pH was controlled by adding drops of 1.1 M HCl as necessary. In drift-pH experiments, the final pH was 8.0-8.5 independent of the initial pH, as a result of solutions equilibrating with atmospheric CO_2. All experiments were replicated 2 to 5 times.

Measurements of As(III-V), Fe, Si, P, Ca and Mg were performed by inductively coupled plasma optical emission spectrometry (ICP-OES, PerkinElmer 5300 DV, measurement error

typically < 5%). Unfiltered and filtered (0.45 µm nylon filters) 5 mL samples digested with 1 mL 1.1 M HCl were analyzed to determine total and dissolved concentrations of ions respectively. Concentrations of adsorbed ions were calculated as the difference between total and dissolved concentrations. The concentration of Fe(II) was equated to the concentration of Fe in filtered samples because Fe(III) is insoluble at circumneutral pH. For As(III) measurements, digested samples were diluted 50 times in 0.25 M disodium citrate and analyzed by ICP-OES with hydride generation[58].

Table 2-1: Detailed electrolyte composition for model calibration experiments (constant pH) and pH-drift experiments. Major differences from Synthetic Bengal groundwater (SGW) are highlighted in red.

	***MODEL CALIBRATIONS* (constant pH)**						***REALISTIC SCENARIO***	
	Measurement of adsorption constants		**Measurement of oxidation rate constants**		**Model optimization**		**pH drift experiments**	
	Avg.	*St. dev.*	Avg.	*St. dev.*	Avg.	*St. dev.*	Avg.	*St. dev.*
As(III) (µM)	2031	*75*	1972	*37*	522	*14*	470	*42*
Ca^{2+} (mM)	103	*7*	102	*2*	103	*5*	103	*6*
Mg^{2+} (mM)	44	*2*	43	*1*	49	*2*	47	*3*
Si (mM)	35	*2*	34	*1*	34	*2*	35	*3*
P (mM)	20	*2*	4	*1*	4	*0*	4	*1*
HCO_3^- (mM)	500	*6*	500	*6*	500	*6*	500	*6*
Na^+ (mM)	609	*13*	576	*8*	576	*10*	578	*13*
Cl^- (mM)	294	*18*	289	*6*	304	*14*	300	*18*

Table 2-2: Detailed operating conditions for all experiments conducted in chapter 2.

	***MODEL CALIBRATIONS* (constant pH)**												***REALISTIC SCENARIO***		
	Measurement of adsorption constants				**Measurement of oxidation rate constants**				**Model optimization**				**pH drift experiments**		
Electrolyte	SGW with high As/P				SGW with high As				SGW				SGW		
Fe dosage type	Fe-EC				$FeSO_4$				Fe-EC				Fe-EC		
pH	6.6	7.0	7.5	8.1	6.6	7.0	7.5	8.1	6.6	7.0	7.5	8.1	6.0	7.0	8.0
Fe dosage rate (C/L/min)	9.2				NA				2.2				3.1	0.93 3.1 9.3	3.1
Total Fe dosage (mg/L)	30.0				30.0				20.9 40.7	20.2 30.0 33.3	20.1 30.4 37.6	18.5 36.6	7.2; 14.5; 28.9; 72.4		
Post-dosage mixing time (min)	240	90	60	60	60	60	20	8	240	90	60	60	120		

2.2. Computational Model

We adapted the computational model described in *Li et al.*[49], which predicts As(III-V) removal in the Fe-EC system assuming second-order kinetics for both Fe(II) oxidation by O_2 and As(III) oxidation by reactive intermediates, and Langmuir adsorption isotherms for As(III-V), P and Si. Accordingly, the equations governing this model are:

$$\frac{d[Fe(II)]}{dt} = D - k_{app} * [Fe(II)] * [O_2] \quad \text{(Equation 2-1)}$$

$$\frac{d[As(III)]_{oxidized}}{dt} = \frac{\beta}{1+\frac{k_1\,[Fe(II)]}{k_2\,[As(III)]}} * k_{app} * [Fe(II)] * [O_2] \quad \text{(Equation 2-2)}$$

$$[As(III), As(V), P, Si]_{adsorbed} = \frac{q_{max} * [Fe(III)] * K_{As(III),As(V),P,Si} * [As(III),As(V),P,Si]}{1+K_{As(III)}[As(III)]+K_{As(V)}[As(V)]+K_{Si}[Si]+K_P[P]} \quad \text{(Equation 2-3)}$$

where D (M s^{-1}) is the Fe dosage rate; k_{app} (M^{-1} s^{-1}) is the second order rate constant for Fe(II) oxidation by O_2; β is the yield of reactive intermediates (Fe(IV)) from Fe(II) oxidation by O_2 and was determined to be ~ 0.25 by Li et al.[49]; k_1/k_2 is the relative affinity of reactive intermediates for Fe(II) compared to As(III); q_{max} is the adsorption capacity of EC precipitates generated in SGW, and $K_{As(III),As(V),P,Si}$ are the adsorption affinities of EC precipitates for As(III), As(V), Si and P, respectively. We added a fourth equation to describe the time-dependent concentration of O_2, in which $[O_2]_{saturation}$ = 0.25 mM at 25ºC and k_r (s^{-1}) is the O_2 recharge rate resulting from mixing and aeration:

$$\frac{dO_2}{dt} = k_r * ([O_2]_{saturation} - [O_2]) - k_{app} * [Fe(II)] * [O_2] \quad \text{(Equation 2-4)}$$

K_{Si} and $K_{As(III)}$ are not expected to vary significantly between pH 6.6 and 8.1[56] because Si and As(III) do not deprotonate in this pH range (first pK_As of H_4SiO_4 and H_3AsO_3 > 9)[59]. Therefore, we used values measured by *Li et al.*[9], K_{Si} =$10^{2.94}$ and $K_{As(III)}$ =$10^{3.81}$, which were comparable to values reported in other studies for very similar systems[58,60]. In contrast, k_{app}, k_1/k_2, $K_{As(V)}$, K_P and q_{max} may all be pH-dependent. The computational model was implemented in Python 2.7.

2.3. Determining Adsorption and Oxidation Rate Constants at Different pHs

To determine $K_{As(V)}$, K_P and q_{max} experimentally, Fe-EC experiments were conducted at an Fe dosage rate of 9.2 C/L/min and at a Fe dosage of 30 mg/L in SGW amended with high concentrations of As and P (~2000 µg/L and 20 mg/L respectively, Tables 2-1). Dissolved and adsorbed concentrations of Si, P, As(III) and As(V) at equilibrium were measured by ICP-OES according to the procedure described above (section 2.1) and computed in Equations 2-5, 2-6 and 2-7, which derive from Equation 2-3:

$$K_{As(V)} = K_{Si} * \frac{[Si]}{[As(V)]} * \frac{[As(V)]_{adsorbed}}{[Si]_{adsorbed}} \quad \text{(Equation 2-5)}$$

$$K_P = K_{Si} * \frac{[Si]}{[P]} * \frac{[P]_{adsorbed}}{[Si]_{adsorbed}} \quad \text{(Equation 2-6)}$$

$$q_{max} = \frac{[Si]_{adsorbed}}{K_{Si}*[Si]} * \frac{1+K_{As(III)}[As(III)]+K_{As(V)}[As(V)]+K_{Si}[Si]+K_P[P]}{[Fe(III)]} \quad \text{(Equation 2-7)}$$

To determine k_{app} and k_1/k_2 experimentally, SGW amended with a high concentration of As(III) (~2000 µg/L) was dosed instantly with 30 mg/L $FeSO_4$ and mixed in open air for 6 to 60 minutes depending on pH (Table 2-2). Fe(II) and total As(III) were measured at regular time intervals by ICP-OES (Figure 2-1). k_{app} was determined by fitting the concentration of Fe(II) as a function of time to Equation 2-8, which derives from Equation 2-1 (D=0 after $FeSO_4$ addition). The concentration of O_2 was assumed to be saturated (0.25 mM), which is likely verified in a 200 mL beaker stirred vigorously.

$$[Fe(II)](t) = [Fe(II)]_{t=0} * e^{-k_{app}*[O_2]*t} \quad \text{(Equation 2-8)}$$

Then, using the value thus found for k_{app}, k_1/k_2 was determined by fitting the concentration of As(III) over time to Equation 2-2 (β=0.25[49]). An example of this procedure at pH 7.0 is shown in Figure 2-1.

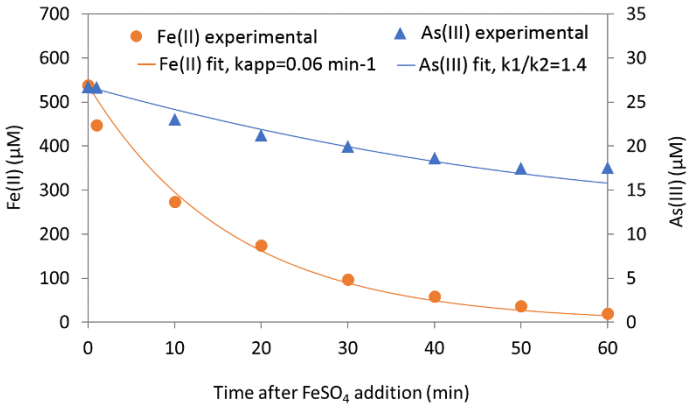

Figure 2-1: Example of procedure to derive k_{app} and k_1/k_2 by fitting Fe(II) and As(III) concentrations as a function of time to Equations 2-8 and 2-2 respectively.

The means and 95% confidence intervals of adsorption and oxidation rate constants measured in duplicate at pH 6.6, 7.0, 7.5 and 8.1 are compiled in Figure 2-2a-b and Table 2-3. Model simulations using mean adsorption and oxidation rate constants are compared with experimental arsenic removal in Figure 2-2c. The Fe dosage rate used in these experiments (2.2 C/L/min, see "Model optimization" in Tables 2-2) was chosen to be representative of field operations[47]. For each pH, k_{app}, k_1/k_2, $K_{As(V)}$, K_P and q_{max} were adjusted within the range of duplicate measurements to optimize the fit between modeled and measured arsenic removal by Fe-EC in SGW. Adjusted ("best-fit") adsorption and oxidation rate constants are indicated in red in Figure 2-2a-b and Table 2-3. The resulting "best fit" between modeled and experimental arsenic concentrations is shown in Figure 2-2d. Model simulations conducted in the rest of the paper used "best-fit" adsorption and oxidation rate constants.

Table 2-3: Adsorption and oxidation rate constants for model equations measured at pH 6.6, 7.0, 7.5 and 8.1. Averages (in black) and 95% confidence intervals (in grey) from duplicate experiments are indicated, as well as the constants chosen in the final model ("best fit", in red).

pH	6.6	7.0	7.5	8.1
log k_{app} (M^{-1} s^{-1})	0.15 (-0.24 ; 0.54) 0.30	0.73 (0.51 ; 0.94) 0.73	1.82 (1.74 ; 1.91) 1.78	2.67 (2.28 ; 3.06) 2.67
k_1/k_2	0.95 (0.85 ; 1.05) 0.90	1.50 (1.30 ; 1.70) 1.50	2.15 (1.46; 2.84) 2.15	2.63 (1.89 ; 3.36) 2.63
log K_P	6.04 (5.64 ; 6.44) 6.04	5.75 (5.34 ; 6.16) 5.75	5.54 (5.32 ; 5.75) 5.54	5.04 (4.89 ; 5.18) 5.04
log $K_{As(V)}$	5.43 (5.18 ; 5.69) 5.54	5.08 (4.86 ; 5.31) 5.19	4.91 (4.76 ; 5.07) 4.83	4.55 (3.99 ; 5.11) 4.75
q_{max}	1.04 (0.81 ; 1.27) 0.81	1.08 (0.78 ; 1.37) 0.93	1.20 (0.88 ; 1.51) 1.04	1.48 (1.44 ; 1.52) 1.5

2.4. Model Simulations

The model was operated for initial As(III), As(V), Si and P concentrations of 500 µg/L, 0 µg/L, 34.2 mg/L and 3.7 mg/L respectively. To investigate the effect of pH on the mechanisms of arsenic removal, simulations were conducted at pH 6.6, 7.0, 7.5 and 8.1 for a range of Fe dosages (5 to 50 mg/L, in 3 mg/L increments), using an Fe dosage rate of 3 C/L/min. Analyzing the respective concentrations of dissolved and adsorbed As(III)/As(V) allowed to identify the processes limiting arsenic removal at each pH. Then, to investigate the effect of operating conditions on arsenic removal, simulations were conducted for a range of Fe dosage rates (0.5 to 80 C/L/min) and O_2 recharge rates (2.0 and 4.6 hr^{-1} and at O_2 saturation), using an Fe dosage of 30 mg/L. 2.0 hr^{-1} is the oxygen recharge rate in a 200 mL beaker with an area-to-volume ratio of 0.3 (assuming an air-water exchange coefficient of $1.9x10^{-3}$ cm/s, consistent with [61]), while 4.6 hr^{-1} is a typical oxygen recharge rate in actively-aerated reactors in wastewater treatment plants[62]. Unless indicated otherwise, simulations included a post-electrolysis mixing period long enough to achieve 99.99% Fe(II) oxidation, which we defined as "equilibrium". When equilibrium required over 100 min post-electrolysis mixing, which is a realistic upper bound for field operations, we reported arsenic removal both at equilibrium and after 100 min mixing.

2.5. Comparison between Model Simulations and Experiments Representative of Field Conditions

A series of experiments was conducted in SGW without holding pH constant to reproduce realistic field conditions where pH evolves due to the solution equilibrating with atmospheric CO_2. These experiments were performed for four dosages (7.2, 14.5, 28.9 and 72.4 mg/L) at three Fe dosage rates (0.93, 3.1 and 9.3 C/L/min) and three initial pHs (6.0, 7.0 and 8.0, Table 2-2). The

robustness and generalizability of the trends - with respect to pH and Fe dosage rate- predicted by the model, which operates at constant pH, were assessed against these drift-pH experiments.

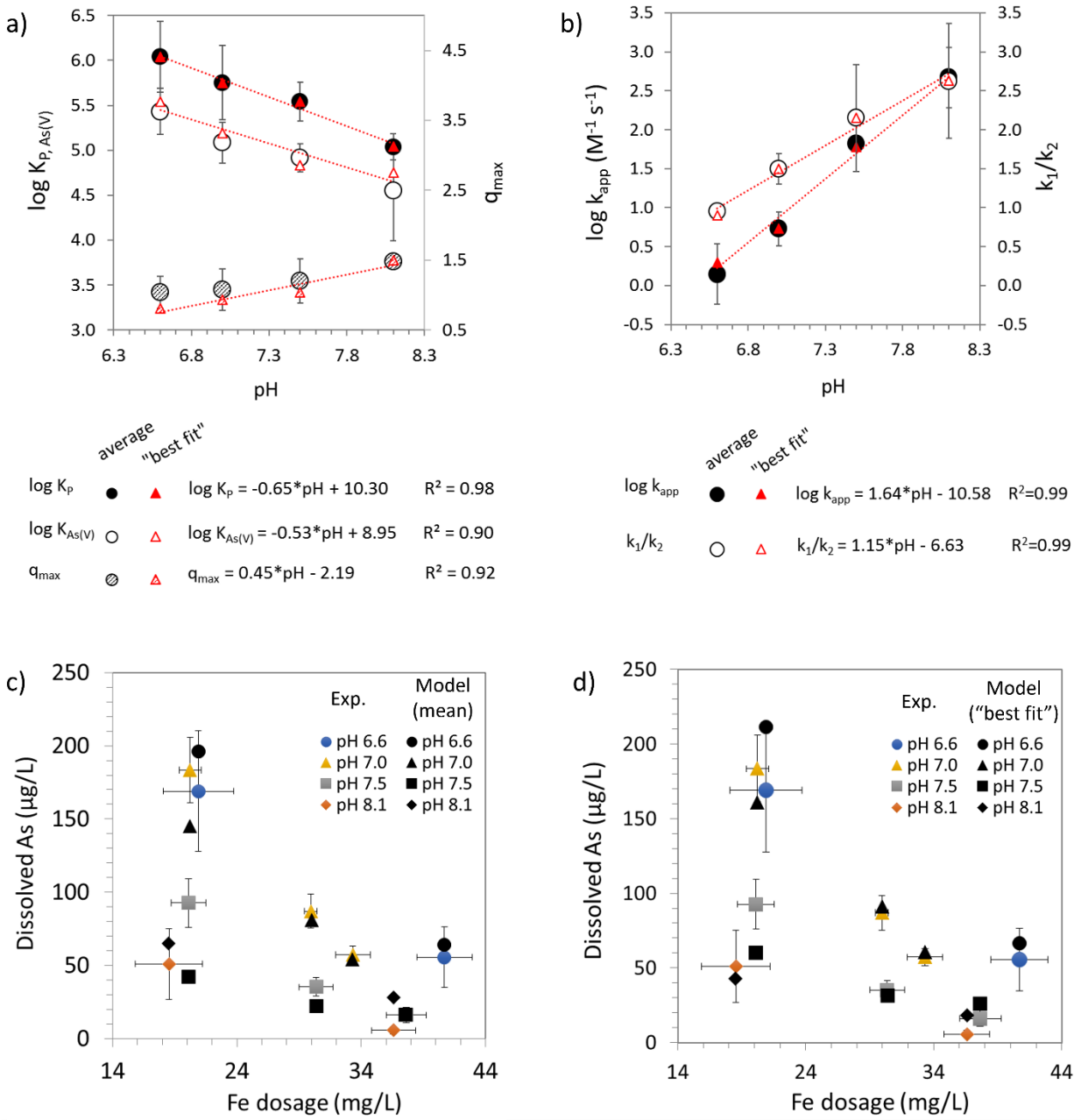

Figure 2-2: Adsorption (panel a) and oxidation (panel b) rate constants measured at pH 6.6, 7.0, 7.5 and 8.1. Averages and 95% confidence intervals from duplicate experiments are indicated, as well as the constants chosen in the final model ("best fit", in red). Numerical values are given in Table 2-3. Panels c and d show comparisons of post-treatment arsenic concentrations between experiments and model simulations using mean and "best fit" constants, respectively.

3. RESULTS AND DISCUSSION

3.1. Adsorption and Oxidation Rate Constants

Experimentally determined adsorption constants, K_P, $K_{As(V)}$ and q_{max}, are presented in Figure 2-2a and Table 2-3. Higher adsorption affinities for P than for As(V) are consistent with previous studies in similar systems[57,58,60]. We found that the affinity of EC precipitates for P and As(V) decreases by 0.65 and 0.53 log, respectively, for each unit increase in pH. Consistent with previous studies reporting lower As(V)/P adsorption to Fe(III) (oxyhydr)oxides at increasing pH[55,56], this result can be explained by the deprotonation of precipitate surface groups at higher pH, which raises the electrostatic barrier to anions. Values of $K_{As(V)}$ determined in this study were generally consistent with existing data on As(V) adsorption to hydrous ferric oxides (see a comparison in Figure 2-3)[56]. Interestingly, the adsorption capacity of EC precipitates, q_{max}, was found to slightly increase with pH. ICP-OES measurements also indicated substantial increases in Ca and Mg uptake between pH 6.6 and 8.1 (~ + 200% on average). Previous work has shown that the uptake of bivalent cations by Fe(III) precipitates, which occurs both electrostatically and via ternary surface complexes (e.g. Ca-P-Fe or Ca-As(V)-Fe), increases the removal of oxyanions[57]. Presumably, such improvement in oxyanion uptake is partly due to increased precipitate capacity in the presence of bound bivalent cations, which may provide additional adsorption sites or increase the accessibility of existing ones (by decreasing the electrostatic barrier). Therefore, we propose that the observed increase in q_{max} results from enhanced bivalent cation uptake, which may be favored at higher pH due to P/As(V) deprotonation ($pK_{a,2}$ = 7.2 and 6.9 respectively).

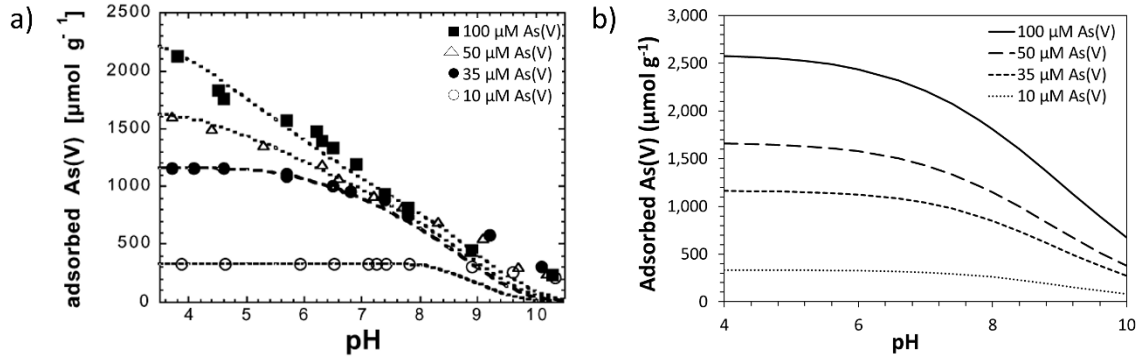

Figure 2-3: As(V) adsorption on hydrous ferric oxides as a function of pH, as reported in Dixit and Hering, 2003[56] (panel a). Using As(V) adsorption affinities ($K_{As(V)}$) measured in our study, we calculated As(V) adsorptions corresponding to the concentrations of adsorbent and adsorbate in Dixit and Hering, 2003[56] (panel b).

Experimentally determined oxidation rate constants are shown in Figure 2-2b and Table 2-3. We found that the oxidation rate of Fe(II) by O_2 in SGW, k_{app}, increases by 1.6 orders of magnitude for each unit increase in pH, which is very comparable to the pH-dependency measured in other carbonated systems in the same pH range (~1.7)[63,64]. We also found that k_1/k_2 increases approximately threefold between pH 6.6 and 8.1, which indicates a decrease in the affinity of reactive intermediates for As(III) relative to Fe(II). Although As(III) and Fe(II) both get easier to

oxidize at higher pH due to increased concentrations of deprotonated and carbonated species, respectively,[63,65] our results suggest that this effect is slightly stronger for Fe(II) in SGW.

Modeled and experimental post-treatment arsenic concentrations are presented in Figure 2-2d, showing a good agreement in the majority of cases. However, our model overestimates removal for low Fe dosages (< 25 mg/L) at pH 7.0 and 7.5, and underestimates it for high dosages (>35 mg/L) at pH 8.1. Adsorption and oxidation rate constants, which are assumed to be independent of the Fe concentration in our model, were measured at an Fe dosage of 30 mg/L (Table 2-2). The observed discrepancies between model and experiments at Fe dosages significantly different from 30 mg/L suggest that model constants may actually depend on the Fe dosage. For example, Langmuir isotherms may not be able to precisely model adsorption processes in systems such as Fe-EC, where the structure and reactivity of the adsorbent strongly depend on the molar ratios of Fe : oxyanions : bivalent cations[66,57].

3.2. Effect of pH on Arsenic Removal with Fe-EC

Figure 2-4a shows post-treatment arsenic concentrations as a function of Fe dosage according to model simulations at different pHs. Except at pH 6.6, 99.99% Fe(II) oxidation is achieved with post-electrolysis mixing times below 100 min (1, 10 and 100 min at pH 8.1, 7.5 and 7.0, respectively). At pH 6.6, approximately 99% of Fe(II) is oxidized after 100 min mixing, whereas full (>99.99%) oxidation requires 300 min. For mixing times below 100 min, arsenic removal is improved at higher pH, despite decreased precipitate affinity for As(V) ($K_{As(V)}$) and decreased As(III) competitiveness for reactive intermediates (k_2/k_1) (Figure 2-2a-b). The model predictions in Figure 2-4a indicate that these detrimental factors are outweighed by the beneficial effect of faster Fe(II) oxidation kinetics at higher pH, which limit the accumulation of Fe(II) and

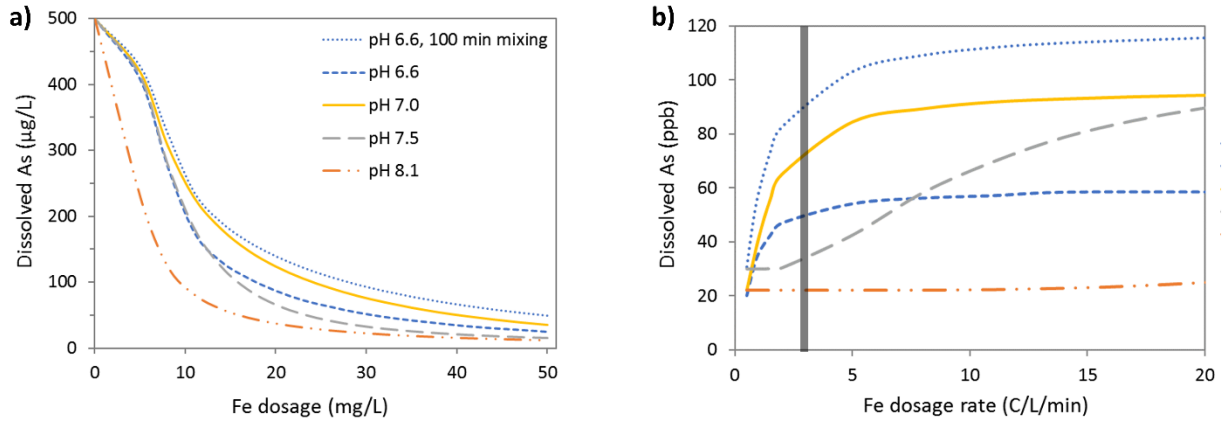

Figure 2-4: Post-treatment arsenic concentrations as a function of Fe dosage (panel a, Fe dosage rate of 3 C/L/min) and Fe dosage rate (panel b, Fe dosage of 30 mg/L) according to model simulations at pH 6.6, 7.0, 7.5 and 8.1, assuming O_2 saturation. We report arsenic concentrations at "equilibrium", defined as the time required to reach 99.99% Fe(II) oxidation (400, 100, 10 and 1 min of post-electrolysis mixing at pH 6.6, 7.0, 7.5 and 8.1 respectively). At pH 6.6, post-treatment arsenic concentrations are also given for a more realistic post-electrolysis mixing time of 100 min, at which 99% Fe(II) oxidation was achieved. On panel b, a vertical line is drawn at 3 C/L/min, which is the Fe dosage rate used in the simulations presented in Figure 2-5.

thus the scavenging of reactive intermediates needed to oxidize As(III) to As(V). Simulations at pH 6.6 show that arsenic removal is significantly enhanced (20 to 60 µg/L depending on the Fe dosage) when the mixing time is extended from 100 to 300 min to improve Fe(II) oxidation from 99% to 99.99%. During the late stages of mixing, competition for reactive intermediates is minimized because Fe(II) is present in trace concentrations, resulting in significant As(III) oxidation and thus arsenic removal. This result illustrates that substantial improvements in arsenic removal can be achieved by increasing the post-electrolysis mixing time to oxidize trace levels of Fe(II).

Figure 2-5 shows the speciation of arsenic in the same simulations. At all pHs and all dosages, adsorbed As(III) is much smaller than adsorbed As(V), indicating that As(V) adsorption

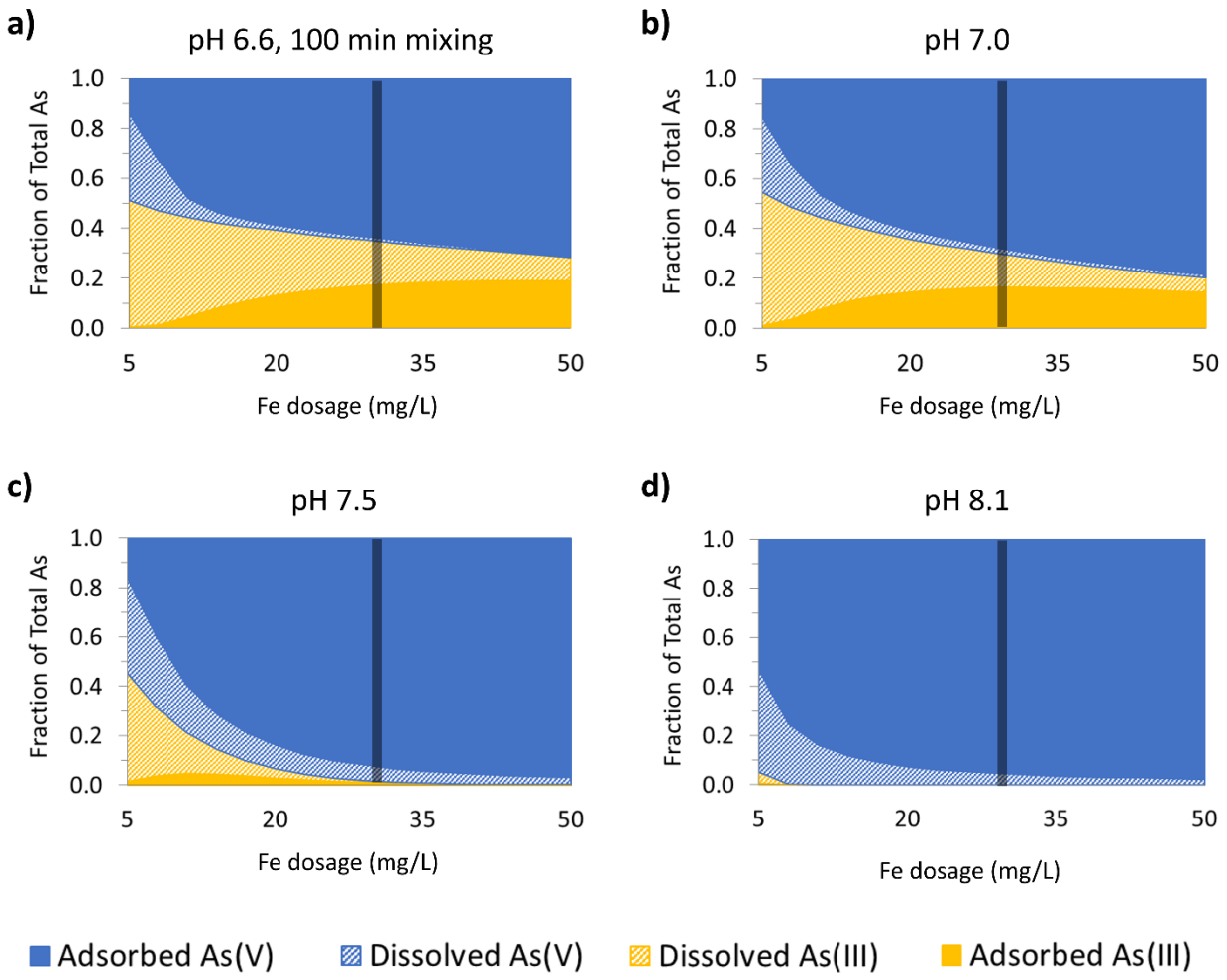

Figure 2-5: Post-treatment arsenic speciation as a function of Fe dosage according to model simulations assuming O_2 saturation, for an Fe dosage rate of 3 C/L/min, at pH 6.6 (panel a), 7.0 (panel b), 7.5 (panel c) and 8.1 (panel c). Except for pH 6.6, we report arsenic concentrations "at equilibrium", defined as the time required to reach 99.99% Fe(II) oxidation (100, 10 and 1 min of post-electrolysis mixing at pH 7.0, 7.5 and 8.1 respectively). At pH 6.6, arsenic concentrations are reported for a post-electrolysis mixing time of 100 min, at which 99% Fe(II) oxidation was achieved. On each panel, a vertical line is drawn at 30 mg/L, which is the Fe dosage used in the simulations presented in Figure 2-4b.

is either the primary (pH 6.6 and 7.0) or the only (pH 7.5 and 8.1) mechanism of arsenic removal. At pH 6.6 and 7.0, As(III) accounts for the vast majority of dissolved arsenic, and As(III) adsorption does not increase for Fe dosages above 30 mg/L, indicating that arsenic removal is limited by the oxidation of As(III) to As(V). By contrast, at pH 8.1, As(V) accounts for the entirety of dissolved arsenic, indicating that removal is limited by As(V) adsorption. pH 7.5 represents an intermediary situation: at low Fe dosages (<20 mg/L), dissolved arsenic is composed of both As(III) and As(V) and arsenic removal is limited by both As(III) oxidation and As(V) adsorption. However, at higher dosages (>20 mg/L), As(V) accounts for the entirety of dissolved arsenic and removal is therefore limited by As(V) adsorption, similar to pH 8.1.

As pH increases, the process limiting arsenic removal thus shifts from As(III) oxidation to As(V) adsorption. This shift can be interpreted as follows. At lower pHs (6.6 and 7.0), the affinity of EC precipitates for As(V) ($K_{As(V)}$) is the highest and As(V) is adsorbed as soon as it forms, as supported by negligible concentrations of dissolved As(V) for Fe dosages > 20 mg/L in Figures 2-5a and 2-5b. However, slow Fe(II) oxidation kinetics lead to the accumulation of Fe(II), which competes with As(III) for reactive intermediates, leaving a large fraction of arsenic unoxidized and dissolved. By contrast, faster Fe(II) oxidation kinetics at higher pHs (7.5 and 8.1) favor the oxidation of As(III), which disappears for Fe dosages >30 mg/L at pH 7.5 and >10 mg/L at pH 8.1 (Figures 2-5c and 2-5d). At these higher pHs, decreased precipitate affinity for As(V) limits adsorption, explaining the higher concentrations of dissolved As(V) compared to lower pHs.

3.3. Impact of Fe Dosage Rate on Arsenic Removal at Different pHs

Figure 2-4b shows post-treatment arsenic concentrations as a function of Fe dosage rate in model simulations at different pHs, using a constant Fe dosage of 30 mg/L. The impact of Fe dosage rate on arsenic removal strongly depends on pH. At lower pHs (6.6 and 7.0), increasing the Fe dosage rate from 0.5 to 5 C/L/min strongly degrades arsenic removal, while further increases in dosage rate have a minimal impact. At pH 7.5, increases in Fe dosage rate between 2 and 20 C/L/min lead to a milder but gradual decrease in arsenic removal. By contrast, at pH 8.1, arsenic removal is independent of Fe dosage rate between 0.5 and 20 C/L/min.

The Fe dosage rate affects the accumulation of Fe(II) and thus the kinetics of As(III) oxidation (Equation 2-2)[49]. Consequently, the Fe dosage rate is expected to have a strong impact when arsenic removal is limited by As(III) oxidation (e.g. at 3 C/L/min for pH 6.6 and 7.0, see Figures 2-5a and 2-5b), and a much more limited impact when arsenic removal is limited by As(V) adsorption (e.g. at 3 C/L/min for pH 7.5 and 8.1, see Figures 2-5c and 2-5d), which is consistent with the model predictions in Figure 2-4b. At pH 7.5, the increasing sensitivity of arsenic removal to Fe dosage rate between 0.5 and 10 C/L/min reflects a shift in the process limiting arsenic removal from As(V) adsorption to As(III) oxidation (see Figure 2-6a-b).

For pH 6.6, 7.0 and 7.5, the lines in Figure 2-4b level off at high dosage rates, indicating that arsenic removal becomes independent of the Fe dosage rate. However, we note that this behavior off does not reflect a change in the process limiting arsenic removal, which remains As(III) oxidation (see Figure 2-6c). At high Fe dosage rates, which lead to large concentrations of Fe(II), Equation 2-2 becomes Equation 2-9. The kinetics of As(III) oxidation are therefore no

longer controlled by the concentration of Fe(II), and they are consequently independent of the Fe dosage rate.

$$\frac{d[As(III)]_{oxidized}}{dt} = \beta * \frac{k_2}{k_1} * k_{app} * [O_2] * [As(III)] \qquad \text{(Equation 2-9)}$$

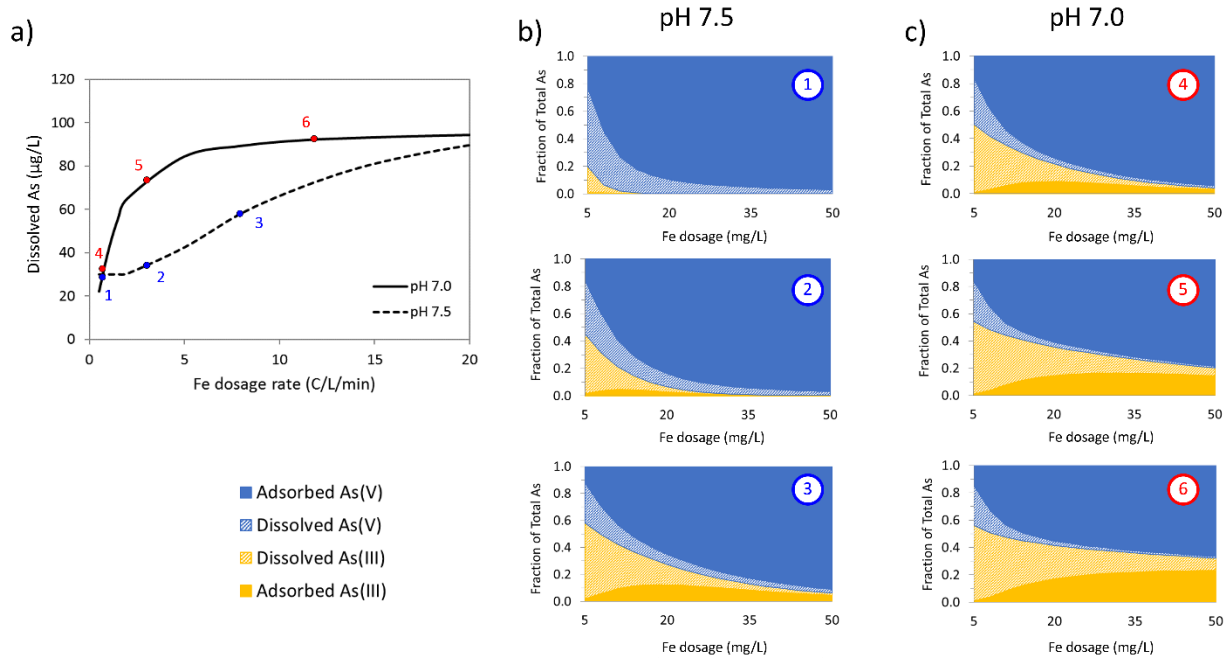

Figure 2-6: Panel a: post-treatment arsenic concentrations as a function of Fe dosage rate (Fe dosage of 30 mg/L) according to model simulations at pH 7.0 and 7.5, assuming O_2 saturation. Dots 1-6 reference the pH and dosage rate conditions investigated in panels b and c. Panels b and c: post-treatment arsenic speciation as a function of Fe dosage according to model simulations (assuming O_2 saturation) at pH 7.0 for Fe dosage rates of 1, 3 and 12 C/L/min (panel b) and at pH 7.5 for Fe dosage rates of 1, 3 and 8 C/L/min (panel c). We report arsenic concentrations at "equilibrium", defined as the time required to reach 99.99% Fe(II) oxidation (100 and 10 min of post-electrolysis mixing at pH 7.0 and 7.5 respectively).

Figure 2-7 shows the effect of Fe dosage rate on arsenic removal for several O_2 recharge rates. Overall, the model predicts lower arsenic removal when O_2 consumption by Fe(II) oxidation is taken into account. O_2 recharge rates of 2.0 and 4.6 hr^{-1} are not sufficient to prevent significant O_2 depletion during treatment. For example, at pH 7.0 and 3 C/L/min, O_2 levels decrease down to 28% and 49% saturation for recharge rates of 2.0 and 4.6 hr^{-1}, respectively, O_2 depletion being more pronounced at higher pHs and larger Fe dosage rates. Lower O_2 concentrations promote Fe(II) accumulation, which inhibits As(III) oxidation and degrades arsenic removal. Figure 2-7 shows that O_2 depletion exacerbates the sensitivity of arsenic removal to Fe dosage rate, indicating that arsenic removal is predominantly limited by As(III) oxidation when O_2 saturation is not maintained.

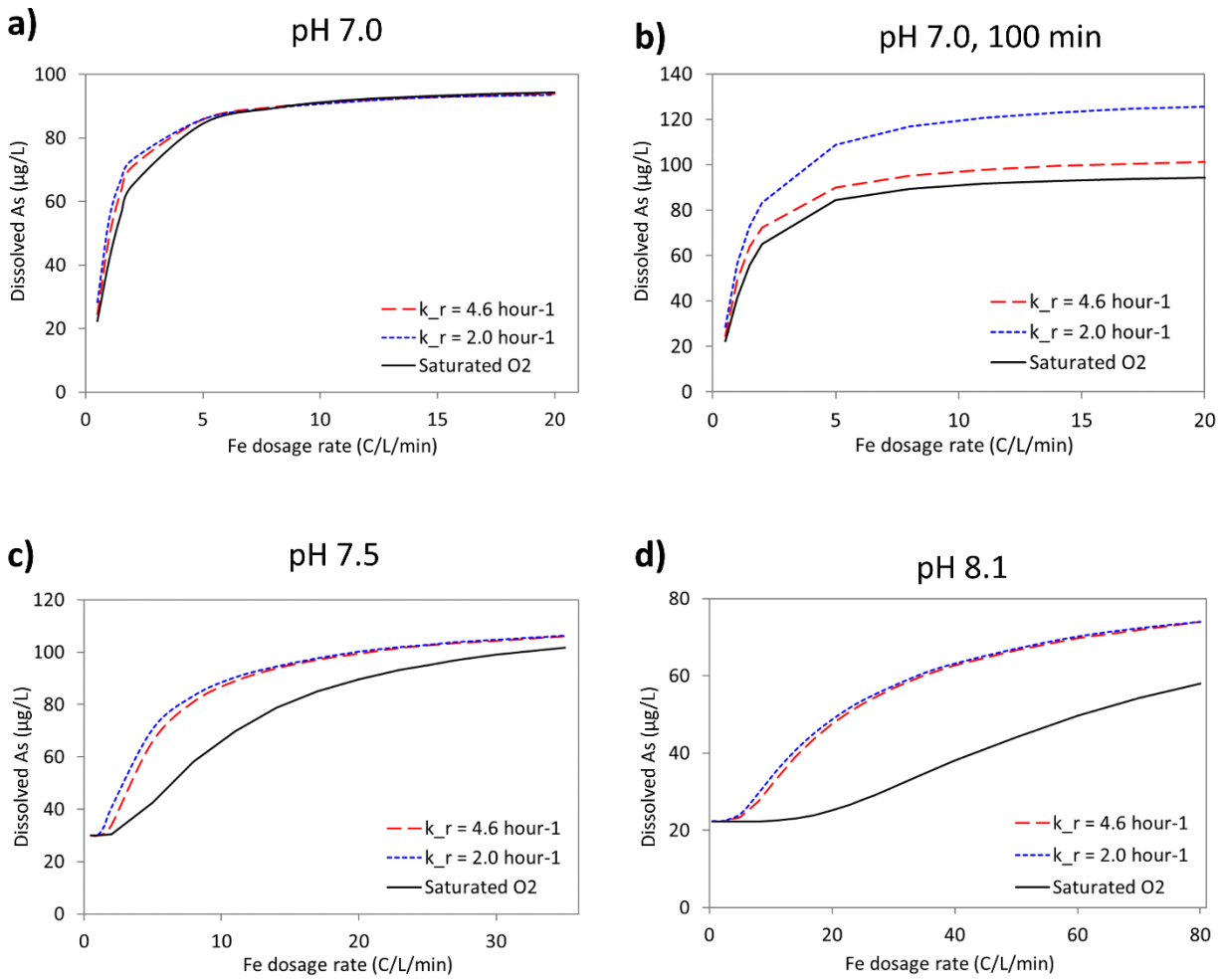

Figure 2-7: Post-treatment arsenic concentrations as a function of Fe dosage rate according to model simulations in three O_2 recharge scenarios, at pH 7.0 (panels a and b), pH 7.5 (panel c) and pH 8.1 (panel d). We report arsenic concentrations at "equilibrium", defined as the time required to reach 99.99% Fe(II) oxidation (post-electrolysis mixing time up to 250 min for pH 7.0 and up to 100 min for pH 7.5 and 8.1, depending on the O_2 recharge scenario). At pH 7.0, post-treatment arsenic concentrations are also given for a more realistic post-electrolysis mixing time of 100 min, at which 99.8% Fe(II) oxidation was achieved.

3.4. Comparison between Model Simulations and Experiments Representative of Field Conditions

Figure 2-8a shows post-treatment arsenic concentrations and pHs as a function of Fe dosage in pH-drift experiments with initial pHs of 6.0, 7.0 and 8.0. Results from model simulations are shown to depict the expected effect of pH when it is held constant. pH-drift experiments exhibited a trend of improved arsenic removal at higher initial pH, even though converging final pHs significantly attenuated the effect of pH compared to model predictions.

Figure 2-8b presents post-treatment arsenic concentrations as a function of Fe dosage for drift-pH experiments conducted at an initial pH of 7.0 and at Fe dosage rates of 0.93 and 9.3

C/L/min. Arsenic concentrations after 20 and 120 min post-electrolysis mixing are reported, as well as corresponding solution pHs. Results from model simulations are shown to depict the effect of Fe dosage rate expected at constant pH. In pH-drift experiments, pH invariably increased from 7.0 to 8.0-8.5. Therefore, arsenic removal could have been expected to be less limited by As(III) oxidation (Figure 2-5) and less sensitive to Fe dosage rate (Figure 2-4b) compared to constant-pH experiments. By contrast, lowering the Fe dosage rate in pH-drift experiments improved arsenic removal more than predicted by the constant-pH model. As shown in Figure 2-8b, arsenic concentrations did not vary significantly after 20 min of post-electrolysis mixing, indicating that ultimate arsenic removal had been reached before the end of the mixing period. Consequently, in experiments at 9.3 C/L/min, arsenic removal took place at pH <7.7-8.1 (Figure 5b). By contrast, in experiments at 0.93 C/L/min, which had tenfold longer dosage times, pH increased up to 8.2-8.6 before ultimate arsenic removal was achieved. Consequently, arsenic removal at 0.93 C/L/min overall took place at substantially higher pHs than in experiments at 9.3 C/L/min, likely contributing to the improved performance at lower Fe dosage rates. We propose that in field-like conditions where pH increases over time as carbonate-rich groundwater equilibrates with atmospheric CO_2, improved Fe-EC performance at lower Fe dosage rates is partly explained by the deferment of reactions until pH has significantly increased, which favors arsenic removal (Figure 2-4a).

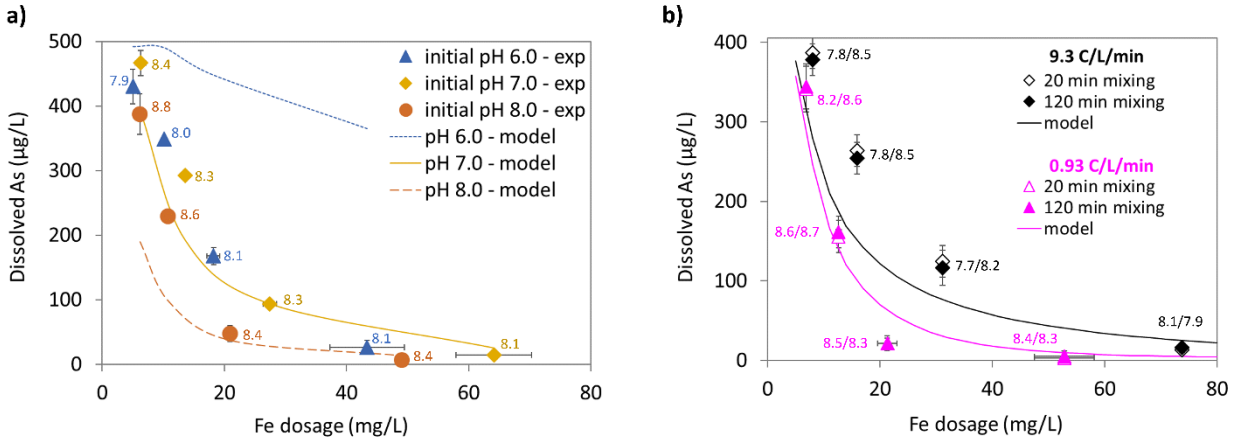

Figure 2-8: Post-treatment arsenic concentrations in pH-drift experiments at different initial pHs (panel a, Fe dosage rate of 3.1 C/L/min) and at different Fe dosage rates (panel b, initial pH 7.0). We report averages and standard deviations of duplicate experiments. Post-treatment solution pH is indicated next to the corresponding data point. Model simulations (assuming O_2 saturation) are shown (lines) to indicate the effect of pH and Fe dosage rate on arsenic removal when pH is held constant.

3.5. Implications for Water Treatment by Fe-EC

This chapter shows that pH controls the impact of operating conditions on arsenic removal in Fe-EC. While a previous study at pH 7.1 had found that decreasing the Fe dosage rate can improve the performance of Fe-EC[49], we demonstrated that this finding only applies when arsenic

removal is limited by As(III) oxidation, i.e. at low pH (< 7.5). By contrast, decreasing the Fe dosage rate at pH>8.0 would only extend the duration of treatment without any benefits to arsenic removal. However, we also found that if oxygen saturation cannot be maintained, decreasing the Fe dosage rate is preferable at any pH. Finally, our results show that increasing the O_2 recharge rate without achieving O_2 saturation can have little to no effect on arsenic removal, especially at higher pHs.

We found that the trends predicted by our constant-pH model, such as improved arsenic removal at higher pH and lower Fe dosage rate, were still valid –even though not with the same magnitude- in more realistic experiments where pH was not held constant. This result indicates that our model can serve as a useful tool to inform decisions about the operation of Fe-EC in the field. We note that the pH drift in our lab experiments may be larger than during typical field treatment (a < 0.5 pH increase was observed in a field trial of Fe-EC in West Bengal, India[47]), possibly due to better air-water exchange in the lab setup. The actual effect of initial pH in the field may therefore be larger than estimated in Figure 2-8a, while the actual effect of Fe dosage rate may be smaller than estimated in Figure 2-8b.

Finally, there is still room to improve our model. Although it already accounts for a number of groundwater characteristics (pH, concentrations of oxyanions) and operating conditions (Fe dosage rate, post-electrolysis mixing time, O_2 recharge rate), more work is needed to incorporate the beneficial effect of bivalent cations on the uptake of oxyanions by Fe(III) (oxyhydr)oxide precipitates[57,67].

CHAPTER 3. *E. coli* attenuation by Fe-EC in synthetic Bengal groundwater: effect of pH and natural organic matter

1. INTRODUCTION

Arsenic-contaminated groundwater serves as the primary drinking water source for tens of millions of people in Bangladesh and India[68]. Previous research aiming to improve the quality of arsenic-contaminated groundwater in the Bengal Basin has focused on arsenic removal alone, largely ignoring possible concurrent microbial contamination of shallow aquifers. However, recent studies have reported the presence of fecal indicators and pathogens (rotavirus, *Shigella*, *Vibrio cholera*, pathogenic *E. coli* and adenovirus) in shallow tubewell water in Bangladesh[37–39]. A study of 125 tubewells in rural Bangladesh found that 30% of wells with arsenic levels above 50 µg/L had detectable levels of *E. coli*[37], indicating significant concurrent arsenic and fecal contamination. Although fecal contamination of groundwater is typically lower than that of surface water (fecal coliform concentrations in tubewells < 10^1-10^2 CFU/100 mL[25,37–39,69,70] compared to 10^2-10^4 CFU/100 mL in ponds and dug wells[25,71] and up to 200,000 CFU/100 mL in Ganga river[72]), it is suspected to contribute to the sustained prevalence of diarrheal diseases in the region[40,73]. Addressing arsenic and microbial groundwater contamination simultaneously and at low-cost would thus have significant implications for access to safe water in Bengal.

Iron electrocoagulation (Fe-EC) relies on the rapid dissolution of a sacrificial Fe(0) anode to produce Fe(II), which then oxidizes in the presence of dissolved oxygen to form Fe(III) precipitates with high specific surface area and a high affinity for arsenic adsorption[48]. Arsenic-laden precipitates can be removed subsequently by gravitational settling. In the Fe-EC process, strong oxidants generated in Fenton-type reactions convert As(III) into As(V), which is easier to remove at circumneutral pH[49]. Previous work has shown that Fe-EC effectively removes arsenic at low cost and is a realistic option for sustainable groundwater remediation in Bengal[46,47,51]. However, microbe reduction by Fe-EC in arsenic-contaminated groundwater and its effect on arsenic remediation have not been examined. Such investigation is necessary to assess the potential of Fe-EC to address safe water needs in Bengal.

Two processes in the Fe-EC system may contribute to microbe attenuation. The first process is the production of Fe(III) precipitates with an affinity for the surface of microorganisms, leading to their encapsulation in flocs and physical removal by settling. In many natural environments, Fe oxides are found in close association with bacterial cells or exopolymers[74–76], which suggests strong sorption affinities and has prompted the use of Fe oxides to remove bacteria[77–79] and viruses[80,81] in engineered systems. The second process is the transient presence of Fe(II) that can lead to oxidative stress and inactivation. Fe(II) oxidation in Fenton-type reactions produces strong oxidants (Fe(IV), OH•) that can inactivate bacteria[82] and viruses[83]. The processes leading to both physical removal with flocs and inactivation are largely governed by electrolyte composition, which can impact the phase, size and surface charge of EC precipitates[66,57], the rate of Fe(II) oxidation[63] and the lifetime of strong oxidants (HCO_3^-, Cl^-, As(III) and natural organic

matter can quench Fe(IV) and OH•). Although some Fe-EC research has focused on microbe attenuation, these studies were performed in electrolytes designed to replicate surface water[81,84,85] and cannot be extrapolated to arsenic-contaminated groundwater, where significant concentrations of oxyanions likely modify the structure and surface charge of EC precipitates and thus the mechanisms and extent of microbe attenuation. In addition, research on microbe reduction in EC systems has primarily involved viruses[81,85–87]. The mechanisms of bacteria attenuation, specifically the respective roles of removal and inactivation, remain largely unknown.

In addition to electrolyte composition, solution pH is likely to be a key factor affecting Fe-EC performance because it controls (1) the rate of Fe(II) oxidation[63] and thereby the residence time of potentially bactericidal Fe(II) as well as the rate at which Fe(III) precipitates are generated, and (2) the surface charge of Fe(III) precipitates and their electrostatic interactions with microorganisms. The pH of arsenic-contaminated groundwater (defined as [As] > 10 μg/L) in Bengal varies between 6.4 and 8.4[36]. In addition, pH may increase during Fe-EC field treatment as a result of groundwater equilibrating with atmospheric CO_2. Therefore, understanding the effect of pH on microbe attenuation is essential to predict treatment efficiency in the field. Furthermore, since pH controls processes potentially leading to removal and inactivation, varying solution pH can help unravel the mechanisms of microbe attenuation in Fe-EC systems.

Natural organic matter (NOM) is present at non-negligible concentrations in arsenic-contaminated groundwater in Bengal (1-5 mg-C/L)[36,88] and may interfere with microbe attenuation by Fe-EC in several ways: quenching of strong oxidants, complexation of dissolved Fe(II)/Fe(III)[89], and alteration of the surface characteristics of Fe(III) precipitates and microorganisms. NOM is known to inhibit microbe-mineral interactions by increasing electrostatic repulsion[90,91], and has been shown to reduce the effectiveness of Fe-based microbe reduction processes[77,81,91]. It is therefore important to determine the impact of NOM on *E. coli* attenuation with Fe-EC.

The goals of this chapter are to: (1) examine the concurrent removal of arsenic and bacteria by Fe-EC in synthetic Bengal groundwater; (2) investigate the effects of pH and NOM on this process; and (3) determine the mechanism of bacteria attenuation, with particular focus on distinguishing removal from inactivation. Using *Escherichia coli (E. coli) K12* as a model for gram-negative fecal bacteria, we first demonstrate concurrent arsenic and bacteria attenuation. Next we investigate the pH-dependence of *E. coli* attenuation in Fe-EC by (1) comparing Fe-EC with Fe chemical coagulation controls, (2) analyzing ζ-potential measurements of EC precipitates and *E. coli*, and (3) varying Fe-EC operating parameters such as iron dosage rate and settling time. We combine these results with live-dead staining and transmission electron microscopy images to propose a mechanism for *E. coli* attenuation. Lastly, we discuss the effect of NOM on *E. coli* reduction by Fe-EC.

2. METHODS

2.1. Synthetic Bengal Groundwater Preparation

The recipe for synthetic Bengal groundwater (SGW) was designed to reproduce the average chemical composition of arsenic-contaminated Bangladesh tubewells (defined as [As] > 10 µg/L), as determined by a large sampling campaign by the British Geological Survey (BGS)[36]. Concentrations of background electrolytes (8.2 mM HCO_3^-, 11.1 mM Na^+ and 9.0 mM Cl^-) and bivalent cations (2.6 mM Ca^{2+} and 1.9 mM Mg^{2+}) were selected to be within the range of the average BGS measurements. Concentrations of oxyanions (0.16 mM P, 1.3 mM Si and 6.1 µM (460 µg/L) As(III)), which affect Fe-EC by decreasing the surface charge of precipitates, inhibiting their aggregation and by competing for surface sites[66], were significantly higher in SGW than average BGS measurements to represent worst-case scenarios for arsenic removal. Arsenic was added as As(III), which is generally more difficult to remove in natural waters than As(V). SO_4^{2-} was not included because we concluded from previous work that SO_4^{2-} concentrations in the range of BGS measurements (0.2 ± 0.6 mM) do not significantly affect the Fe-EC process for groundwater remediation. Although the average Fe concentration in BGS-sampled tubewells was 3.4 mg/L, Fe was not included to avoid redundancy with our Fe-EC dosage. All other ions measured by the BGS (Al, B, Ba, Co, Cr, Cu, Li, Mn, Sr, V and Zn) were trace elements (average concentrations < 11 µM), except K^+ (average concentration of 0.14 mM), which we did not include in SGW because it is a background ion similar to Na^+ (already present at 11.1 mM). A comparison of SGW composition with BGS measurements is presented in Table 3-1. The low conductivity of SGW (~2.1 mS/cm, estimated on the basis of Table 3-1) did not inhibit operating the EC cell at low voltage.

Table 3-1: SGW composition compared to real Bangladesh tubewell water. Concentrations of HCO3-, Ca2+ and Mg2+ in SGW are close to average levels in arsenic-contaminated tubewells (defined as [As]>10 µg/L), while concentrations of Si, P and As represent worst-case conditions for As removal. a Values obtained from the BGS database on Bangladesh tubewells[36]. pH, HCO3, Cl- and dissolved organic carbon (DOC) values come from Special Study Areas (n=271); all other values comes from the National Survey Data (n=3534).

Groundwater component	**SGW**	**Bangladesh tubewells [a]**	
		Mean ± st. dev.	***% wells with [x]>[x]$_{SGW}$***
HCO_3^- (mM)	8.2	8.2 ± 2.3	28.4
Ca^{2+} (mM)	2.6	1.6 ± 1.3	9.9
Mg^{2+} (mM)	1.9	1.1 ± 0.9	4.9
P (mM)	0.16	0.05 ± 0.05	3.3
Si (mM)	1.3	0.7 ± 0.2	0.1
As(III) (µM)	6.1	1.7 ± 2.1	2.3
pH	6.6 or 7.5	7.1 ± 0.2	
DOC (mg/L)	0-3	3.0 ± 2.8	20.7
Na^+ (mM)	11.1	4.1 ± 8.0	3.9
Cl^- (mM)	9.0	2.2 ± 5.6	3.7

Stock solutions of the reagents were autoclaved prior to use. The procedure to prepare SGW was similar to Roberts et al[58]. The day of an experiment, 200 mL batches of SGW were prepared by adding 8.2 mM $NaHCO_3$ to 18 MΩ deionized water (Millipore Milli-Q Integral 5), bubbling CO_2(g) to decrease pH to 6.2, and subsequently adding 1.3 mM Na_2SiO_3, 2.6 mM $CaCl_2$, 1.9 mM $MgCl_2$, 0.16 mM Na_2HPO_4 and 6.1 µM (460 µg/L) $NaAsO_2$ (As(III)). Finally, CO_2(g) was allowed to escape until pH reached the target value (6.6 or 7.5), which was maintained throughout an experiment by adding drops of 1.1 M HCl as needed. Total HCl added was between 2 and 10 mM, resulting in a less than 43% increase in ionic strength. Concentrations of As, Ca, Mg, P and Si were measured by inductively coupled plasma optical emission spectrometry (ICP-OES, PerkinElmer 5300 DV, measurement error typically < 5%). Initial concentrations of all ions varied by less than 10% in replicate batch experiments. ICP-OES with hydride generation was used to measure low (<20 µg/L) final arsenic concentrations. For NOM experiments, 3 mg-C/L of Suwanee River Fulvic Acid (International Humic Substance Society) was added to SGW. The concentration of NOM was measured with a TOC-V analyzer (Shimadzu).

2.2. *E. coli* Preparation and Enumeration

We used a non-pathogenic and kanamycin-resistant strain of the gram-negative bacterium *Escherichia coli K12* (NCM 4236) obtained from the late Dr. Sydney Kustu (UC Berkeley). Two days before an experiment, a frozen *E. coli* culture was thawed and inoculated into tryptic soy broth containing 0.025 g/L of kanamycin and grown overnight at 37º C. This culture was re-propagated twice in fresh broth (8 and 16 hours respectively) to minimize bacterial shock after thawing. On the morning of an experiment, 1.3 mL of stationary-phase *E. coli* was harvested by centrifugation (5200g for 5 min), rinsed three times with phosphate buffer (20 mM P, 145 mM NaCl) and resuspended in phosphate buffer. For bacteria attenuation experiments, 200 mL SGW was spiked with 200 µL of this *E. coli* harvest, resulting in concentrations of $10^{6.1}$-$10^{6.7}$ CFU/mL.

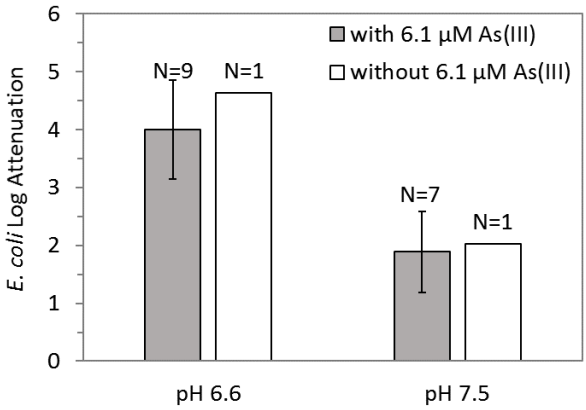

Figure 3-1: *E. coli* attenuation with Fe-EC in SGW with and without 6.1 µM As(III). Fe dosage was 0.5 mM. The number of replicates is indicated above each bar. This Figure illustrates the absence of arsenic toxicity to *E. coli* in SGW.

E. coli concentrations were enumerated in duplicate in 100 µL aliquots as colony forming units (CFU) using the spread plate technique on agar with 0.025 g/L kanamycin. It has been shown that 1 mM As(III) does not affect the survival or mutagenicity of *E. coli*[92,93]. Therefore, arsenic toxicity to *E. coli* is not expected in SGW, where the concentration of arsenic is much lower ([As]=6.1 µM). Similar *E. coli* attenuation in the presence and absence of 6.1 µM As(III) (Figure 3-1) confirmed the absence of arsenic toxicity to *E. coli* in our system. In addition, there was no detectable arsenic uptake by *E. coli* (Table 3-2), consistent with a study showing that arsenic uptake by bacterial cells is minimal when [P]>>[As][94] (in SGW, [P]=160 µM and [As]=6.1 µM).

Table 3-2: Comparison of As(III) removal by Fe-EC in SGW with and without *E. coli.* In all experiments, the Fe dosage was 0.5 mM and the Fe dosage rate was 46.4 µM/min. We report average concentrations ± one standard deviation in µg/L. Post-treatment arsenic speciation was not measured, but previous work in a very similar electrolyte and with comparable operating conditions[49] allows us to estimate that the majority of arsenic in post-treatment samples was As(III), since most As(V) is adsorbed on EC precipitates at circumneutral pH.

Without *E. coli* (n=6)		**With $10^{6.5}$ CFU/mL *E. coli* (n=7)**	
Initial As (µg/L)	***Final As (µg/L)***	***Initial As (µg/L)***	***Final As (µg/L)***
458 ± 37	117 ± 17	465 ± 30	116 ± 15

2.3. Fe-EC Experiments

All glassware was washed in 10% HNO_3, rinsed with 18 MΩ deionized water and autoclaved prior to use. EC experiments were conducted by immersing two 1 cm x 8 cm Fe(0) electrodes (98% Fe, 0.5 mm thick, 0.5 cm apart, anodic submerged area of 3 cm^2) in 200 mL SGW spiked with *E. coli*. Electrodes were cleaned with sand paper before each experiment to remove any rust or solid deposits. Within the tested current density range (0.33 to 10 mA/cm^2), the Fe dosage rate *D* (M Fe/s) is related to the applied current *I* (A or Coulombs/s) according to Faraday's law:

$$D = \frac{I}{V*Z*F} \qquad \text{(Equation 3-1)}$$

where *V* is the reactor volume (L), *Z* is the number of electrons involved (equivalents/mol) and *F* is Faraday's constant (96485 Coulombs/mol). We assumed Z=2 based on Lakshmanan et al.[95]. Unless specified otherwise, we used an Fe dosage rate of 46.4 µM/min (current density of 10 mA/cm^2) and the dosage time was adjusted to reach the desired final Fe concentration (varying from 0.1 to 2.5 mM). Voltage was <5V, resulting in an electric field <10 V/cm, orders of magnitude lower than bactericidal electric fields[96–98]. Operating conditions were selected based on previous work[46,48,60,99] to avoid the anodic production of chlorine or oxygen and the formation of mixed-valent Fe oxides. We note that we found that *E. coli* attenuation was similar by Fe-EC and by chemical coagulation with an Fe(II) salt (see later part 3.3 and Figure 3-6), confirming that chlorine production in Fe-EC was negligible.

Fe-EC led to the formation of hydrous ferric oxide precipitates[48,50]. After dosing, the solution was stirred in open air for 90 to 120 min to allow for Fe(II) oxidation and formation of Fe(III) precipitates. These stages are referred to as "dosing-mixing" hereafter. The suspension was then left to settle overnight. Unfiltered and filtered (0.45 μm nylon filters) samples were taken before dosing, after dosing-mixing and after overnight settling for measurement of Fe, As, Ca, Mg, P and Si with ICP-OES. All samples were digested with 1.1 M HCl prior to ICP-OES analysis. Unfiltered samples were used to measure total Fe (Fe(II) + Fe(III)). Because Fe(III) is insoluble at circumneutral pH, Fe in filtered samples was considered to be Fe(II). Across all experiments, unfiltered Fe in bulk solution after dosing was 95% ± 7% (across 69 experiments) of the Faradaic value. Fe in the filtrate (soluble Fe(II)) after dosing-mixing was <0.1% of the total Fe dosed for experiments at pH 7.5, and 19% ± 6%, (across 18 experiments) of the total Fe dosed for experiments at pH 6.6. Although complete (99.9%) oxidation of Fe(II) in our SGW at pH 6.6 requires over 9h (Figure 3-2b), we chose not to prolong mixing beyond 120 min to remain representative of field conditions.

a)

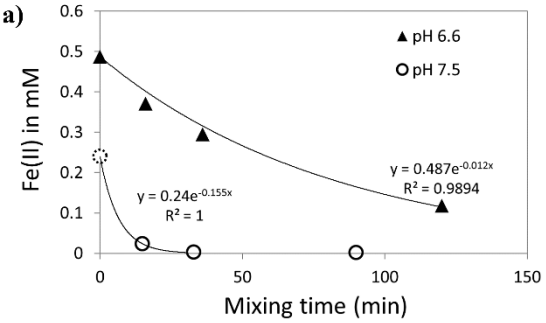

b)

pH	k_{eff} (min^{-1})	t_{50} (min)	t_{99} (min)	$t_{99.9}$ (min)
6.6	0.012	58	384	576
7.5	0.155	4.5	30	45

Figure 3-2: (a) Experimental derivation of Fe(II) oxidation rates (keff) in SGW at pH 6.6 and 7.5 in the presence of $10^{6.5}$ CFU/mL of *E. coli*. (b) Resulting keff and required times to achieve 50, 99 and 99.9 % Fe(II) oxidation (t_{50}, t_{99} and $t_{99.9}$ respectively).

Samples for *E. coli* enumeration were taken before dosing and after settling (from the supernatant, ~ 3 cm below the surface). The supernatant was not sampled until Fe concentrations were <5% of the total Fe dosed, which typically required overnight settling. *E. coli* attenuation was calculated as the difference between CFU concentrations in the pre-dosing and post-settling samples. Overnight settling allowed separating individual *E. coli* cells from cells associated with Fe(III) precipitates, because individual cells do not settle in this time frame (Stokes settling velocity of 1 μm particles with a density of 1.16 g/cm^{3}[100] is about 1 cm/day). This assumption was verified in preliminary experiments, which showed that: (1) concentrations of *E. coli* cells suspended in SGW did not change after two days (less than 4.5% change), and (2) *E. coli* CFUs at different depths in the supernatant in EC experiments varied by less than 0.2 log.

2.4. Fe-EC Experiments with Alum

To isolate the effects of removal and inactivation on *E.coli* attenuation during the settling period, several experiments were conducted with $Al_2(SO_4)_3$ coagulant (alum), which allowed to

decrease the time needed for settling of EC precipitates and quickly separate cells associated with flocs from free cells in the supernatant. Alum was selected instead of an Fe-based coagulant, because using the latter would have modified the amount of Fe in the system. After dosing-mixing, 0.1 mL of a 370 mM alum solution was added to the suspension, resulting in an Al concentration of 0.19 mM. After rapid mixing (700 rpm, 2 min) and slow mixing (60 rpm, 20 min), large flocs formed that settled in approximately 2 hours, as opposed to 18 hours in regular EC experiments, allowing us to sample the supernatant after 2, 5 and 24 hours for bacteria culturability testing.

2.5. *E. coli* Attenuation by Coagulation with $FeSO_4$, $FeCl_3$ and Pre-Synthesized Ferrihydrite

To constrain the mechanisms of *E. coli* attenuation with Fe-EC and to elucidate the effect of pH, chemical coagulation experiments with Fe salts were conducted as controls. Stock solutions of $FeSO_4$ (100 mM, acidified with 1 mM HCl to avoid premature Fe(II) oxidation), $FeCl_3$ (100 mM) and pre-synthesized ferrihydrite (200 mM) were prepared. The latter was synthesized following Schwertmann and Cornell[101] by dissolving 4g of $Fe(NO_3)_3$ in 50 mL of 18 MΩ deionized water and adding approximately 36 mL of 1 M KOH to neutralize pH to 7. The red precipitates were then harvested by centrifugation, rinsed and resuspended in 50 mL 18 MΩ deionized water. Adequate volumes of the $FeCl_3$, $FeSO_4$, or ferrihydrite stock solutions were added to 200 mL SGW adjusted to pH 6.6 or 7.5 to achieve Fe concentrations of 0.5 mM. Solutions were stirred open to the atmosphere for 100-130 min, then left to settle overnight. Sampling followed the same procedure as in EC experiments.

2.6. *E. coli* Attenuation at Varying Generation Rates of Fe(III) Precipitates

At circumneutral pH, Fe(III) precipitates instantaneously relative to Fe(II) oxidation. Therefore, the rate at which Fe(III) precipitates are generated in Fe-EC, r, is effectively the amount of Fe(II) oxidized per minute (μM-Fe precipitated/min) and can be calculated according to Equation 3-2, where the concentration of Fe(II) as a function of time is the solution of differential Equation 3-3:

$$r = \left|\frac{dFe(II)_{ox}}{dt}\right| = k_{eff} * Fe(II) \qquad \text{(Equation 3-2)}$$

$$\frac{dFe(II)}{dt} = q - k_{eff} * Fe(II) \qquad \text{(Equation 3-3)}$$

with q the Fe dosage rate (μM/min) and k_{eff} (min^{-1}) the effective rate of Fe(II) oxidation in SGW, which depends on pH[63]. We measured k_{eff} (in the presence of *E. coli*) by fitting Equation 3-3 to the concentration of Fe(II) in two different scenarios:

- at pH 7.5, in an Fe-EC experiment (q=45.5 μM/min, t_{dosage}=10.8 min), where the concentration of Fe(II) can be expressed as:

$$Fe(II)\left(t_{mixing}\right) = \frac{q}{k_{eff}}\left(1 - e^{-k_{eff}*t_{dosage}}\right) * e^{-k_{eff}*t_{mixing}} \qquad \text{(Equation 3-4)}$$

with t_{dosage} (min) the EC dosage time and t_{mixing} (min) the post-EC mixing time. We measured k_{eff} = 0.155 min^{-1} (Figure 3-2).

- at pH 6.6, in a chemical coagulation experiment with $FeSO_4$ (Fe_{tot} = 0.5 mM), where the concentration of Fe(II) can be expressed as:

$$Fe(II)(t_{mixing}) = Fe_{tot} * e^{-k_{eff} * t_{mixing}} \quad \text{(Equation 3-5)}$$

with Fe_{tot} the total amount of Fe dosed. We measured k_{eff} = 0.012 min^{-1} (Figure 3-2).

Our measurements (Figure 3-2b) were consistent with studies conducted in carbonated systems, which found that Fe(II) oxidation was approximately 50 times faster for each pH unit increase between pH 6 and 8[63,64].

At pH 7.5, Fe(II) oxidation is rapid ($t_{1/2}$ = 4.5 min in SGW, see Figure 3-2b) and the generation rate of precipitates is mainly controlled by the Fe dosage rate. In order to investigate the impact of the generation rate of Fe(III) precipitates on *E. coli* attenuation, Fe-EC experiments were conducted at pH 7.5 at three different Fe dosage rates (1.1, 2.6 and 46.4 µM/min, corresponding to current densities of 0.33, 0.67 and 10 mA/cm^2 respectively) and three different total dosages (0.1, 0.2 and 0.5 mM), as summarized in Table 3-3. The corresponding precipitate generation rates, calculated according to Equation 3-2, are shown in Figure 3-3. One experiment was carried out with $FeCl_3$ at pH 7.5 where 6 µL of 100 mM $FeCl_3$ were added to the reaction beaker every minute in order to mimic a dosage rate of 3.1 µM/min. A reaction time (dosing-mixing) of 100 min was kept constant across all experiments.

Table 3-3: List of experiments with varying precipitate generation rates: operating conditions and resulting average and maximum precipitate generation rates.

	Dosage rate (µM/min)	**Current (mA)**	**Current density (mA/cm^2)**	**Dosage time (min)**	**Total Fe dosage (mM)**	**pH**	**Precipitate generation rate (µM/min)**	
							Average	***Maximum***
Fe-EC	46.4	30	10	10.8	0.5	7.5	17.6	39.1
	46.4	30	10	4.3	0.2	7.5	9.8	24.0
	46.4	30	10	2.2	0.1	7.5	6.4	15.4
	2.6	2	0.67	80	0.2	7.5	2.4	2.6
	1.1	1	0.33	100	0.1	7.5	1.0	1.1
	46.4	30	10	10.8	0.5	6.6	3.1	6.0
$FeCl_3$	all at once	NA	NA	NA	0.5	7.5	23.5	77.5
	all at one	NA	NA	NA	0.2	7.5	11.2	32.5
	3.1	NA	NA	80	0.2	7.5	2.6	3.1

All *E. coli* attenuation experiments were conducted in triplicate or more. We report average log attenuations ± one standard deviation.

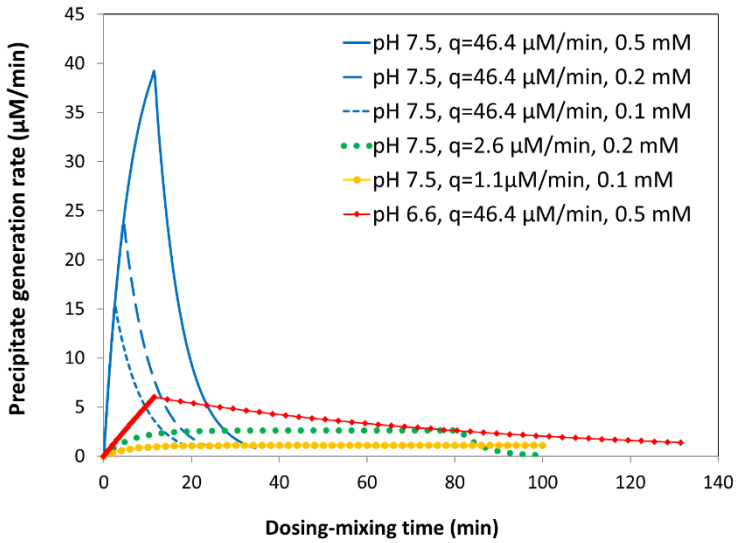

Figure 3-3: Precipitate generation rate as a function of time for Fe-EC experiments with varying dosage rates. Experimental conditions are detailed in Table 3-3. Plots were obtained from solving Equations 3-2 and 3-3.

2.7. Bacterial Viability Tests

Quantifying *E. coli* inactivation by direct plating would require enumerating viable cells in the supernatant as well as in the settled flocs. To recover bacterial cells associated with flocs, standard elution methods use a high pH (9-10, in the presence of beef extract) to dissolve Fe(III) precipitates[81,102]. However, EC precipitates generated in SGW did not dissolve at pH 9-10 over several days, likely due to the adsorption of oxyanions (silicate, phosphate, arsenate), which slows dissolution kinetics[103]. Rapid dissolution of EC precipitates was only observed at pH<3, where the viability and culturability of *E. coli* are compromised[104]. As a result, separating *E. coli* from Fe(III) precipitates was not possible and a different method was used to estimate *E. coli* inactivation during Fe-EC.

We used the BacLight LIVE-DEAD kit (Invitrogen) to assess the degree of membrane permeabilization, a proxy for *E. coli* inactivation. This test relies on two fluorescent nucleic acid stains: green fluorescing SYTO9 enters all cells while red fluorescing PI only enters cells with damaged membranes. As a result, cells with intact membranes ("live") appear green, and cells with damaged membranes ("dead") appear red. Samples were first concentrated 10 times by centrifugation (8200g for 10 minutes). Next, 100 µL of the concentrated samples were reacted with 0.3 µL of 1:2.5 SYTO9-PI solution for one hour in the dark, then analyzed with a Zeiss AxioImager fluorescent microscope (63x Plan-Apochromat objective, EndoGFP and mCherry filters, U.C. Berkeley CNR Biological Imaging Facility). Pictures of Fe(III) precipitates and stained *E. coli* cells were taken in transmission and fluorescent modes respectively, and images were superimposed. At least 10 pictures were taken per sample and visually analyzed to produce representative results.

We applied this procedure to evaluate *E. coli* inactivation during the two treatment stages: dosing-mixing and overnight settling. For the former, samples were collected from the mixed suspension at the end of dosing-mixing in EC experiments (at pH 6.6 and 7.5). For the latter, sampling the supernatant after settling did not allow for quantitative fluorescent microscopy analysis because *E. coli* concentrations were too low. We therefore mimicked supernatant conditions at pH 6.6 with 200 mL solutions of SGW amended with 0.18 mM $FeSO_4$ and spiked with $10^{7.5}$ CFU/mL *E. coli.*

2.8. Bacteria and Precipitates Characterization

Transmission electron microscopy (TEM) was carried out on the precipitate-microorganism aggregates with a FEI Tecnai 12 Transmission Electron Microscope operated at 120 kV (UC Berkeley Electron Microscope Lab). TEM samples were prepared by depositing 5 µL of post dosing-mixing suspensions onto copper grids coated with a carbon film, and were allowed to settle for 2 minutes before the liquid was wicked off with filter paper.

ζ -potential measurements were conducted at different pHs for (1) Fe(III) precipitates generated by Fe-EC in SGW with and without NOM (Fe dosage = 0.5 mM) and (2) *E. coli* suspended in SGW ($10^{6.5}$ CFU/mL). To prepare samples, the suspension pH was adjusted with 1.1 M HCl to different values between 1.9 and 8.1 (resulting in ionic strength increases from 20.4 to 39.3 mM). Suspensions of Fe(III) precipitates were sonicated for 10 min in order to disaggregate flocs. Samples were then loaded into Malvern DTS1061 capillary cells to minimize settling during measurements. Electrophoretic mobility was measured in triplicate by dynamic light scattering with a Malvern Zetasizer Nano-ZS at 633 nm, and converted to ζ-potential using the Smoluchowski approximation. Each measurement gave a distribution of ζ-potentials characterized by its mean and standard deviation. For each set of triplicate measurements, we report the averaged means and the error calculated as the largest of: (1) the 3 individual standard deviations, or (2) the standard deviation of the 3 means.

3. RESULTS AND DISCUSSION

3.1. Concurrent arsenic and *E. coli* Attenuation

Figure 3-4 shows concurrent arsenic and *E. coli* attenuation in SGW at pH 7.5. For Fe dosages of 0.5, 1.5 and 2.5 mM, Fe-EC achieved log attenuations of 1.9, 3.7 and 4.4 respectively. Arsenic was reduced from 450 µg/L to 116 µg/L at 0.5 mM Fe, and to below the WHO recommended maximum contaminant level (MCL) of 10 µg/L[45] at Fe dosages > 1.5 mM. Similar arsenic removal in SGW with and without *E. coli* (Table 3-2) suggests that Fe-EC can attenuate bacteria without detriment to arsenic remediation. At Fe dosages of more than 2 mM, which are typical of current field operation[47], Fe-EC achieved over 4-log attenuation of *E. coli* and thus met the WHO guideline for household drinking water treatment requiring 4-log bacteria reduction[105]. Because WHO drinking water guidelines characterize waters as low risk if *E. coli* < 1 CFU/100

mL[45], this level of treatment is likely sufficient to eliminate the need for an additional disinfection step for most groundwaters.

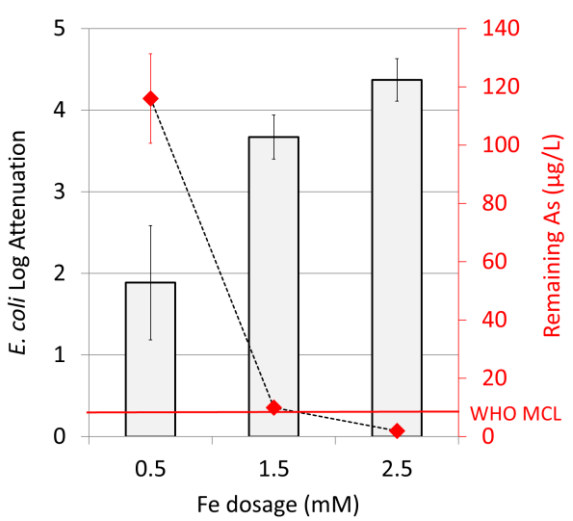

Figure 3-4: Concurrent arsenic and *E. coli* attenuation by Fe-EC in SGW at pH 7.5 for Fe dosages of 0.5, 1.5 and 2.5 mM. The initial arsenic concentration was 450 µg/L as As(III). The columns represent *E. coli* log attenuation, whereas the diamonds indicate dissolved arsenic concentrations (measured by ICP-OES with hydride generation). The solid red line indicates WHO recommended maximum contaminant level (MCL) for arsenic, 10 µg/L.

3.2. Surface Charge Characterization of EC Precipitates and *E. coli*

Figure 3-5 shows the ζ-potentials of EC precipitates and *E. coli* in SGW between pH 1.5 and 8.5. The isoelectric point (IEP) of *E. coli* was found to be between 2 and 3, which is consistent with reported IEP of gram-negative bacteria[106]. Above pH 5, the ζ-potential of *E. coli* cells was less negative than that observed previously in a KCl electrolyte[107], which could be due to Ca^{2+} and

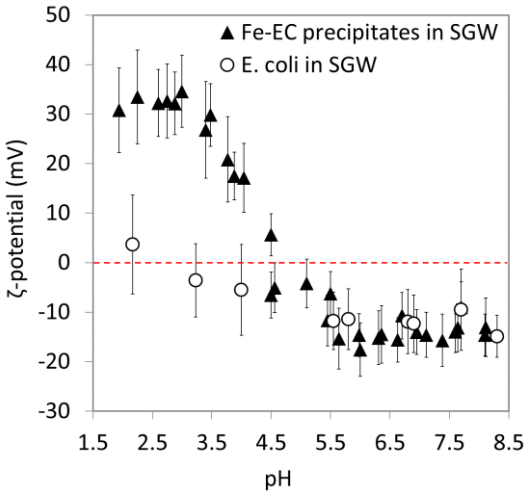

Figure 3-5: ζ-potential of Fe-EC precipitates (0.5 mM Fe) and *E. coli* in SGW measured by dynamic light scattering (633 nm).

Mg^{2+} complexation by negatively charged residues on the cell surface[108]. Past studies have shown that Fe-EC in SGW leads to the formation of short-range ordered hydrous ferric oxide[48,66]. We found the IEP of EC precipitates to be between 4 and 5, which is lower than IEP values typically reported for poorly ordered Fe(III) precipitates (between 6 and 9)[109,110]. This difference can be attributed to the adsorption of silicate and negatively charged phosphate (Si:Fe and P:Fe of 0.028±0.08 and 0.24±0.02 mol:mol, across 7 experiments), which are known to decrease the IEP of ferrihydrite upon adsorption[110,111]. Our ζ-potential measurements indicate that EC precipitates and *E. coli* are both negatively charged at circumneutral pH in SGW, and that their surface charge does not significantly vary between pH 5.5 and 8.5.

3.3. Effect of pH on *E. coli* Attenuation

In Figure 3-6, *E. coli* attenuation at pH 6.6 and 7.5 is compared for 4 different scenarios (Fe-EC, chemical coagulation with ferrous and ferric salts, and coagulation with pre-synthesized ferrihydrite) at an Fe dosage of 0.5 mM. These 4 scenarios have been shown to generate the same type of precipitates[48,58,60,112] and only differ by the form and rate with which Fe is released into SGW: as Fe(II) for Fe-EC and $FeSO_4$ (released progressively and in a single dose respectively), as dissolved Fe(III) for $FeCl_3$, and as colloidal Fe(III) for pre-synthesized ferrihydrite (both released in a single dose). With Fe-EC, *E. coli* attenuation was significantly higher at lower pH: 4.0 log removal at pH 6.6 compared to 1.9 at pH 7.5. A similar trend was observed for $FeSO_4$ (4.3 log at pH 6.6 and 2.0 log at pH 7.5). Conversely, pH had no significant effect on *E. coli* attenuation with $FeCl_3$ and with pre-synthesized ferrihydrite, indicating that possible changes in colloid surface charge or SGW chemistry between pH 6.6 and 7.5 have no impact on bacteria-precipitate surface interactions. Consequently, the increased *E. coli* reduction with Fe-EC and $FeSO_4$ at pH 6.6 cannot be attributed to a difference in colloid surface charge, which is supported by our ζ-potential measurements showing that both EC precipitates and *E. coli* cells have nearly identical net surface charge at pH 6.6 and 7.5 (ζ-potential ~ -12.0 mV and -13.4 mV respectively, Figure 3-5).

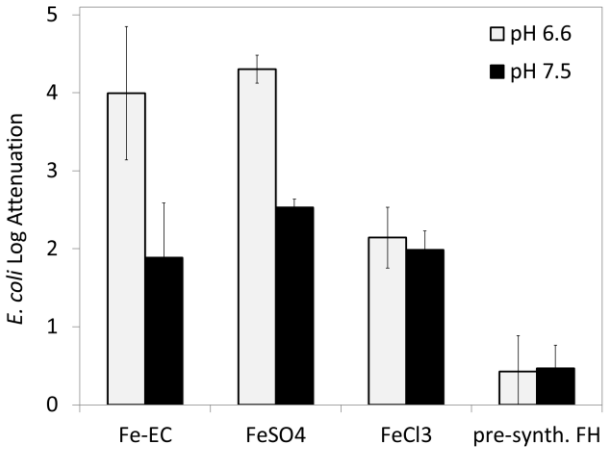

Figure 3-6: Effect of pH on *E. coli* attenuation by Fe-EC and chemical coagulation with $FeSO_4$ salt, $FeCl_3$ salt and pre-synthesized ferrihydrite (FH). The Fe dosage for all experiments was 0.5 mM.

E. coli attenuation with $FeSO_4$ exhibited the same pH dependence as Fe-EC, suggesting that increased attenuation at lower pH is related to the transient presence of Fe(II). The rate of Fe(II) oxidation in SGW at pH 6.6 (k_{eff} = 0.012 min^{-1}, Figure 3-2) is significantly slower than at pH 7.5 (k_{eff} = 0.155 min^{-1}, Figure 3-2), which leads to: (1) a slower generation rate of Fe(III) precipitates, and (2) a longer lifetime of bactericidal Fe(II). In the two following sections, we investigate the impacts of these two factors on *E. coli* attenuation by Fe-EC.

3.4. Effect of the Generation Rate of Fe(III) Precipitates on *E. coli* Attenuation

The generation rate of Fe(III) precipitates controls the rate at which they aggregate into flocs, and may thus affect bacteria-precipitate interactions. To probe the impact of the precipitate generation rate on *E. coli* attenuation, the Fe dosage rate *q*, which controls the flux of Fe(II) delivered by the anode, was decreased from 46.4 to 2.6 and 1.1 µM/min at pH 7.5. As calculated with Equation 3-2, *q* = 2.6 µM/min at pH 7.5 leads to a precipitate generation rate comparable to that of experiments at pH 6.6 with *q* = 46.4 µM/min (see Figure 3-3). Figure 3-7 shows that lower dosage rates, resulting in lower precipitate generation rates, did not significantly improve *E. coli* attenuation by Fe-EC at pH 7.5. Similarly, no significant difference in *E. coli* attenuation was observed between single dose versus low dosage rate for chemical coagulation with $FeCl_3$ at pH 7.5. We concluded that the lower precipitate generation rate at pH 6.6 cannot account for increased *E. coli* attenuation compared to pH 7.5.

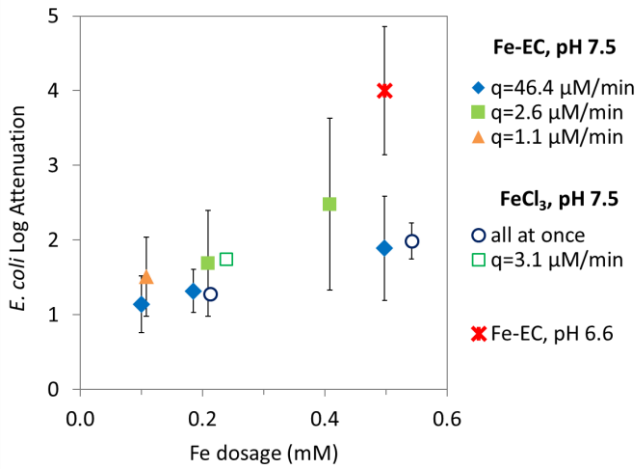

Figure 3-7: Effect of dosage rate (or precipitate generation rate) on *E. coli* attenuation at pH 7.5 by Fe-EC and chemical coagulation with $FeCl_3$. *E. coli* attenuation by Fe-EC at pH 6.6 is shown with a red cross.

3.5. Evolution of *E. coli* Attenuation during Settling in Experiments with Alum

The use of alum in EC experiments significantly accelerated settling of Fe(III) precipitates and allowed us to quickly separate *E. coli* cells associated with precipitates from free cells in the supernatant. As a result, this experimental design enabled us to track the viability of suspended *E. coli* cells in the supernatant during the 24-hour settling period. We found that the difference in *E.*

coli attenuation between pH 6.6 and pH 7.5 increased over the 24-hour settling period (Figure 3-8). After 2-hour settling, *E. coli* attenuation was only slightly higher at pH 6.6 compared to pH 7.5 (2.5 and 1.8 log respectively). The discrepancy significantly increased over time and was comparable to that of regular EC experiments after 24-hour settling (5.0 and 2.5 log attenuation at pH 6.6 and 7.5 with alum, compared to 4.0 and 1.9 log attenuation at pH 6.6 and 7.5 in regular EC experiments). In contrast to experiments at pH 7.5, those at pH 6.6 contained a significant concentration of unoxidized Fe(II) at the beginning of settling (0.10 ± 0.04 mM, corresponding to 19% ± 6% of the total Fe dosed, across 9 experiments), most of which oxidized during the 24-hour settling period. Consequently, our results indicate that the longer lifetime of Fe(II) at pH 6.6 leads to additional *E. coli* attenuation in the supernatant during settling. Figure 3-8 shows a correlation at pH 6.6 between the increase of *E. coli* attenuation during overnight settling and the amount of Fe(II) oxidized in the supernatant. This correlation could point to the bactericidal action of Fe(II) on *E. coli* in the supernatant. To further investigate this possibility, we conducted live-dead staining of the bacteria.

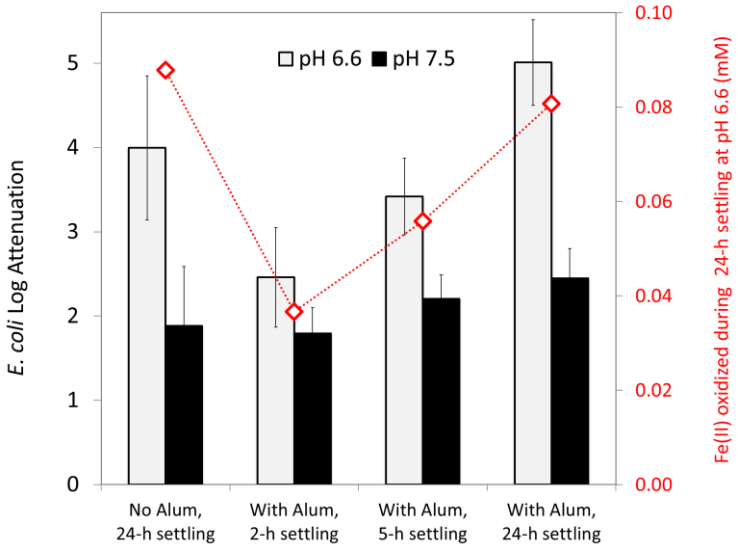

Figure 3-8: *E. coli* attenuation by Fe-EC as a function of settling time in experiments with alum, at pH 6.6 and 7.5 (bars). Diamonds indicate the amount of Fe(II) oxidized during the 24-hour settling period at pH 6.6. For comparison, results for regular Fe-EC experiments (without alum) are given on the left. The Fe dosage for all experiments was 0.5 mM.

3.6. *E. coli* Inactivation

Bacterial viability tests conducted immediately after dosing-mixing showed that *E. coli* inactivation during dosing-mixing was limited, both at pH 6.6 and 7.5, with less than 20% of the cells appearing red on fluorescent microscopy images (representative examples shown in Figure 3-9). Bacterial viability tests on the supernatant after overnight settling at pH 6.6 showed a majority of red cells (see Figure 3-10a-b), suggesting *E. coli* inactivation during the settling period at pH 6.6. However, *E. coli* concentrations in the supernatant were too low for quantitative fluorescent

microscopy analysis. Therefore, we conducted separate experiments to mimic supernatant conditions at pH 6.6 with higher *E. coli* concentrations. This was achieved by adding $10^{7.5}$ CFU/mL and 0.18 mM $FeSO_4$ to SGW. In images taken after 18 h, approximately 50% of the cells appeared red (Figure 3-10c), suggesting that reactive species produced from Fe(II) oxidation in the supernatant at pH 6.6 caused significant membrane damage (confirmed by culturability measurements indicating a 0.8 log reduction in CFUs). The identity of the reactive oxidant causing inactivation (Fe(IV) or OH•) could not be determined, but the inability of 5 mM formate or methanol to hinder *E. coli* attenuation at pH 6.6 (Figure 3-11) rules out OH• [113].

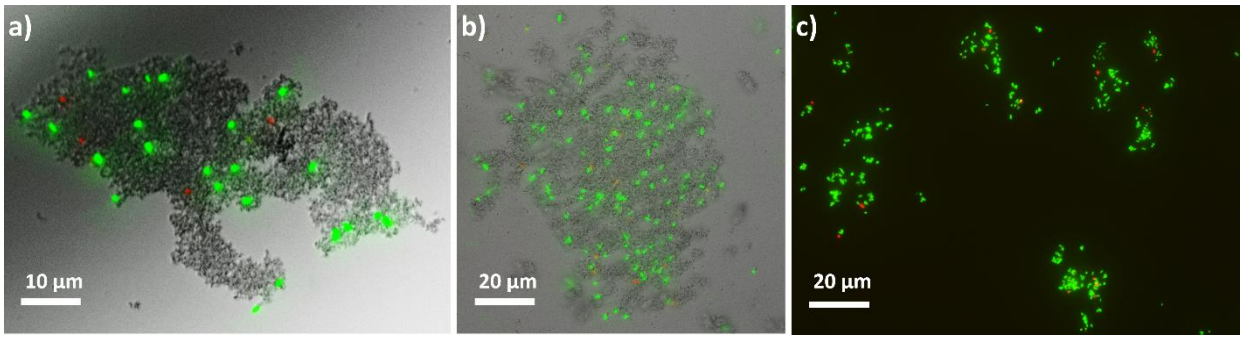

Figure 3-10: Fluorescent microscopy images of live-dead stained *E. coli* cells (green=live, red=dead) immediately after dosing-mixing. On a) and b), EC precipitate flocs are visible in grey, surrounding *E. coli* cells. a) *E. coli* counts: $10^{6.3}$ CFU/mL, pH 7.5, Fe dosage=1.5 mM. b) *E. coli* counts: $10^{6.5}$ CFU/mL, pH 6.6, Fe dosage=0.5 mM. c) *E. coli* counts: $10^{7.2}$ CFU/mL, pH 6.6, Fe dosage=0.5 mM.

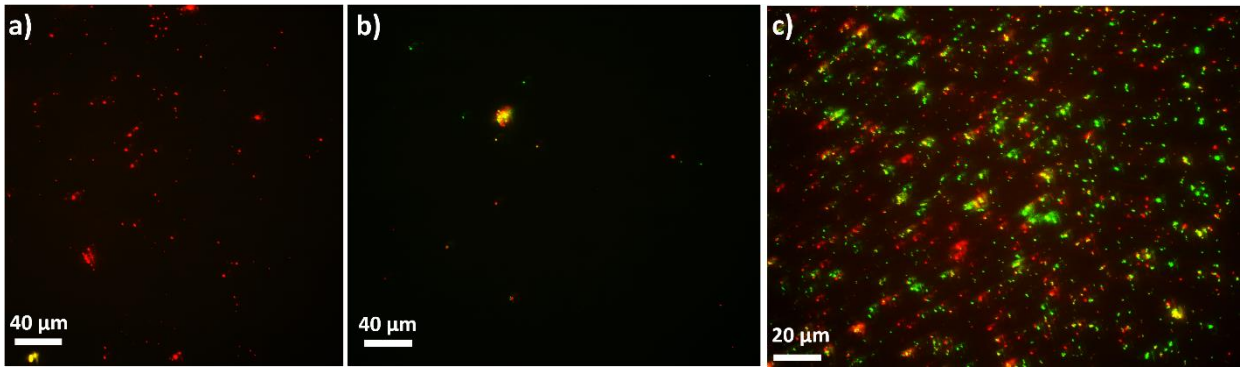

Figure 3-9: Fluorescent microscopy images of live-dead stained *E. coli* cells (green= live, red=dead) from the supernatant after overnight settling at pH 6.6, in Fe-EC experiments with 0.5 mM Fe (panels a and b, $10^{7.3}$CFU/mL *E. coli*) and in mock-supernatant experiments with 0.18 mM $FeSO_4$ (panel c, $10^{7.6}$ CFU/mL *E. coli*).

3.7. Mechanism of *E. coli* Attenuation by Fe-EC

Similar *E. coli* reduction with Fe-EC and $FeSO_4$ (both at pH 6.6 and 7.5, Figure 3-6) indicates that the temporary electric field during electrolysis as well as potential electrochemically-generated chlorine species[86] do not contribute to bacteria attenuation with Fe-EC in SGW.

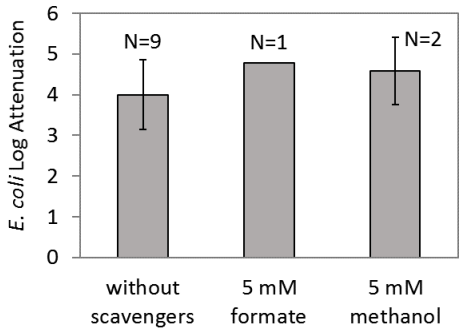

Figure 3-11: *E. coli* attenuation with Fe-EC in SGW at pH 6.6 with and without strong oxidant scavengers. Fe dosage was 0.5 mM. The number of replicates is indicated above each bar.

Consequently, the possible mechanisms of *E. coli* attenuation are (1) physical removal with EC precipitates and (2) inactivation by strong oxidants generated during Fe(II) oxidation.

At pH 7.5, all Fe(II) is oxidized by the end of dosing-mixing. Consequently, minimal inactivation at the end of dosing-mixing (<0.1 log as determined on fluorescent microscopy images, Figure 3-9a) implies that inactivation is overall insignificant and that *E. coli* attenuation is primarily due to physical removal with flocs by gravitational settling. As shown on Figure 3-6, *E. coli* reduction at pH 7.5 with Fe-EC is not significantly different from the attenuation achieved with $FeCl_3$ (pH 6.6 or 7.5). The latter only removes *E. coli* via encapsulation in flocs, since inactivation by germicidal Fe(II) can be ruled out in the case of a ferric salt. Consequently, similar *E. coli* reduction with Fe-EC at pH 7.5 and with $FeCl_3$ further supports that removal with flocs is the primary mechanism of *E. coli* attenuation by Fe-EC at pH 7.5.

By contrast, our results suggest that both removal and inactivation contribute to *E. coli* reduction at pH 6.6. Inactivation after dosing-mixing at pH 6.6 was insignificant (<0.1 log as determined from fluorescent microscopy images, Figure 3-9b-c), suggesting that the attenuation observed at the earliest stage of settling (2.5 log after 2h, Figure 3-8) is mostly due to removal with flocs. The additional ~2 log attenuation occurring in the supernatant during overnight settling is likely attributable to inactivation, supported by the increase in dead cells in the supernatant (Figure 3-10a-b) and mock supernatant (Figure 3-10c). Note that the live-dead stain is likely a conservative measure of inactivation, as loss of viability may occur well before membranes become permeable to PI[114]. In addition, the higher bacteria concentration in the mock supernatant compared to regular supernatant conditions could have lowered the steady-state concentration of reactive oxidants through scavenging, explaining the limited inactivation (0.8-log loss of culturability) in the mock supernatant.

We established that the largest fraction of *E. coli* cells (1.9 log at pH 7.5, ~2 log at pH 6.6, Figures 6 and 8) is physically removed with flocs. Figures 9a-b illustrate the association of *E. coli* cells with large Fe(III) flocs. TEM images provide further insight, illustrating the intimate spatial arrangement between EC precipitates and bacteria surfaces (Figures 3-12a-b). Precipitates bridging individual cells (Figure 3-12a) lead to large precipitate-bacteria networks that can be readily removed by gravitational settling (Figure 3-12c). Although our ζ-potential measurements indicate that EC precipitates and *E. coli* are both negatively charged at circumneutral pH in SGW

(Figure 3-5), adhesion of EC precipitates to *E. coli* may be enabled by a combination of 1) charge heterogeneities on cell surfaces, 2) hydrophobic interactions, and 3) hydrogen or covalent bonds. Due to their small size relative to *E. coli* cells (apparent in Figures 12a-b), EC precipitates may be sensitive to heterogeneities in *E. coli* surface composition, allowing localized adhesion. For example, surface proteins carrying positively charged amine groups could constitute preferential adhesion sites. In addition, phosphate and carboxyl residues, which can form covalent bonds with iron oxides[115], may provide chemical bonding sites for EC precipitates. Significantly lower *E. coli* removal with pre-synthesized ferrihydrite (0.5-log at pH 7.5, Figure 3-6) compared to Fe-EC, $FeSO_4$ and $FeCl_3$ (~2-log at pH 7.5, Figure 3-6) shows that precipitates are less effective when they are produced and aggregated into flocs before coming into contact with *E. coli* cells. This result supports that bacteria-precipitate interactions are facilitated when precipitates are small relative to *E. coli* cells.

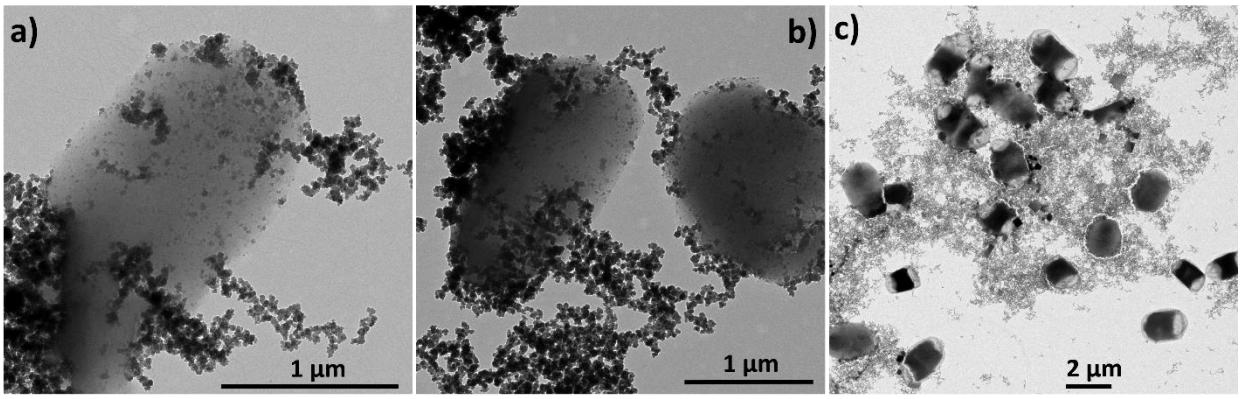

Figure 3-12: Transmission electron microscopy images illustrating the intimate association of EC precipitates and bacteria surfaces: a) EC precipitates adhering to the surface of an *E. coli* cell, b) EC precipitates bridging two *E. coli* cells, c) resulting bacteria-precipitate aggregate with *E. coli* cells trapped in the Fe floc. *E. coli* count: ~$10^{7.0}$ CFU/mL, Fe dosage=0.5 mM.

3.8. Effect of NOM on *E. coli* Attenuation

3 mg-C/L of Suwanee River Fulvic Acid had a minimal impact on *E. coli* attenuation both at pH 6.6 (0.5 mM Fe) and 7.5 (1.5 mM Fe), as illustrated on Figure 3-13a. The ζ-potential of EC precipitates, shown in Figure 3-13b, was not affected by NOM between pH 5.5 and 8.5. ICP-OES analysis of filtered samples after dosing-mixing indicated that Ca^{2+}/Mg^{2+} uptake did not increase in the presence of NOM, ruling out bivalent cation bridging of EC precipitates and NOM. Taken together, these results suggest that NOM did not significantly interact with EC precipitates, and therefore did not interfere with the adhesion of EC precipitates to *E. coli* cells.

These results are unexpected given the accounts of NOM adsorbing to ferric (oxyhydr)oxides[90,116,117] and inhibiting MS2 attenuation by Fe-EC in a $CaCl_2$ electrolyte[81], but may be explained by the composition of SGW. NOM may not effectively compete with silicate and phosphate for surface sites on EC precipitates: decreased NOM adsorption on Fe oxides in the

presence of silicate and phosphate has been observed elsewhere[118,119]. In addition, EC precipitates have a net negative charge in SGW, and electrostatic repulsion may inhibit interactions with NOM. Conversely, EC precipitates formed in $CaCl_2$ are expected to be positively charged at circumneutral pH and more prone to interact with NOM, likely explaining the results of Tanneru and Chellam[81]. In their paper, they also proposed that quenching of OH• and Fe(IV) by NOM may inhibit inactivation of MS2[81]. In our system, 3 mg-C/L of NOM did not have a significant effect on overall attenuation at pH 6.6, possibly because NOM concentrations were lower (C:Fe mass ratios of 0.03-0.1 in our experiments, compared to 0.5 in Tanneru and Chellam[81]). It is possible that higher NOM concentrations would cause a larger decrease in *E. coli* attenuation at pH 6.6 due to greater quenching of reactive oxidants. Finally, we note that 3 mg-C/L of Suwanee River Fulvic Acid did not significantly affect arsenic removal by Fe-EC in SGW (Figure 3-13a).

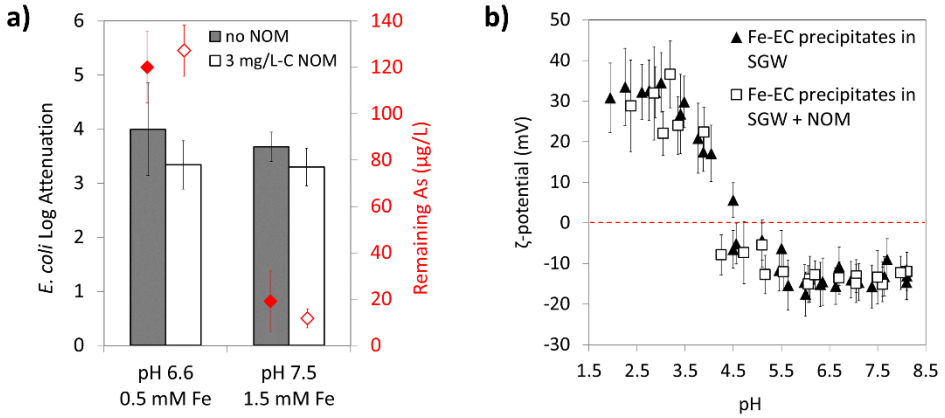

Figure 3-13: (a) Effect of NOM on *E. coli* attenuation and arsenic removal by Fe-EC in SGW at pH 6.6 and 7.5. The initial arsenic concentration was 440 µg/L as As(III). The columns represent *E. coli* log attenuation, whereas the diamonds indicate dissolved arsenic concentrations (measured by ICP-OES without hydride generation). (b) ζ-potential of EC precipitates generated in SGW with and without 3 mg-C/L NOM.

3.9. Implications for Water Treatment

In this work, we show that Fe-EC can adequately reduce bacterial contamination from synthetic Bengal groundwater without detriment to arsenic removal, even in the presence of 3 mg-C/L NOM. Groundwater remediation with Fe-EC in arsenic-affected areas may therefore not need to be followed by chlorination or UV disinfection. More research on virus attenuation by Fe-EC is needed to reinforce this claim. Additionally, Bengal groundwater treatment with Fe-EC does not present a risk of disinfection byproducts formation since no chlorine is electrochemically produced. Although possible rust build-up on electrodes in the long-term field operation of Fe-EC might change the bacteria attenuation efficiency and the power consumption, the relative roles of removal and inactivation identified in this laboratory study should not change as long as chlorine is not electrochemically produced. Because bacterial inactivation during dosing-mixing is very limited, settled flocs may contain viable pathogens, presenting a risk if sludge is not handled properly. Consequently, adequate sludge treatment such as high-temperature drying (70 C for 30 min[120]) should be applied to ensure sludge sterilization. Finally, we found that at lower pH, Fe(II)

addition was more efficient than equivalent amounts of Fe(III) because the prolonged lifetime of Fe(II) at lower pH led to increased attenuation. This result suggests that the use of ferrous salts (as opposed to ferric salts) in primary water and wastewater treatment might improve microbe reduction when the pH of the influent is mildly acidic. More generally, our results suggest that conditions promoting Fe(II) build-up in the Fe-EC process, such as a low pH, a short post-EC mixing time, or a high dosage rate causing O_2 depletion, may lead to increased bacteria reduction.

CHAPTER 4. Bacteria attenuation by Fe-EC governed by interactions between bacterial phosphate groups and Fe(III) precipitates

1. INTRODUCTION

In Chapter 3, we demonstrated that Fe-EC can attenuate the model fecal bacterium *Escherichia coli* (*E. coli*) from synthetic Bengal groundwater (SGW) without detriment to arsenic removal[121], confirming that Fe-EC has promising applications for low-cost groundwater remediation[47]. Fe-EC can also attenuate microbial contamination in surface water[84] and industrial wastewater[122], and may therefore have useful applications beyond groundwater treatment. In Chapter 3, we showed that two processes contribute to bacteria attenuation in Fe-EC: (1) physical removal, caused by bacteria enmeshment in Fe(III) flocs and subsequent settling, and (2) inactivation by reactive species produced upon Fe(II) oxidation by O_2. Fundamental aspects of the mechanisms underlying these two processes remain unknown. For example, the type of chemical interactions governing bacteria enmeshment in flocs is not well understood. In addition, the effect of major groundwater components, such as HCO_3^-, Ca, Mg, Si, and P, which can interfere with both inactivation and removal, has not been investigated. Finally, the impact of bacteria surface structure (Gram-positive versus Gram-negative, smooth versus rough Gram-negative) on attenuation has not been studied. Such detailed knowledge would considerably improve our predictions of Fe-EC performance in various water matrices containing different types of bacterial contamination.

Based on Chapter 3, bacteria inactivation in Fe-EC can likely be attributed to reactive intermediates such as $O_2^{\bullet-}$, H_2O_2, and Fe(IV), which are generated in Fenton-type reactions[52,123] and have been associated with bactericidal effects[113,124–127]. Because HCO_3^- can react with these intermediates, this ubiquitous ion might affect the nature and reactivity of the strong oxidants generated during Fe-EC, and thus the level of bacteria inactivation.

The results of Chapter 3 also suggest that the adhesion of EC precipitates to cell walls, which is apparent on TEM images (Figure 3-12), is a key process in bacteria enmeshment in flocs. Specifically, much higher bacteria removal by Fe-EC than by coagulation with pre-synthesized ferryhydrite (for the same Fe(III) concentration, Figure 3-6) indicates that removal cannot be solely attributed to the mechanical sweeping of bacterial cells by Fe(III) flocs (sweep flocculation). In addition, increased removal at higher Fe dosages (Figure 3-4) indicates a stoichiometric relationship between Fe(III) precipitates and bacterial surfaces, consistent with the primary role of precipitate adhesion to cell walls. However, important questions remain regarding bacterial functional groups involved in such adhesion, the type of interaction (electrostatic versus specific bonding), and the effects of groundwater chemistry and cell wall structure.

Four types of surface functional groups, present at comparable densities on bacterial cell walls[128], may mediate the adhesion of EC precipitates: hydroxyl (pK_a =8.9-9.7), amine (pK_a =8.9-

9.7), carboxyl (pK_a =4.3-5), and phosphate groups (pK_{a1} =3.1-3.2, pK_{a2} =6.5-6.9)[128–133]. At circumneutral pH, hydroxyl moieties are protonated (uncharged) and are not expected to strongly interact with iron oxides[134]. Although amine moieties do not have a strong affinity for iron oxides[135,136], these groups are positively-charged at circumneutral pH. Therefore, amine groups may be involved in electrostatic interactions with EC precipitates, which can have a net negative charge depending on electrolyte composition. In contrast to hydroxyl and amine groups, carboxyl and phosphate moieties have strong affinities for Fe(III) (oxyhydr)oxides[57,137–141]. Studies using Attenuated Total Reflectance Fourier-Transform Infrared spectroscopy (ATR-FTIR) in controlled laboratory systems and simple water matrices have shown direct bonding between Fe(III) oxide surfaces and bacterial phosphate and carboxyl groups[115,136,142]. However, it is unclear whether such strong specific interactions take place in Fe-EC, where precipitates and bacteria interact in an agitated suspension and in more complex electrolytes. For example, bivalent cations (Ca and Mg) can be complexed by bacterial phosphate and carboxyl groups[108,130,133,143,144], which might inhibit interactions with EC precipitates. In addition, strongly adsorbing oxyanions, such as Si and P[49,111,137], can decrease the availability of bonding sites on the surface of EC precipitates, and thus decrease bacteria removal. Examining the individual and interdependent effects of Ca, Mg, Si and P on bacteria attenuation is not only essential to predict the performance of Fe-EC in real groundwater, but can also help us constrain the bacterial functional groups involved in the adhesion of EC precipitates.

In addition to the electrolyte composition, a number of previous studies have shown that the structure of bacterial cell walls can affect bacteria interactions with mineral surfaces[77,107,145–147]. Different biomolecules on the surface of Gram-negative and Gram-positive bacteria, as well as different surface roughness between smooth (with O-antigen) and rough (without O-antigen) Gram-negative strains, may affect cell attachment through variations in surface charge, hydrophobicity and steric hindrance[77,107,145–147]. Because waterborne pathogenic bacteria and indicator organisms span the range of Gram-positive, smooth and rough Gram-negative strains[45], understanding the impact of cell wall structure on bacteria attenuation with Fe-EC is essential to generalize our findings to all bacterial species relevant to water quality.

Spectroscopic techniques such as ATR-FTIR, X-ray fluorescence (XRF) and X-ray absorption spectroscopy (XAS) have been used to study bacteria-Fe systems[115,136,142,148–150]. However, these techniques are not adapted to determine bacteria-Fe(III) interactions in systems where Fe(III) is co-precipitated with bacteria in complex electrolytes approaching the composition of groundwater. For example, distinguishing between P-Fe bonds from bacteria-precipitate interactions and P-Fe bonds from sorption of aqueous P to Fe(III) precipitates is largely impossible with P K-edge XAS and ATR-FTIR. Additionally, ATR-FTIR is not suited to investigate interactions taking place inside large flocs due to the low penetration length of infrared beams in aqueous medium (~1µm). To circumvent these limitations, the present study proposes an innovative approach, where macroscopic data -bacteria attenuation in systematically varied electrolytes- is combined with ζ-potential measurements to elucidate the molecular interactions between bacteria and EC precipitates. Although this approach can only provide indirect evidence for specific interactions between bacteria surfaces and precipitates, it builds upon previous spectroscopic studies, which identified bacteria-Fe oxide bonding processes in simple controlled

systems[115,136,142] and structures of Fe-EC precipitates in complex water matrices[50,57], to gain information about bacteria removal mechanisms in groundwater-like electrolytes.

The goals of this chapter are to: (1) determine the impact of HCO_3^-, Ca, Mg, P and Si on bacteria attenuation with Fe-EC, (2) identify the bacterial functional groups involved in the adhesion of EC precipitates to cell walls and investigate the type of interaction (electrostatic versus specific), and (3) test the generalizability of these conclusions to various bacteria types. To achieve these objectives, we first compared Fe-EC with $FeCl_3$ coagulation to distinguish the contributions of inactivation and enmeshment in flocs to overall bacteria attenuation in Fe-EC as a function of the HCO_3^- concentration. Inactivation results were confirmed using live-dead staining. Second, we systematically investigated the effect of ionic strength, Ca/Mg and P/Si on *E. coli* attenuation, both in single and multiple solute electrolytes, to identify the bacterial surface groups involved in precipitate adhesion to cell walls. ζ-potential, a proxy for surface charge, was used to assess the interaction of major groundwater ions with the surface of EC precipitates or *E. coli* cells. Third, we validated our proposed mechanism with 3 bacteria strains bearing different surface structures (smooth and rough Gram-negative, and Gram-positive). Our results strongly suggest that Fe-EC can be used to remove various types of bacteria from a wide range of water matrices representative of regions affected by arsenic and microbial contamination of drinking water sources. More generally, this study can help predict the performance of Fe-EC, and other Fe-based coagulation processes, to reduce bacterial contaminants from drinking water and wastewater.

2. METHODS

2.1. Bacteria Preparation and Enumeration

Two Gram-negative and one Gram-positive bacterial strains was used: *Escherichia coli* K12 (NCM 4236, kanamycin-resistant), *Escherichia coli* ECOR 10 (from STEC center[151], ampicillin-resistant[152]) and *Enterococcus faecalis* (ATCC 19433, no antibiotic resistance). K12 is a rough strain (no O-antigen)[153] whereas ECOR 10 is a smooth strain (O-antigen present, serotype O6)[151]. After three propagations in growth media amended with appropriate antibiotics, stationary-phase bacteria were rinsed 3 times and resuspended in 100 mM NaCl following the same procedure as in Chapter 3. Growth media were bacto tryptic soy broth for the two *E. coli* strains, and beef heart infusion broth for *E. faecalis*. Antibiotics were kanamycin (25 mg/L) for *E. coli* K12 and ampicillin (15 mg/L) for *E. coli* ECOR 10 (no antibiotics for *E. faecalis*). We did not harvest bacteria in a phosphate buffer to avoid subsequent phosphate contamination of Fe-EC electrolytes. Bacteria were spiked in Fe-EC electrolytes to achieve initial concentrations of $10^{6.1\text{-}6.7}$ CFU/mL ($10^{5.0\text{-}5.8}$ CFU/mL for *E. faecalis*). Bacteria concentrations were enumerated in duplicate in 0.1 mL aliquots as colony forming units (CFU) using the spread plate technique on agar (modified Luria Bertani for the two *E. coli* strains and m-Enterococcus for *E. faecalis*) amended with appropriate antibiotics (detection limit of 10 CFU/mL).

2.2. Electrolytes

The list of electrolytes used in bacteria attenuation experiments is specified in Table 4-1. In summary, we first varied the concentration of HCO_3^- (0.1-8.0 mM) to examine its impact on bacteria inactivation. Second, a range of ionic strengths was investigated by varying NaCl (in deionized water and in SGW) or $NaClO_4$ (in 1 mM $CaCl_2$). Then, concentrations of bivalent cations (Ca: 0-13.5 mM and Mg: 0-10.6 mM) and oxyanions (P: 0-0.4 mM and Si: 0-0.4 mM) were systematically varied, in single and composite electrolytes, to elucidate their effect on bacteria removal. Finally, synthetic Bengal groundwater (SGW), containing 8.2 mM HCO_3^-, 2.7 mM Ca, 2.0 mM Mg, 1.3 mM Si, 0.15 mM P, and 6.3 µM As(III), was prepared as described in Chapter 3 and used as the electrolyte in some experiments. All experiments were conducted at pH 7.0 ± 0.3, except for the comparisons between the three bacterial strains, which were conducted at pH 7.5 ± 0.2. The pH was held constant throughout experiments by adding HCl, NaOH or $NaHCO_3$ as needed. Electrolytes were selected in part to overlap with previous work on the structure of EC precipitates[48,50,57], which we leverage in our interpretations of bacteria attenuation and ζ-potential measurements.

Table 4-1: List of experiments conducted for this chapter, with detailed electrolytes, bacteria, pH and experimental conditions. Concentrations are given in mM.

Bacteria	**HCO_3^-**	**Si**	**P**	**Ca**	**Mg**	**NaCl**	**$NaClO_4$**	**pH**	**Alum**
E. coli K12	0.1-8.0	0	0	0	0	0-2	0	7.0	no
E. coli K12	0.1	0	0	0	0	2-200	0	7.0	no
E. coli K12	0.1	0	0	1	0	0	0-300	7.0	no
E. coli K12	0.1	0	0	0-12.9	0	0-2	0	7.0	no
E. coli K12	0.1	0	0	0	0-10.6	0-2	0	7.0	no
E. coli K12	0.1	0-0.4	0	0	0	2	0	7.0	yes
E. coli K12	0.1	0	0-0.4	0	0	2	0	7.0	yes
E. coli K12	8.0	1.2	0-0.4	2.3-9.1	0	0	0	7.0	no
E. coli K12	8.0	1.2	0-0.4	0	4.7-8.0	0	0	7.0	no
E. coli K12	8.0	1.2	0.4	1.1-13.5	0	0	0	7.0	no
E. coli K12	8.0	1.2	0.4	0	2.4-10.5	0	0	7.0	no
E. coli K12	8.0	1.2	0.4	0-13.4	4.7	0	0	7.0	no
E. coli K12	8.2	1.3	0.2	2.5	1.8	0-220	0	7.5	no
E. coli ECOR 10	8.2	1.3	0.2	2.5	1.8	0	0	7.5	no
E. faecalis	8.2	1.3	0.2	2.5	1.8	0	0	7.5	no
0.6 mM citrate-C	0.1	0-0.4	0-0.5	0	0	2	0	7.0	yes

2.3. Fe-EC and $FeCl_3$ Experiments

All glassware was washed in 9% HNO_3, rinsed with 18 MΩ deionized water, and autoclaved prior to use. The procedure used for Fe-EC experiments is the same as in Chapter 3. Two 1 cm × 8 cm Fe(0) electrodes (98% Fe, 0.5 mm thick) were submerged in 200 mL of electrolyte spiked with bacteria (anodic submerged area of 3 cm^2). Electrodes were cleaned with sandpaper before each experiment to remove any rust or solid deposits. In all experiments, a current density of 10 mA/cm^2 was applied for 11 min, resulting in a Faradaic Fe dosage of 0.5 mM. Current density was selected based on previous work to avoid the anodic production of chlorine or oxygen[46,48,49]. The total cell voltage was <15 V in all experiments, resulting in an electric field <30 V/cm, orders of magnitude lower than bactericidal electric fields[96–98]. After the electrolysis stage, suspensions were stirred open to the atmosphere for 90-180 min to allow for complete Fe(II) oxidation and formation of Fe(III) precipitates. Suspensions were then left to settle overnight, which permitted the separation of individual cells from cells associated with EC precipitates, as described in Chapter 3. When required for floc formation and settling (Table S1), 5 mg/L-Al of $Al_2(SO_4)_3$ (alum) was added at the end of the mixing period, along with approximately 1.5 mM $NaHCO_3$ to avoid a pH drop. After alum addition, solutions were mixed rapidly (700 rpm, 5 min), then slowly (60 rpm, 25 min), to improve floc formation. Preliminary tests confirmed that the addition of alum did not significantly impact *E. coli* attenuation in two different electrolytes (2 mM NaCl pH 7 and SGW pH 7.5), as shown in Figure 4-1. Solution pH was not controlled during the settling stage. In a subset of experiments, coagulation by $FeCl_3$ addition was used instead of Fe-EC to isolate the contribution of removal from that of inactivation. In these experiments, 1 mL of a 100 mM $FeCl_3$ solution was added to the electrolyte and the solution pH, which dropped to ~3 during $FeCl_3$ addition, was re-adjusted to 7.0±0.1 in less than 5 min.

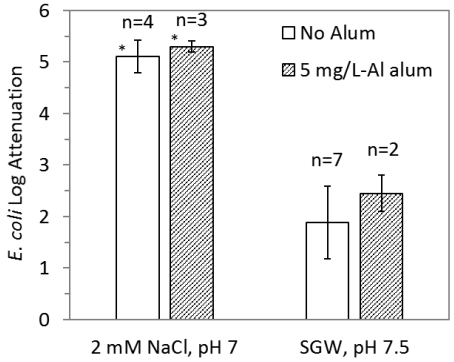

Figure 4-1: *E. coli* attenuation by Fe-EC with and without the addition of 5 mg/L-Al of alum before settling (Fe dosage = 0.5 mM). The number of replicate experiments is indicated. Asterisks indicate that the detection limit for bacteria attenuation was reached for some of the replicate experiments.

Unfiltered and filtered (0.45 μm nylon filters) samples were taken before Fe-EC, and before and after overnight settling, for measurements of Fe, As, Ca, Mg, P, and Si by ICP−OES (PerkinElmer 5300 DV, measurement error typically < 5%). All samples for ICP-OES analysis were digested in 0.2 M HCl. Filtered and unfiltered samples were used to measure Fe(II) and total

Fe (Fe(II) + Fe(III)), similarly to Chapter 3. Across the 113 bacteria attenuation experiments reported here, the total Fe concentration after Fe-EC (Fe dosage) was 96% ± 7% of the value predicted by Faraday's law (0.5 mM). Unoxidized Fe(II) (before settling) and unsettled Fe (after settling) were <1.2% and <4.7% of the total Fe dosed, respectively. Bacteria attenuation was calculated as the difference between log CFU concentrations before Fe-EC and after settling (samples taken from the supernatant, ~ 3 cm below the surface), and therefore accounts for both inactivation and enmeshment in flocs. Bacteria attenuation experiments were generally replicated three or more times, except for 12 experiments conducted in duplicate or less (indicated in Table 4-2). We report average bacteria attenuations ± one standard deviation across replicates.

Table 4-2: List of experiments that were not conducted in triplicate or more in this chapter.

Figure	Experiment	# of replicates
Figure 4-6d	9 mM Ca	1
	5 mM Mg	1
	8 mM Mg	1
	5 mM Mg + 13 mM Ca	1
Figure 4-7c	all	2
Figure 4-7d	9 mM Ca	1
	8 mM Mg	1
Figure 4-5	8 mM NaCl	2
	100 mM NaCl	1
	200 mM NaCl	2
	27 mM $NaClO_4$	2
	297 mM $NaClO_4$	2

In the groundwater-like electrolyte containing 8 mM HCO_3^- and 0.4 mM P, the formation of calcite, magnesite and hydroxyapatite solids was thermodynamically possible for the high Ca/Mg experiments: at 13.5 mM Ca and 10.6 mM Mg, the saturation indices for calcite, magnesite and hydroxyapatite are 12.5, 2.0 and 2.3 respectively, assuming an open-system at pH 7.0. To assess the amount of Ca/Mg/P that could possibly be removed through this process, we conducted control experiments in the absence of Fe. We added 13.5 mM Ca or 10.6 mM Mg to the groundwater-like electrolyte (8 mM HCO_3^-, 0.4 mM P, 1.2 mM Si) and the solution was mixed in open air at pH 7.0 for 2 hours before allowing the potential solids to settle overnight. ICP-OES measurements showed that less than 0.1 mM Ca, Mg or P precipitated under these conditions. Because Ca/Mg/P removal in our Fe-EC experiments with solutions oversaturated with respect to calcite, magnesite and hydroxyapatite was typically greater than 0.1 mM (ranging from 0.2 to 0.9 mM for Ca/Mg, and ~0.4 mM for P), we concluded that the precipitation of these Ca/Mg/P-bearing solid phases was minor relative to the uptake of Ca/Mg and P by EC precipitates. Furthermore, a previous study showed that the presence of Fe(III), at P:Fe molar ratios ≤ 1, stops the formation of hydroxyapatite in solutions that are extremely oversaturated with respect to this phase, due to the favorability of P-O-Fe bonds compared to P-O-Ca bonds[67]. Therefore, the formation of hydroxyapatite in our Fe-EC experiments, which had a P:Fe molar ratio of 0-0.8, can be ruled out.

Therefore, we used Ca/Mg/P removal measured by ICP-OES as a proxy for Ca/Mg/P uptake by EC precipitates.

Finally, to assess the effect of P/Si on the uptake of carboxyl moieties by EC precipitates, we performed citrate removal experiments using Fe-EC in the presence and absence of oxyanions under conditions identical to *E. coli* removal experiments, using 10 mg/L-Al of alum before settling (Table 4-1). Citrate concentrations were measured as total C with a TOC-V_{CSH} analyzer (Shimadzu).

2.4. ζ-Potential Measurements

In this chapter, ζ-potential measurements, which are a proxy for surface charge, were used to assess the interaction of major groundwater ions with the surface of EC precipitates or *E. coli K12* cells. ζ-potential measurements of EC precipitates and *E. coli* cells were conducted separately. Approximately 1 mL of electrolyte containing EC precipitates or bacteria was loaded into a Malvern DTS 1070 folded capillary cell, which was used to minimize settling during measurements. Samples with EC precipitates were sonicated for 10-20 min to disaggregate flocs before loading the cell. Electrophoretic mobility was measured in triplicate or more by dynamic light scattering (Malvern Zetasizer Nano-ZS) at 633 nm, and converted to ζ-potential using the Smoluchowski approximation. Each measurement gave a distribution of ζ-potentials characterized by its mean and its variance. For each set of triplicate measurements, we report the average and the standard deviation of the 3 distribution means.

2.5. Bacterial Viability Tests

Qualitative assessments of membrane permeabilization, which were used as a proxy for bacteria inactivation, were performed with the BacLight LIVE-DEAD kit (Invitrogen). This kit uses two fluorescent DNA stains: green fluorescing SYTO9 enters all cells while red fluorescing PI only enters cells with damaged membranes. Samples were first concentrated 10 times by centrifugation (8200g for 10 minutes). Next, 100 μL of the concentrated samples were reacted with 0.3 μL of 1:2.5 SYTO9:PI solution for one hour in the dark, then analyzed with a Zeiss AxioImager fluorescent microscope (63x Plan-Apochromat objective, EndoGFP and mCherry filters, U.C. Berkeley CNR Biological Imaging Facility).

2.6. Model of Ca/Mg Complexation by Bacterial Cell Walls

Following previous approaches[108,129–131], we derived a simple equilibrium surface complexation model, which included three bivalent cation adsorption sites on bacterial cell walls: carboxyl groups, protonated and deprotonated phosphate groups. Amine functional groups were not included because they have not been found to play a role in metal adsorption[108,129–131]. The surface complexation reactions relevant to our model are the following:

$$\equiv H_2POO \rightarrow \equiv HPOO^- + H^+ \qquad K_{A1} \qquad \text{(Equation 4-1)}$$

$$\equiv HPOO^- \rightarrow \equiv POO^{2-} + H^+ \qquad K_{A2} \qquad \text{(Equation 4-2)}$$

$$\equiv HPOO^- + M^{2+} \rightarrow \equiv HPOOM^+ \qquad K_{P1,Ca};\ K_{P1,Mg} \qquad \text{(Equation 4-3)}$$

$$\equiv POO^{2-} + M^{2+} \rightarrow \equiv POOM \qquad K_{P2,Ca};\ K_{P2,Mg} \qquad \text{(Equation 4-4)}$$

$$\equiv HCOO \rightarrow \equiv COO^- + H^+ \qquad K_A \qquad \text{(Equation 4-5)}$$

$$\equiv COO^- + M^{2+} \rightarrow \equiv COOM^+ \qquad K_{C,Ca};\ K_{C,Mg} \qquad \text{(Equation 4-6)}$$

All the constants and their sources are specified in Table 4-3. Among the available literature on Ca complexation constants[108,130,133], we chose to use Johnson *et al.*, 2007[130] because it provided the most comprehensive data (Ca complexation constants to the three relevant functional groups with corresponding pK_as) and was consistent with other studies[108,128,129,131–133]. Because Gram-negative and Gram-positive bacteria have similar metal complexation constants[131,132], it is valid to extrapolate data from Johnson *et al.*, 2007, measured for bacteria consortia, to other types of bacteria. Although Mg adsorption to bacterial surfaces has been reported[143,144], complexation constants have not been documented to the authors' knowledge. Instead, we used the experimental linear relationship between acetate and bacteria complexation constants proposed in Johnson *et al.*, 2007[130]. Acetate-Mg complexation constants were found in Shock *et al.*, 1993[154].

Table 4-3: List of bacterial surface complexation constants used in our model and their sources.

Bacterial surface group	Constants		Source
Phosphate groups	pK_{A1}	3.15	Johnson *et al.*, 2007[130]
	pK_{A2}	6.54	Johnson *et al.*, 2007[130]
	$K_{P1,Ca}$	1.8	Johnson *et al.*, 2007[130]
	$K_{P1,Mg}$	2.4	derived from Johnson *et al.*, 2007[130] and Shock and Koretsky, 1993[154]
	$K_{P2,Ca}$	2.9	Johnson *et al.*, 2007[130]
	$K_{P2,Mg}$	3.3	derived from Johnson *et al.*, 2007[130] and Shock and Koretsky, 1993[154]
Carboxyl groups	pK_A	4.77	Johnson *et al.*, 2007[130]
	$K_{C,Ca}$	2.3	Johnson *et al.*, 2007[130]
	$K_{C,Mg}$	2.5	derived from Johnson *et al.*, 2007[130] and Shock and Koretsky, 1993[154]

By definition, the fraction of bacterial phosphate and carboxyl groups complexed by bivalent cations can be written as:

$$f_{P\ groups\ complexed} = \frac{[\equiv HPOOCa^+]+[\equiv POOCa]+[\equiv HPOOMg^+]+[\equiv POOMg]}{[\equiv H_2POO]+[\equiv HPOO^-]+[\equiv POO^{2-}]+[\equiv HPOOCa^+]+[\equiv POOCa]+[\equiv HPOOMg^+]+[\equiv POOMg]}$$

(Equation 4-7)

$$f_{C\ groups\ complexed} = \frac{[\equiv COOCa^+]+[\equiv COOMg^+]}{[\equiv HCOO]+[\equiv COO^-]+[\equiv COOCa^+]+[\equiv COOMg^+]} \quad \text{(Equation 4-8)}$$

Realizing that each term can be expressed as a function of $[\equiv HPOO^-]$ or $[\equiv COO^-]$ as in Equations 9-14, Equations 7 and 8 can be rearranged into Equations 15 and 16, which predict the percentage of bacterial phosphate and carboxyl groups complexed by Ca and Mg. Resulting model predictions are shown in Figure 4-2.

$$[\equiv H_2POO] = \frac{[\equiv HPOO^-][H^+]}{K_{A1}} \quad \text{(Equation 4-9)}$$

$$[\equiv POO^{2-}] = \frac{[\equiv HPOO^-]K_{A2}}{[H^+]} \quad \text{(Equation 4-10)}$$

$$[\equiv HPOOM^+] = [\equiv HPOO^-][M^{2+}]K_{P1,M} \quad \text{(Equation 4-11)}$$

$$[\equiv POOM] = [\equiv POO^{2-}][M^{2+}]K_{P2,M} = \frac{[\equiv HPOO^-]K_{A2}}{[H^+]}[M^{2+}]K_{P2,M} \quad \text{(Equation 4-12)}$$

$$[\equiv HCOO] = \frac{[\equiv COO^-][H^+]}{K_A} \quad \text{(Equation 4-13)}$$

$$[\equiv COOM^+] = [\equiv COO^-][M^{2+}]K_{C,M} \quad \text{(Equation 4-14)}$$

$$\%_{P\ groups\ complexed} = \frac{K_{P1,Ca}[Ca^{2+}]+K_{P1,Mg}[Mg^{2+}]+\frac{K_{A2}}{[H^+]}(K_{P2,Ca}[Ca^{2+}]+K_{P2,Mg}[Mg^{2+}])}{\frac{[H^+]}{K_{A1}}+1+\frac{K_{A2}}{[H^+]}+K_{P1,Ca}[Ca^{2+}]+K_{P1,Mg}[Mg^{2+}]+\frac{K_{A2}}{[H^+]}(K_{P2,Ca}[Ca^{2+}]+K_{P2,Mg}[Mg^{2+}])} * 100$$

(Equation 4-15)

$$\%_{C\ groups\ complexed} = \frac{K_{C,Ca}[Ca^{2+}]+K_{C,Mg}[Mg^{2+}]}{\frac{[H^+]}{K_A}+1+K_{C,Ca}[Ca^{2+}]+K_{C,Mg}[Mg^{2+}]} * 100 \quad \text{(Equation 4-16)}$$

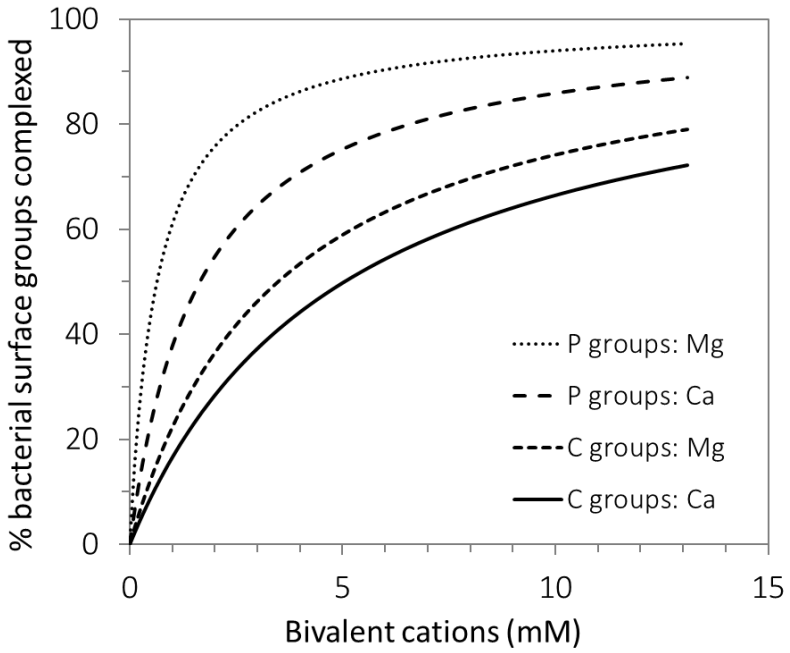

Figure 4-2: Model predictions of the percentage of bacterial phosphate and carboxyl groups complexed by Ca/Mg.

2.7. Estimation of the Concentration of Bacterial Surface Functional Groups in our Experiments

Table 4-4: List of assumptions used to calculate the concentration of bacterial surface functional groups in our experiments.

Density of groups (carboxyl, protonated and deprotonated phosphate groups)[128]:	$25.7 \pm 8.2 \times 10^{-5}$ mol/wet g (9.1 ± 3.8, 11.3 ± 7.0, 5.3 ± 2.1)
Density of a bacterial cell[155]:	1.1 wet g/cm^3
Volume of a bacterial cell (approximated by a sphere of 1 μm diameter):	5.2×10^{-13} cm^3/cell
Number of cells per cell colony forming unit:	~ 1
Bacteria concentration in our experiments:	~ $10^{6.5}$ CFU/mL

Using the assumptions listed in Table 4-4, the total concentration of bacterial surface functional groups in our experiments can be calculated as:

$$25.7 \pm 8.2 * 10^{-5} \frac{mol}{wet\ g} * 1.1 \frac{wet\ g}{cm^3} * 5.2 * 10^{-13} \frac{cm^3}{cell} * 1 \frac{cell}{CFU} * 10^{9.5} \frac{CFU}{L} = 4.7 \pm 1.5 * 10^{-4}\, mM$$

Similarly, the concentrations of carboxyl, protonated and deprotonated phosphate groups are 1.6 ± 0.7, 2.0 ± 1.3 and $1.0 \pm 0.4 * 10^{-4}$ mM respectively.

3. RESULTS AND DISCUSSION

3.1. Effect of HCO_3^- on the Contributions of Removal and Inactivation

The effect of 8 mM HCO_3^- on *E. coli* attenuation by Fe-EC and $FeCl_3$ coagulation is shown in Figure 4-3a. Representative *E. coli* live-dead staining images are presented in Figure 4-3b-e. Whereas 8 mM HCO_3^- did not significantly affect *E. coli* attenuation by coagulation with $FeCl_3$, the presence of HCO_3^- decreased attenuation by Fe-EC by ~1.2 log. Because no reactive oxidants are produced from an Fe(III) salt[156], minimal inactivation occurs during $FeCl_3$ coagulation (consistent with live-dead staining, Figure 4-3b-c), which implies that attenuation via $FeCl_3$ addition is exclusively due to physical removal (enmeshment in flocs). Any difference in precipitate-bacteria adhesion between Fe-EC and $FeCl_3$ coagulation would lead to higher removal

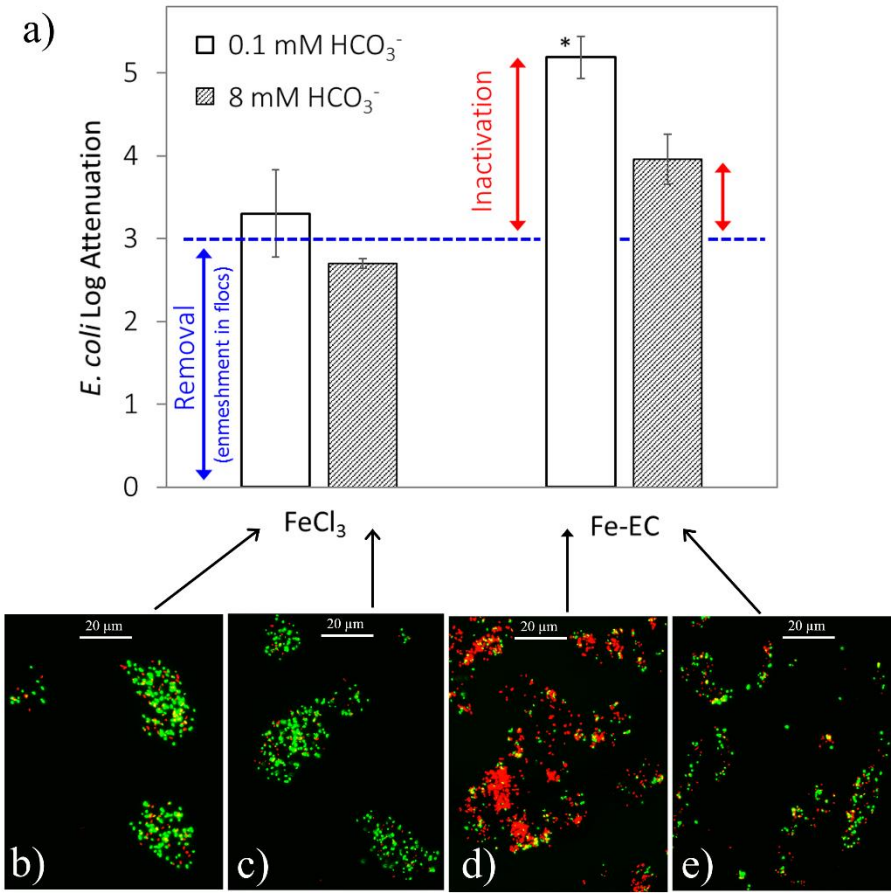

Figure 4-3: *E. coli* attenuation with Fe-EC and $FeCl_3$, with and without 8 mM HCO_3^-. Fe dosage was 0.5 mM in all experiments. Panel a shows *E. coli* log attenuations. The asterisk indicates that the detection limit for bacteria attenuation was reached for some of the replicate experiments. Panels b-e show fluorescent microscopy images of live (green)-dead (red) stained *E. coli* cells. The blue dashed line is the average attenuation in all $FeCl_3$ experiments (with and without HCO_3^-) and represents removal (blue arrow). *E. coli* log attenuations are compared to this baseline to deduce approximate log inactivations (red arrows). All experiments were conducted at pH 7.0. In 0.1 mM HCO_3^- experiments, 2 mM NaCl were added for conductivity.

in the latter, because the precipitates generated by $FeCl_3$ coagulation in a HCO_3^- electrolyte are less crystalline and thus have a higher surface area than Fe-EC precipitates[50,67,101]. Consequently, the difference in attenuations between Fe-EC and $FeCl_3$ coagulation can conservatively be attributed to inactivation.

As shown in Figure 4-3a, HCO_3^- did not affect physical removal, which is consistent with ζ-potential measurements showing that HCO_3^- does not significantly interact with the surface of *E. coli* cells or Fe(III) precipitates (Figure 4-4). By contrast, 8 mM HCO_3^- decreased inactivation substantially by ~1.2 log. We found a strong correlation between inactivation (Figure 4-3a) and membrane permeabilization in Fe-EC (Figure 4-3d-e). Membrane damage may be caused by the reactive species produced as intermediates during Fenton-type reactions, (e.g. $O_2^{\bullet-}$, H_2O_2, and Fe(IV)[52,123]), which have been associated with bactericidal effects[113,124–127]. The inhibitory effect of HCO_3^- on inactivation may be explained by the formation of $CO_3^{\bullet-}$ radicals, which are produced when HCO_3^- or Fe(II)-carbonate complexes react with H_2O_2[52,157]. Table 4-5 compares the reactivity of the strong oxidants produced in Fe-EC. $CO_3^{\bullet-}$ is a stronger oxidant than superoxide and hydrogen peroxide from a thermodynamic standpoint (see E^0_W), which translates into faster oxidation kinetics with the glutathione biomolecule. Although thermodynamic comparisons between $CO_3^{\bullet-}$ and Fe(IV) are more difficult due to the lack of a reliable reduction potential for Fe(IV), oxidation kinetics with formate and phenol (which are functional groups present on the surface of bacteria) indicate that $CO_3^{\bullet-}$ is a similar or stronger oxidant compared to Fe(IV). Overall, $CO_3^{\bullet-}$ seems to be more reactive than $O_2^{\bullet-}$, H_2O_2, and Fe(IV), and is therefore likely to be a much shorter-lived and less selective oxidant. We speculate that large HCO_3^- concentrations reduce membrane damage and inactivation by shifting the nature of reactive species produced during Fe-EC towards a shorter-lived oxidant ($CO_3^{\bullet-}$) that is more likely to die off in the bulk (e.g. reacting with Fe(II), Cl^-, HCO_3^-) than to interact with cell membranes.

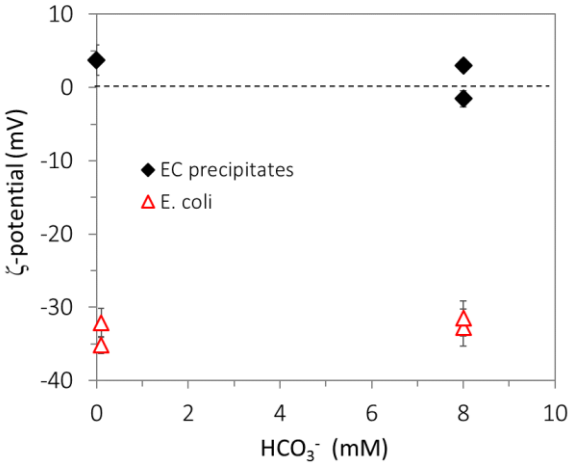

Figure 4-4: Effect of HCO_3^- on the ζ-potential of EC precipitates and *E. coli* cells. This Figure shows that 8 mM HCO_3^- does not significantly affect the surface charge of EC precipitates and *E. coli* cells, indicating that HCO_3^- does not interact with bacteria or precipitate surfaces.

Overall, Figure 4-3 shows that both inactivation and removal (enmeshment in flocs) contribute to *E. coli* attenuation in Fe-EC, and that the concentration of HCO_3^- governs the amount of inactivation. In the rest of the chapter, we will focus on removal. Interactions between EC precipitates and *E. coli* cells are investigated by varying levels of ionic strength, Ca, Mg, P, and Si. Because these ions are not expected to react with oxidants such as $O_2^{\bullet-}$, H_2O_2, or Fe(IV)[49,58,156], nor to interact with lipids aliphatic chains, which are the target of oxidants on cell membranes (lipid peroxidation), they are assumed to have a negligible effect on inactivation. Therefore, their potential impact on *E. coli* attenuation will be solely attributed to changes in removal.

Table 4-5: Reduction potentials and reaction rates of strong oxidants produced in Fe-EC. [a] Reduction potentials at pH 7, calculated based on standard reduction potentials (E^0_{SHE}) found in the literature. [b] GSH stands for glutathione, an anti-oxidant found in plants and used in a study to compare the reactivity of radicals towards biomolecules[158].

Oxidant	Half-cell reaction	E^0_{SHE} (V)	E^0_w(V)[a]	k (M^{-1} s^{-1}) with GSH[b]	k (M^{-1} s^{-1}) with formate	k (M^{-1} s^{-1}) with phenol
$O_2^{\bullet-}$	$O_2^{\bullet-} + 2H^+ + e^- \rightarrow H_2O_2$	1.69 [159]	0.88	10^1-10^3 [158]		$10^{3.1}$ [160]
H_2O_2	$H_2O_2 + H^+ + e^- \rightarrow OH^\bullet + H_2O$	0.97 [159]	0.56	0.9 [158]		
$OH^\bullet$	$OH^\bullet + H^+ + e^- \rightarrow H_2O$	2.49 [159]	2.09	10^{10} [158]		
$CO_3^{\bullet-}$	$CO_3^{\bullet-} + H^+ + e^- \rightarrow HCO_3^-$	2.19 [161]	1.78 [157]	$10^{7.7}$ [158]	$10^{5.0}$ [162]	$10^{6.7\text{-}7.3}$ [162]
Fe(IV)	$FeO^{2+} + 2\ H_2O + e^- \rightarrow Fe(OH)_{3(s)} + H^+$	0.59-1.71 [163,164]	0.99-2.12		$10^{5.5}$ [163]	$10^{3.6}$ [163]

3.2. Effect of Ionic Strength

Increasing ionic strength over 2 orders of magnitude (2-200 mM), which results in increased charge screening (Debye length decreased tenfold), did not significantly affect *E. coli* attenuation by Fe-EC, regardless of the initial electrolyte composition (Figure 4-5). The negligible effect of ionic strength suggests that electrostatic interactions play a secondary role compared to specific interactions in the adhesion of EC precipitates to *E. coli* cells. In the following two sections, we investigate the bacterial surface sites involved in these interactions by systematically varying the concentration of bivalent cations and oxyanions in order to selectively complex adsorption sites on the surface of *E. coli* cells and EC precipitates.

3.3. Effect of Bivalent Cations: Ca and Mg

3.3.1. Single Solute Electrolytes (no oxyanions, no HCO_3^-)

E. coli attenuation as a function of Ca and Mg concentrations is shown in Figure 4-6a. Ca and Mg both decreased *E. coli* attenuation, with a larger inhibitory effect observed for Mg (2.1 log decrease in attenuation when Mg increased from 0 to 10.6 mM) than for Ca (1.3 log decrease in attenuation when Ca increased from 0 to 12.9 mM). Because bivalent cations should not affect inactivation (see 3.1.), these reductions in bacteria attenuation can be interpreted as reductions in *E. coli* removal.

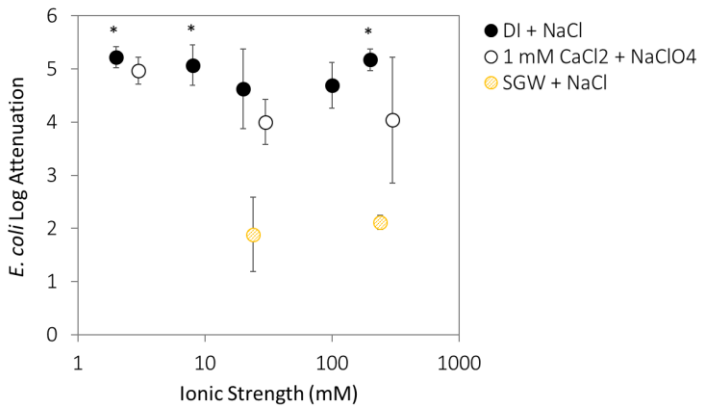

Figure 4-5: Effect of ionic strength on *E. coli* attenuation by Fe-EC in 3 different electrolytes: in deionized water with varying NaCl (pH 7.0), in 1 mM $CaCl_2$ with varying $NaClO_4$ (pH 7.0) and in SGW with varying NaCl (pH 7.5). The Fe dosage was 0.5 mM Fe for all experiments. Because unusual variations in log attenuation were observed between 1 and 2 days of settling (especially in the $NaClO_4$ series), we report averaged log attenuations for 1 and 2 days of settling. Asterisks indicate that the detection limit for bacteria attenuation was reached for some of the replicate experiments.

Figure 4-6b shows the ζ-potential of EC precipitates and *E. coli* cells as a function of Ca/Mg concentrations. In this single Ca/Mg solute electrolyte, EC precipitates were positively charged. Increasing concentrations of Ca/Mg had a limited effect on the ζ-potential of EC precipitates, suggesting that bivalent cations interacted minimally with their surface. This result is expected given the repulsive electrostatic forces between bivalent cations and positively-charged EC precipitates, and is consistent with previous work showing negligible uptake of Ca/Mg by Fe(III) (oxyhydr)oxides at circumneutral pH in the absence of oxyanions[165,166]. By contrast, Ca and Mg caused a significant increase in the ζ-potential of *E. coli* cells, indicating a strong interaction between bivalent cations and bacteria surfaces. Our surface equilibrium model (Figure 4-2) predicts that raising Ca/Mg concentrations from 0 to 13 mM leads to a significant increase in the complexation of carboxyl (from 0 to 70-80%) and phosphate (from 0 to 90-95%) groups, which is consistent with the observed increase in *E. coli* ζ-potential (Figure 4-6b).

Figure 4-6c combines attenuation results (Figure 4-6a) and model outputs (Figure 4-2) to highlight that *E. coli* removal decreases as the percentage of complexed bacterial carboxyl and phosphate groups increases. Stronger inhibition of *E. coli* removal by Mg than by Ca (Figure 4-6a) is consistent with this trend, because Mg has a higher affinity for bacterial surface functional groups[144] (Table 4-3 and Figure 4-2).

3.3.2. Groundwater-like Electrolytes (with oxyanions and HCO_3^-)

Figure 4-6d shows the effect of Ca (0-13.5 mM) and Mg (2.4-10.5 mM) on *E. coli* attenuation in a groundwater-like electrolyte containing 8 mM HCO_3^-, 1.2 mM Si and 0.4 mM P. Similar to the single Ca/Mg solute system, bivalent cations reduced *E. coli* attenuation, with Ca/Mg concentrations above 10 mM leading to a 1-2 log decrease in attenuation.

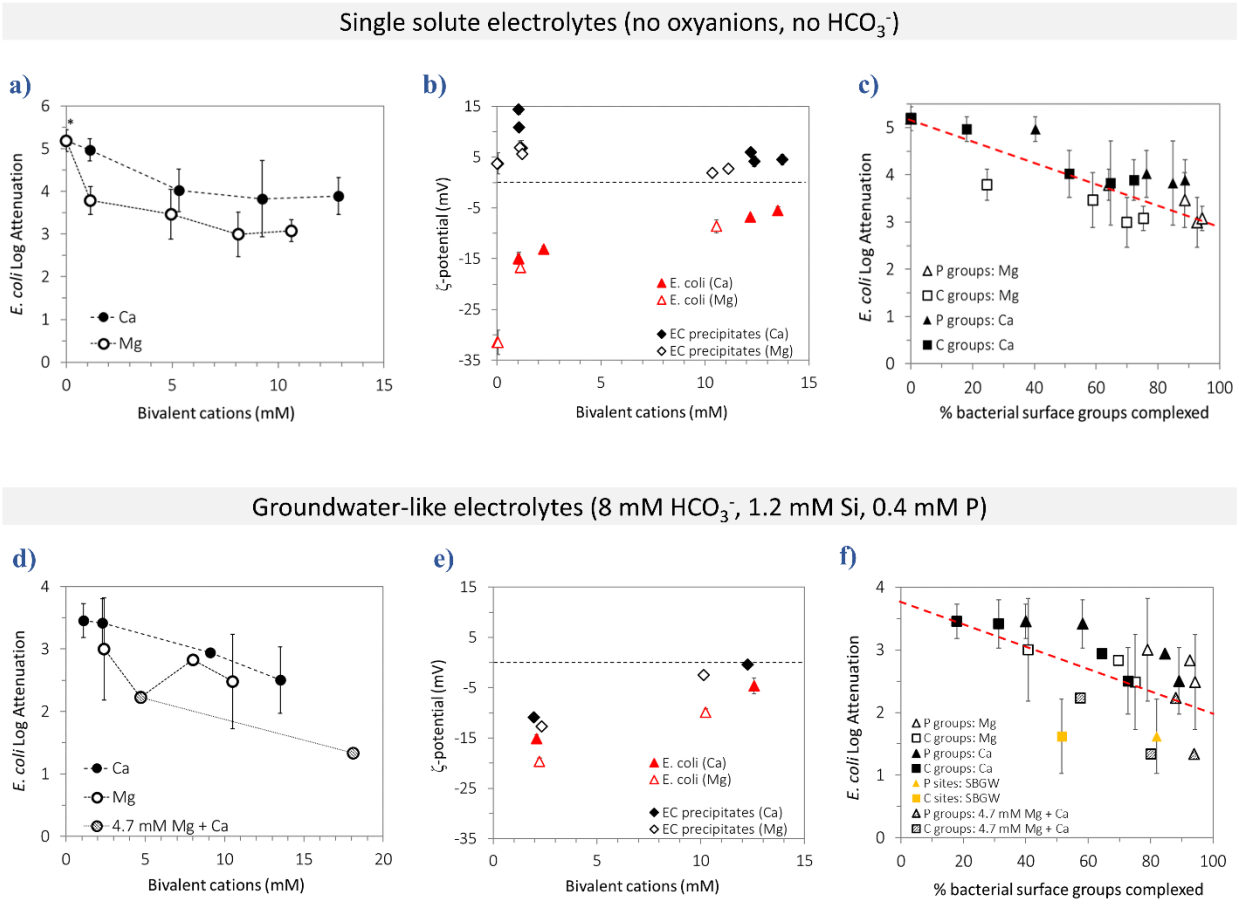

Figure 4-6: Effect of Ca and Mg on *E. coli* attenuation in Fe-EC, in single solute electrolytes (panels a, b and c) and in groundwater-like electrolytes containing 8 mM HCO_3^-, 1.2 mM Si and 0.4 mM P (panels d, e and f). Panels a and d: effect of increasing Ca/Mg concentrations on *E. coli* log attenuation with an Fe dosage of 0.5 mM. The asterisk indicates that the detection limit for bacteria attenuation was reached for some of the replicate experiments. Panels b and e: effect of increasing Ca/Mg concentrations on the ζ-potential of EC precipitates and *E. coli* cells (data points for 0 mM Ca and 0 mM Mg overlap on panel b). Panels c and f: *E. coli* attenuation as a function of complexed bacterial surface groups (combination of Figures 4-6a and 4-2, and 4-6d and 4-2 respectively). The dotted red lines highlight the inverse correlation between *E. coli* attenuation and the complexation of bacterial functional groups. All experiments were conducted at pH 7.0. Experiments with no Ca/Mg (panel a) were conducted in 2 mM NaCl for conductivity.

Figure 4-6e shows ζ-potentials of EC precipitates and *E. coli* cells as a function of Ca/Mg concentrations in the groundwater-like electrolyte. Bivalent cations increased the ζ-potential of *E. coli* cells, consistent with the complexation of phosphate and carboxyl groups on cell walls, as explained in section 3.3.1. In this electrolyte, EC precipitates were negatively-charged due to the sorption of P and, to a lesser extent, Si (P:Fe and Si:Fe molar solids ratios of 0.7 ± 0.1 and 0.06 ± 0.04, respectively). In contrast to the previous experiments without oxyanions (section 3.3.1), bivalent cations significantly interacted with the surface of EC precipitates in the groundwater-like electrolyte, as indicated by a substantially higher ζ-potential at larger Ca/Mg concentrations. This increase in precipitate surface charge coincided with increased Ca/Mg uptake, with solids ratios going from 0.5 ± 0.1 to 1.2 ± 0.7 mol Ca:mol Fe, and from 0.3 ± 0.1 to 0.5 ± 0.4 mol Mg:mol Fe,

respectively. EC precipitates with similar chemical compositions (i.e. Ca/Mg:P:Fe molar ratios) have been documented in previous studies performed in nearly identical electrolytes, but in the absence of bacteria[50,57]. In these studies, Ca was shown to interact with P sorbed to Fe(III) precipitates, via direct Ca-O-P bonds, and to a lesser extent, electrostatically[57]. In the present study, the observed increase in precipitate ζ-potential with Ca/Mg in the groundwater-like electrolyte is consistent with such interactions of Ca/Mg with P sorbed to Fe(III) precipitates.

Figure 4-6f illustrates the inverse relationship between *E. coli* attenuation in the groundwater-like electrolyte and the predicted percentage of bacterial functional groups complexed by Ca/Mg. Figure 4-6f also includes data from Chapter 3 obtained in synthetic Bengal groundwater containing (2.6 mM Ca and 1.9 mM Mg), which are consistent with this trend. Finally, we note that *E. coli* attenuations in groundwater-like electrolytes (Figure 4-6f) are overall ~1 log lower than in single solute systems (Figure 4-6c), which is consistent with the inhibition of inactivation by 8 mM HCO_3^- shown in section 3.1.

Taken together, Figures 4-6a-f show that Ca/Mg decreases *E. coli* removal independent of the electrolyte, and more specifically, independent of the surface charge of EC precipitates: whether Ca/Mg increase (Figure 4-6b, no oxyanions) or decrease (Figure 4-6e, oxyanions present) the electrostatic barrier to precipitate adhesion on cell walls, bivalent cations equally inhibit *E. coli* removal. Combined with the limited impact of ionic strength (Section 3.2 and Figure 4-5), this result confirms the minimal role of electrostatic interactions on *E. coli* removal and instead points to the importance of specific interactions between EC precipitates and bacterial phosphate and/or carboxyl groups. These results are in good agreement with previous ATR-FTIR studies that provided evidence for direct bonding between Fe oxides and bacterial phosphate/carboxyl groups in simple and controlled systems[115,136,142].

3.4. Effect of Oxyanions: P and Si

3.4.1 Single Solute Electrolytes (no bivalent cations, no HCO_3^-)

Figure 4-7a shows the effect of 0.4 mM Si/P on *E. coli* attenuation in electrolytes containing no Ca/Mg. Whereas Si had no detectable effect, P reduced *E. coli* attenuation by 1.6 log. Because Si and P should not affect inactivation, as explained in section 3.1, these effects correspond to changes in removal. ζ-potential measurements of EC precipitates and *E. coli* cells as a function of P/Si concentrations are presented in Figure 4-7b. Si and P had no detectable effect on the ζ-potential of *E. coli* cells, reflecting the absence of interaction between these oxyanions and bacterial cell walls. By contrast, Si and P significantly decreased the ζ-potential of EC precipitates, indicating oxyanion sorption[110,111], which is supported by the uptake of Si and P measured by ICP-OES (Si:Fe and P:Fe molar solids ratios of 0.3 and 0.6, respectively). Because electrostatic interactions do not play a major role in *E. coli* removal, as demonstrated above, lower bacteria removal in the presence of P cannot be explained by the decrease in precipitate surface charge. Rather, the results in Figure 4-7a indicate that inorganic aqueous P competes with bacterial functional groups involved in bonding to EC precipitates. By contrast, our results indicate that Si does not strongly compete with these functional groups.

Because aqueous P and bacterial phosphate groups are structurally and chemically similar, they are expected to compete for precipitate surfaces. However, the competition between P and carboxyl groups is less straight-forward. To assess the effect of P on the adsorption of carboxyl moieties, we measured the removal of citrate (a proxy for carboxyl groups) by Fe-EC in the presence and absence of P. As shown in Figure 4-7c, P decreased citrate removal by nearly 54% (initial P:C molar ratio of 0.9). In *E. coli* attenuation experiments, the molar ratio of aqueous P to bacterial surface carboxyl groups is ~ 2500 mol P: mol C (see section 2.7). Therefore, aqueous P is expected to strongly compete with bacterial carboxyl groups in attenuation experiments.

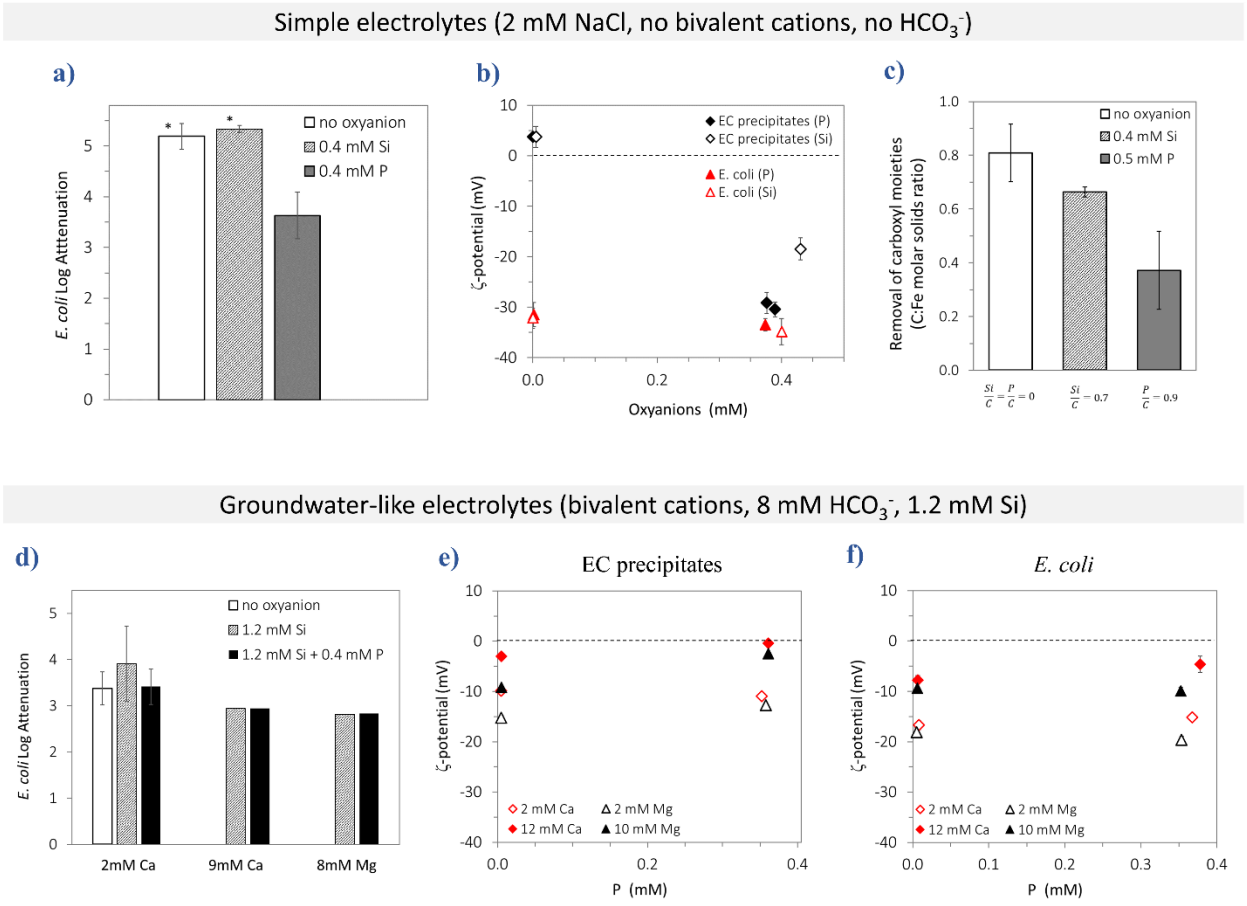

Figure 4-7: Effect of P and Si on *E. coli* attenuation by EC with an Fe dosage of 0.5 mM in single solute electrolytes (0.4 mM P or Si in 2mM NaCl background for conductivity; panels a,b and c) and groundwater-like electrolytes containing 8 mM HCO_3^-,1.2 mM Si and bivalent cations (panels, d, e and f). a) Effect of Si and P on *E. coli* attenuation. Asterisks indicate that the detection limit for bacteria attenuation was reached for some of the replicate experiments. b) Effect of Si (open symbols) and P (solid symbols) on the ζ-potential of EC precipitates and *E. coli* cells. c) Effect of P and Si on the removal of citrate (a proxy for carboxyl moieties) by Fe-EC. d) Effect of P on *E. coli* attenuation at different levels of Ca/Mg. e) Effect of P on the ζ-potential of EC precipitates. f) Effect of P on the ζ-potential of *E. coli* cells. All experiments were conducted at pH 7.0.

Fe(III) (oxyhydr)oxides have a much higher affinity for P than for Si[58,60]. Therefore, Si is not expected to compete with bacterial phosphate groups for precipitate surfaces. However, Figure 4-7c shows that Si decreased citrate removal in Fe-EC by nearly 20% (initial Si:C molar ratio of 0.7). In *E. coli* attenuation experiments, where the molar ratio of Si to bacterial surface carboxyl groups is orders of magnitude higher (~ 2500, see section 2.7), it is thus likely that Si would inhibit bacteria removal if carboxyl groups played an important role in the adhesion of EC precipitates. Because Si had no detectable effect on *E. coli* attenuation (Figure 4-7a), we propose that phosphate groups are the primary sites for the adhesion of EC precipitates to cell walls, with negligible contributions from carboxyl groups.

3.4.2. Groundwater-like Electrolytes (with bivalent cations, HCO_3^-, and Si)

In Figure 4-7d, we show the effect of P (0-0.4 mM) on *E. coli* attenuation in the presence of Ca (2 and 9 mM) or Mg (8 mM), in a groundwater-like electrolyte containing 8 mM HCO_3^- and 1.2 mM Si. In contrast to experiments in electrolytes free of bivalent cations, where P decreased *E. coli* removal by 1.6 log (Figure 4-7a), 0.4 mM P had no effect on *E. coli* removal in the presence of Ca/Mg. We note that lower *E. coli* attenuations in Figure 4-7d compared to Figure 4-7a (~2 log) are due to the inhibition of inactivation by 8 mM HCO_3^- (shown in section 3.1) and to the reduction in removal caused by Ca/Mg (shown in section 3.3).

Figures 4-7e-f show ζ-potential measurements of EC precipitates and *E. coli* cells, respectively, as a function of P concentration in the groundwater-like electrolyte containing bivalent cations. Figure 4-7e shows that P did not interact significantly with bacterial cells, as expected. In contrast to single oxyanion systems (Figure 4-7b), EC precipitates in the groundwater-like electrolyte were negatively-charged for all P concentrations, due to sorbed Si/P. In addition, the ζ-potential of EC precipitates did not decrease when the P concentration increased from 0 to 0.4 mM, despite substantial P uptake by precipitates (P:Fe molar solids ratios of 0.6-0.8, see Table 4-6). This result stands in strong contrast with electrolytes containing no Ca/Mg, where high concentrations of P (0.4 mM) and similar P:Fe solids ratios (0.6 mol:mol) significantly decreased EC precipitate surface charge (Figure 4-7b). In the groundwater-like electrolytes, ICP-OES measurements indicated that Ca/Mg uptake by EC precipitates increased by 20-200 % -depending on the initial Ca/Mg concentration- in the presence of 0.4 mM P (Table 4-6). This co-sorption of Ca/Mg explains the negligible impact of P sorption on the surface charge of EC precipitates.

Based on the co-sorption of Ca/Mg and P, the behavior of precipitate and bacteria surfaces and the negligible effect of P on *E. coli* removal observed in our system, we propose that Ca/Mg can act as a bivalent cation bridge between bacterial phosphate groups and P sorbed to Fe(III) precipitates. This Ca/Mg configuration, which leads to additional sites at the precipitate surface that can interact with bacterial cell walls, is consistent with the Ca-P-Fe configurations documented previously in comparable systems[57,67,167].

Table 4-6: Effect of 0.4 mM P on ion uptake by EC precipitates, as measured by ICP-OES. For different initial concentrations of bivalent cations, this Table indicates (1) P uptake by EC precipitates and (2) the change in Ca/Mg removal upon P addition (comparison between Ca/Mg removal with and without P). * Ca/Mg removal can be used as a proxy for Ca/Mg uptake by EC precipitates, as explained in section 2.3.

Background electrolyte		**P uptake by EC precipitates**		**Change in Ca/Mg removal** *	
		P:Fe solid ratio (mM/mM)		**Ca-Mg:Fe solid ratios (mM/mM)**	
		Average	***St. dev.***	***Average***	***St. dev.***
0.1 mM HCO_3^- + 2 mM NaCl	0 Ca/Mg	0.6	0.0	NA	NA
8 mM HCO_3^- + 1.2 mM Si	2.3 mM Ca	0.8	0.2	+ 0.2 (+ 33%)	0.1
	13.5 mM Ca	0.8	0.1	+ 0.2 (+21%)	0.5
	2.4 mM Mg	0.6	0.0	+ 0.2 (+199%)	0.0
	10.6 mM Mg	0.7	0.0	+ 0.2 (+63%)	0.1

3.5. Attenuation of Different Types of Bacteria

The attenuation of *E. coli* K12, *E. coli* ECOR 10 and *E. faecalis* in SGW with an Fe dosage of 0.5 mM is shown in Figure 4-8. No significant difference between the log attenuations of the three different bacterial strains was observed, despite their considerably different cell wall structures. For example, the surface of Gram-positive *E. faecalis* is composed of a peptidoglycan layer topped with techoic acids, whereas the surface of Gram-negative *E. coli* is made of phospholipids and lipopolysaccharides (LPS)[168]. Furthermore, the two *E. coli* strains differ by the length of their LPS: ECOR 10 is a smooth strain with a full-length LPS (with O-antigen), whereas K12 is a rough strain with a truncated LPS (no O-antigen). Such differences in cell wall composition lead to differences in hydrophobicity, surface charge, surface roughness and steric hindrance to approach mineral surfaces and nanoparticles[77,107,145–147].

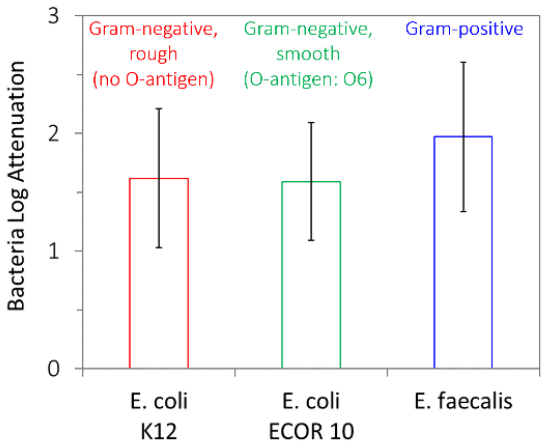

Figure 4-8: Log attenuation of three different bacterial strains by Fe-EC, at an Fe dosage of 0.5 mM. All experiments were conducted at pH 7.5 in SGW (see chemical composition in Table 4-1.

Previous studies have found that cell wall composition and LPS length affect the interactions of bacteria with mineral surfaces (sand, iron-oxide coated sand, and gold nanoparticles) in systems governed by non-specific interactions, such as electrostatic, steric, hydrophobic and van der Waals forces[77,107,145–147]. In contrast to these studies, similar attenuation of *E. coli* K12, *E. coli* ECOR 10 and *E. faecalis* in our system is likely due to the dominant role of specific interactions in bacteria-precipitate adhesion. Phosphate functional groups, which we showed are the primary binding sites for EC precipitates, are present in similar abundance on Gram-negative and Gram-positive bacteria[128,169] (mainly on phospholipids and on techoic acids, respectively), explaining similar removal of *E. coli* and *E. faecalis*. In addition, negligible steric hindrance from longer LPS on *E. coli* is likely due to the small size of EC precipitates compared to bacterial cells (Figure 4-9).

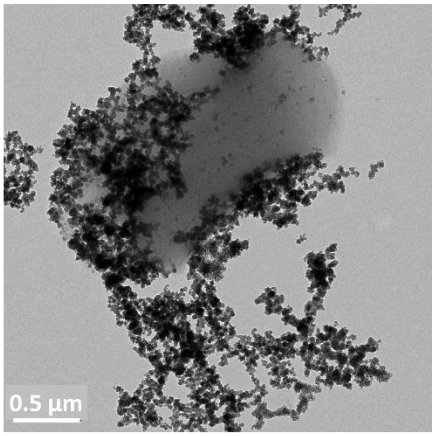

Figure 4-9: Transmission electron microscopy (TEM) image of EC precipitates (~ 50 nm in size) adhering to the surface of *E. coli* cells. Image obtained with a FEI Tecnai 12 operated at 120 kV (UC Berkeley Electron Microscope Lab). Sample preparation followed the procedure described in Chapter 3.

Based on these results, we expect that Fe-EC would be similarly effective for all waterborne pathogenic bacteria, both Gram-negative (e.g. *Vibrio cholera*, *Shigella*, *Salmonella*, pathogenic *E. coli*) and Gram-positive (e.g. *E. faecalis*, *Bacillus cereus*, *Staphylococcus aureus)*. Finally, similar attenuation of *E. coli* K12 and *E. coli* ECOR 10 suggests that fecal pathogens, which are typically smooth strains[170], would be as effectively removed as our model indicator *E. coli* K12. Overall, these results are promising for the application of Fe-EC to drinking water or wastewater treatment.

3.6. Implications for Water Treatment

In this study, we showed that bacteria inactivation, which can be significant in the absence of oxidant scavengers, is largely suppressed by HCO_3^- concentrations characteristic of natural waters. Therefore, we expect physical removal to be the primary process of bacteria attenuation in most water treatment applications. Sludge sterilization before handling and disposal (e.g. via heat treatment) may therefore be necessary because flocs may contain viable pathogens.

We showed that removal is driven by the interactions of EC precipitates with bacterial phosphate groups, which may bind to Fe(III) surfaces directly or via a Ca/Mg bridge to P sorbed on precipitates. The removal mechanisms elucidated in this chapter are summarized in Figure 4-10. These mechanisms, as well as the observed effects of silicate and phosphate, can be used to predict the impact of various oxyanions on bacteria removal with Fe-EC. Specifically, oxyanions with a substantially lower affinity for Fe(III) (oxyhydr)oxides than phosphate moieties, such as bicarbonate, arsenite (present in groundwater), borate (present in wastewater effluent) or nitrate (present in agricultural runoff and wastewater effluent), are not expected to affect bacteria removal significantly. By contrast, oxyanions with a sorption affinity comparable to that of phosphate moieties, such as arsenate, are expected to decrease bacteria removal, unless bivalent cations are present in sufficient concentrations to induce bridging.

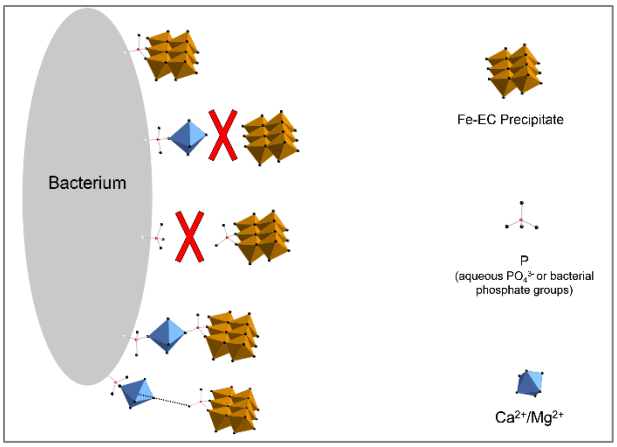

Figure 4-10: Summary diagram of the mechanisms elucidated in chapter 4 regarding the adhesion of EC precipitates to bacterial cell walls. Precipitates interact with bacterial phosphate groups, either directly or via a Ca/Mg bridge (bond or electrostatic). Bivalent cations inhibit adhesion by complexing bacterial phosphate groups. Oxyanions with a strong affinity for Fe(III) precipitates, such as P, inhibit adhesion by competing with bacterial phosphate groups for sorption.

Similarly, our results allow us to predict the impact of hardness and natural organic matter. Because Ca and Mg were found to decrease bacteria removal by complexing bacterial surface groups, Fe-EC is expected to be more effective in soft waters (e.g. most surface water) compared to hard waters (e.g. > 0.6 mM Ca/Mg[171], as in some groundwater). The main functional groups on natural organic matter (NOM) are carboxyl and hydroxyl moieties[172,173], which likely have a lower sorption affinity for Fe(III) (oxyhydr)oxides than bacterial phosphate moieties. Therefore, NOM is not expected to inhibit bacteria removal by Fe-EC substantially, consistent with our previous finding in synthetic Bengal groundwater (Chapter 3). However, in electrolytes where bacteria inactivation by strong oxidants is significant (e.g. at low HCO_3^- concentrations), NOM could potentially quench reactive species and decrease attenuation[81].

Consistent with the universal presence of phosphate groups on bacteria surfaces, Fe-EC is equally effective towards Gram-positive and Gram-negative bacteria, rough and smooth alike. Therefore, our results strongly suggest that Fe-EC, which is a technology applicable to decentralized water treatment in low-resource settings[47,53], can effectively remove all types of

bacterial contamination from a wide range of surface and ground water sources. However, the generalization of the results to wastewater treatment needs to be carefully examined, because wastewater can contain non-negligible concentrations of bivalent cations (e.g. Cu^{2+}, Cd^{2+}, Pb^{2+}, Zn^{2+})[174,175] with a higher affinity for bacterial surfaces than Ca/Mg[130], which could significantly inhibit bacteria removal. Finally, virus attenuation by Fe-EC must be evaluated to assess the potential of this technology to substitute for existing disinfection methods, and field validation is needed before Fe-EC is implemented.

CHAPTER 5. Use of alternatives to arsenic-contaminated groundwater in rural West Bengal, India

1. INTRODUCTION

In rural West Bengal, India, groundwater tubewells supply drinking water to 80% of 13.8 million households[18]. Tubewell coverage is dense and yields are adequate[35], but the quality of shallow groundwater (typically 15-60 m deep) is poor. Toxic levels of naturally-occurring arsenic put an estimated 9.5 million people at risk of skin lesions, impaired cognitive functions, cardiovascular and lung diseases, cancers, and premature death[1,20,21]. In addition, high levels of iron[14,36] alter the color and taste of water, and may cause adverse health effects[42] such as gastrointestinal (GI) disorders[43]. Finally, due to the sustained prevalence of open defecation (51%)[18] and the close proximity of latrines to tubewells, which are not always adequately sealed, shallow groundwater contains non-negligible fecal contamination[37,39,41], potentially causing diarrheal illnesses.

Alternatives to shallow groundwater in the region can be sorted into three categories: source switching (e.g. publicly-provided deep tubewells and piped water), household water treatment, and purchased water from small-scale independent providers (SSIPs, predominantly informal). Deep tubewells have lower levels of iron and microbial contamination than shallow tubewells[36,37], and can also be arsenic-safe if sufficiently deep (typically deeper than 150 m)[1]. Domestic filters, generally made of sand or ceramic, remove iron and some fecal contamination, and can also remove arsenic if they have an additional iron or activated alumina component[1]. Municipal piped water (treated), which is available in some areas, is supplied for free at public taps. Finally, 20-L containers of treated water can be purchased from local private (or non-profit) water providers who operate small treatment plants.

Identifying what motivates households to use alternatives to shallow groundwater is crucial to design effective arsenic mitigation strategies. Interventions in the region have focused on disseminating information about arsenic levels in wells[176,177], but there is growing evidence that behavioral factors may play at least as significant of a role in changing water practices as knowledge about contaminants[178,179]. Studies in rural Bangladesh found that social norms, self-efficacy, taste and convenience influence the use of arsenic-safe alternatives[180,181]. However, these studies focused on arsenic alone. The impact of more tangible groundwater problems, such as iron and gastric illness, on the use and avoidance of shallow tubewells has not been investigated. Understanding how water sources are chosen when several contaminants co-occur will contribute to the literature about the respective roles of information, perceptions, and behavioral factors in shaping water practices (e.g. [182]). In addition, while socioeconomic status (SES) may affect the use of safe water options[183], identifying drivers of behavior change that do not depend on SES can help in designing inclusive interventions.

This chapter also investigates the potential for arsenic-safe water provision through SSIPs. SSIPs are prevalent worldwide in areas where formal public water provision is insufficient[184]. Their critical role in filling a service gap for the poor and their ability to tailor services to low-income customers has been recognized[185–187]. In addition, they can be financially sustainable without subsidies[185], and as cost recovery has become a priority in water supply[188,189], SSIPS have gained attention. SSIPs are active in areas such as rural West Bengal: in Murshidabad district alone, there are approximately 700 "mini-plants" –predominantly informal– treating an estimated 1,200,000 liters of water per day[190]. However, little is documented about the number, type, and water consumption practices of households served by SSIPs in rural West Bengal. Such knowledge would help assess to what extent the supply of treated water through SSIPs, which is in effect a case of privatization[191,192], can be part of the solution to the arsenic crisis.

In this context, four questions motivated this chapter: (1) To what extent do households in rural West Bengal use alternatives to shallow groundwater? (2) What are the factors driving the use of alternatives? (3) How do households choose between different competing alternatives? (4) Where purchased water is available, to what extent can it be a solution to shallow groundwater contamination? In this work, "alternatives" include all water sources *perceived* by households to be of better quality than private tubewells, irrespective of the actual safety of these sources. This approach is legitimate because household decisions regarding drinking water are known to be driven by perceptions of water quality, which are not always correlated with actual quality[193,194].

We conducted a systematic survey of 501 households in the severely arsenic-affected and relatively poor district of Murshidabad, in West Bengal, India. We surveyed two distinct areas with different sets of alternatives to shallow groundwater. For Area 1 (n=409), we investigated the socioeconomic and behavioral factors predicting the use of filters, purchased water from SSIPs, and government (deep) tubewells. We further investigated the factors influencing the consumption of water from SSIPs, locally known as *kena jol* (literally, "purchased water"; henceforth KJ). Area 2 (n=92) allowed us to investigate changes in household water practices up to 18 months after free piped water became available. Overall, our results show that, after SES, risk perception of gastric illness or dissatisfaction with iron are the primary predictors of the use of alternatives to shallow groundwater, prevailing over arsenic risk perception. This finding indicates that households react primarily to readily noticeable water problems, rather than to arsenic contamination. Finally, despite a significant literature suggesting that SSIPs can serve the poor, we found that KJ does not provide universal access to treated drinking water in our study site, as both the use and the degree of use of this alternative are strongly associated with SES. Overall, this chapter provides insights into household drinking water decisions in rural West Bengal, India, and analyzes the competition amongst different alternatives to arsenic-contaminated groundwater. Our results can inform arsenic mitigation interventions in the region.

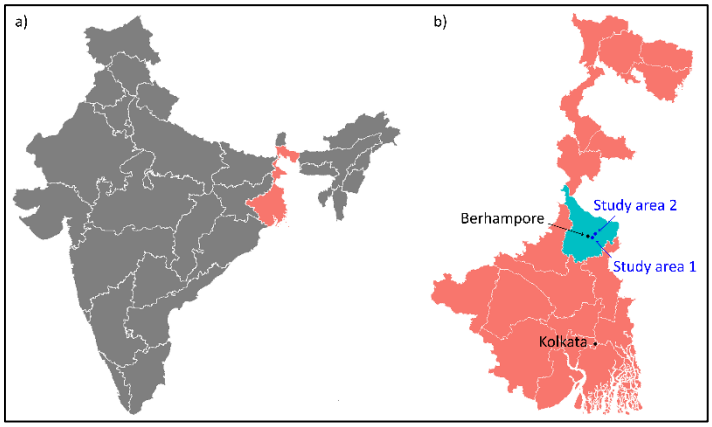

Figure 5-1: Location of study areas. a) Map of Indian states showing West Bengal in red. b) Map of West Bengal districts showing Murshidabad district in blue, with study areas 1 and 2.

2. METHODS

2.1. Selection of Field Site

West Bengal, neighbor to Bangladesh, has 19 districts and a population of 91.3 million people[18]. Murshidabad district's (Figure 5-1) population of 7.1 million is predominantly Muslim (66%) and rural (80%)[18]. It is one of the poorest[195] and most severely arsenic-affected districts in the state[21]. Arsenic mitigation efforts of the last decades largely failed[14], thus much of the population remains exposed to arsenic-unsafe groundwater.

We selected our study areas based on three criteria: (1) the extent of arsenic contamination, which we conservatively defined as the fraction of shallow wells tested by PHED exceeding 50 µg/L of arsenic[196] (the WHO MCL is 10 µg/L[45]), (2) the population size[18], and (3) the availability of alternatives to shallow groundwater. These criteria led us to Berhampore block, within which we identified three highly arsenic-affected villages with populations large enough to yield our desired samples. Two of these villages (Purbba Narayanpur and Putijol) were in effect a single geographical study area (Area 1, 2945 households) and the third was geographically distinct (Area 2, 1370 households).

Areas 1 and 2 are both classified as "rural" by the Census of India but they are located close to Berhampore city (population: 195,000 in 2011) (Figure 5-1). Their demographic and socioeconomic characteristics, shown in Table 5-1, indicate that they are broadly representative of rural West Bengal. According to the 2011 Census, tubewells are the main source of water for over 99% of households in both areas[18]. Arsenic measurements conducted by the National Rural Drinking Water Program (NRDWP) in 2014 indicate high levels of arsenic for Area 1 (20 to 210 µg/L, n=20) and Area 2 (10 to 220 µg/L, n=9)[197]. Our own measurements in Area 1 (n=30) showed even higher levels (30-300 µg/L). Iron concentrations in tubewell water were high, as we regularly observed from water discoloration, and as confirmed by NRDWP measurements of 0.4 mg/L - 5.0 mg/L (n=28) in 2014 (the WHO MCL is 0.3 mg/L)[197]. In addition, high rates of open defecation

(41% Area 1 and 60% in Area 2, Table 5-1) increase the risk of fecal contamination of groundwater.

Area 1 had three alternatives to shallow groundwater: government-provided (deep) public tubewells, domestic filters and KJ. KJ was mainly sourced from a "mini-plant" operated by an informal local entrepreneur (Figure 5-2); water packaged in 20L plastic containers was delivered for INR 20-30 (INR 61 = USD 1 in 2014). Filters varied widely in type and price (Figure 5-3, INR 100-14,000), from self-made sand-based filters to purchased filters using fine pore-size (ceramic) or more selective (e.g. activated alumina) media. Area 2 also offered three alternatives: filters, KJ and piped water. Piped water had become available 1-18 months prior to our survey and was intermittent (twice a day for ~3 hours) at seven, reportedly self-installed and unauthorized, free public taps. We analyzed these areas as separate case studies without pooling the data.

Table 5-1: Demographic and socioeconomic description of Areas 1 and 2 based on 2011 census data. Comparison with broader rural Berhampore block, Murshidabad district and West Bengal, and with survey sample.

	Census of India, 2011					**Our survey, 2014**	
	West Bengal (state) Rural	**Murshidabad (district) Rural**	**Berhampore (block) Rural**	**Study area 1**	**Study area 2**	**Study area 1 (n=409)**	**Study area 2 (n=92)**
Demography (% population)							
Scheduled caste or tribe	35	14	18	5	23	0	52
Literate	63	56	61	58	58	70	65
Religion (Muslim:Hindu)	31:66	69:31	63:36	-	-	100:0	45:55
Income source (% workers)							
Cultivation	61	59	66	74	67	-	-
Other	39	41	34	26	33	-	-
Assets (% households)							
Banking services	40	33	33	24	28	88	87
Radio/TV	34	25	28	20	15	42	38
Computer	5	5	4	2	1	0	0
Mobile phone	34	28	30	30	27	83	75
Bicycle	58	53	63	66	61	86	84
Motorcycle	6	4	4	3	4	21	11
No above asset	29	36	29	28	32	6	7
Dwelling (% households)							
Finished floor	23	21	29	14	26	38	32
Pacca or mixed walls	34	46	60	49	54	78	67
Mud, bamboo, or thatch walls	62	54	39	51	45	22	33
Built roof (as opposed to tiles or hay)	17	26	32	20	19	51	30
Main source of drinking water (% households)							
Tubewell	80	92	93	99	100	-	-
Sanitation (% households)							
Improved latrine	41	31	38	40	26	-	-
Open defecation	51	64	55	41	60	-	-

Figure 5-2: Production and distribution of 20 L containers of treated water in Area 1. a) Treatment unit including several filters and a reverse osmosis membrane. b) Storage tank and filling station. c) Distribution of treated water to households.

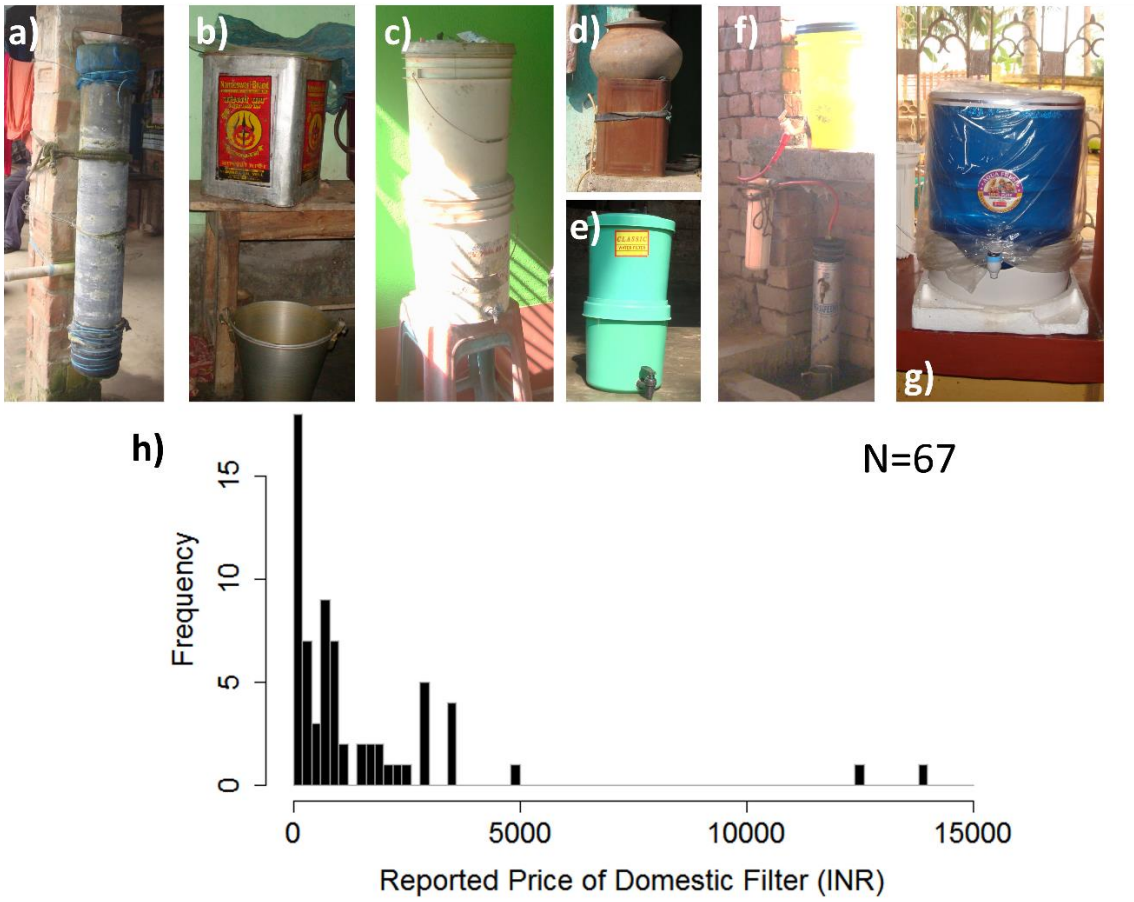

Figure 5-3: Overview of domestic filters in Area 1. Self-made filters: pipe (a) or tin jar (b) filled with sand and gravel; plastic bucket (c) or ceramic pot (d) filled with sand and gravel feeding into a storage container. Purchased filters: two-bucket "candle" filter (e), activated-alumina filter (f), and reverse-osmosis filter (g). h) Distribution of reported prices of domestic filters, from 100 INR (~1.5 USD) to 14,000 INR (~200 USD).

2.2. Data Collection

For this exploratory study we decided *a priori* on an overall sample size of 500. We allocated ~ 80% of this sample size to Area 1 (n=409), where household water practices varied more than in Area 2 (n=92) (Figures 5-6 and 5-12). We used a systematic sampling strategy in which we interviewed every 4th household, starting from the beginning of a street. If household members were unavailable or unwilling, the next house was selected. 52.7% of respondents were female. Tables 5-1, 5-2 and 5-3 present socioeconomic and demographic characteristics of the surveyed households.

Table 5-2: Demographic and socioeconomic characteristics of surveyed households in Areas 1 and 2. When appropriate, 5th and 95th percentiles are indicated. INR 61 = USD 1 in 2014. When applicable, averages and 90% confidence intervals (CI, 5th and 95th percentiles) are reported.

	Study area 1 (n=409)	**Study area 2 (n=92)**
Respondents		
Gender	51.3% F, 48.7% M	58.7 % F; 41.3 % M
Age	41.6 (22.3-65.0)	38.6 (20.6-57.5)
Years of schooling	4.5 (0-12)	4.0 (0-13)
> 0 years of schooling (≈ literacy rate)	70.2 %	65.2 %
Household concerns (% times listed in top three)		
Poverty	53.5	60.9
Health, diseases	39.6	28.3
Water	38.9	17.4
Food	32.3	51.1
Education, school	27.6	34.8
Unemployment	18.8	23.9
Households		
Religion	100% Muslim	44.6 % Muslim; 55.4 % Hindu
Size	4.1 (2-7)	4.3 (2-6)
Number of children	1.5 (0-4)	1.5 (0-3)
Number of rooms	2.8 (1-5)	2.9 (1-5)
Land ownership	59.2 %	20.7 %
Metered electricity connection	82.9%	80.4%
Member abroad	9.0 %	1.1 %
Member away in country	9.3 %	14.0 %
Type of income source	54.5 % cultivation 42.1 % daily labor 24.7 % business 17.6 % remittances	16.3 % cultivation 66.3 % daily labor 20.7 % business 15.1 % remittances
Monthly expenditures	Phone: INR 205 (0-600) Soap, cosmetics: INR 259 (40-800) Cigarettes: INR 157 (0-600)	Phone: INR 140 (0-490) Soap, cosmetics: INR 157 (40-400) Cigarettes: INR 156 (0-434)

Higher socioeconomic indicators in our sample compared to census data (Table 5-1) could result from three factors. First, asset ownership may be under-reported in government census surveys, for fear of losing social benefits targeted towards the poor. Second, mobile phone ownership in rural India increases by 20% per year[198], consistent with the substantial discrepancy between the two datasets. Third, despite our efforts to ensure that our sampling strategy was followed, our surveyors may have been subject to sampling bias towards wealthier households.

Our household survey collected detailed information on all the sources of drinking water, their frequency of use, and the household members using them. We collected data on a number of demographic, socioeconomic, behavioral and risk perception factors. Questions testing factual knowledge about arsenic were asked at the end to avoid biasing respondents' answers during the survey. A translator external to the research team translated the survey instrument from English to Bangla.

The survey was piloted and administered by four enumerators, residents of Murshidabad district and with at least high-school education, who were trained and supervised by our research team. Data were collected on Android tablets (Datawind UbiSlate 3G7) using Open Data Kit Collect (version 1.4.4). Each household interview took 45 to 60 min. The lead author (with working knowledge of Bangla) accompanied enumerators in the field every day and attended 25% of household interviews. At the end of each sampling day, the lead author and the enumerators checked the new datasets for quality and completeness.

Table 5-3: Primary community problems, household concerns and health concerns according to survey respondents in Areas 1 and 2. These questions were asked at the very beginning of each interview.

	Study area 1 (n=409)	**Study area 2 (n=92)**
Community problems (% times listed in top three)		
Water	81.7	58.7
Roads	48.2	45.7
Sanitation	40.3	28.3
Poverty	29.1	45.7
Household concerns (% times listed in top three)		
Poverty	53.5	60.9
Health, diseases	39.6	28.3
Water	38.9	17.4
Food	32.3	51.1
Education, school	27.6	34.8
Unemployment	18.8	23.9
Household health concerns (% times listed in top three)		
"Gas" (gastrointestinal disorders)	63.3	51.1
Fever	63.1	87.0
Cough	39.3	48.9
Arsenic	0.0	0.0

2.3. Definition of Outcome and Explanatory Variables

Our outcome variable was the use of alternatives to drinking untreated water from private tubewells. An "alternative" was defined as any water source that was not a private tubewell, irrespective of the actual microbial and chemical safety of this source. Government tubewells were not counted as an alternative for households that did not have a private tubewell (or access to a neighbor's tubewell). We found 60-200 µg/L of arsenic in the four government tubewells that we sampled, even though they were considered safer than private tubewells. Our observations of the technologies used in the mini-plant in Area 1 and in most filters in use, suggest that many alternatives were not optimized for arsenic removal, though we did not directly test water quality from these alternatives.

Surveyed households displayed five levels of adoption in the use of alternatives: (1) no use; (2) occasional use, for celebrations, visitors, or when a household member was sick; (3) regular use by only some household members; (4) regular use by all household members, but concurrent with private tubewells; (5) exclusive use. Unless indicated otherwise, our analyses focused on regular use, aggregating levels of adoption 3, 4 and 5.

Drawing from the literature on safe water uptake[178,180,183,193,199–202], we selected 13 potential explanatory variables for the adoption of alternatives to shallow groundwater. SES has been linked to the adoption of safe water and sanitation behaviors[183,199]. Using principal components analysis (PCA) to assign weights to each asset and expenditure, we derived an SES index from asset ownership and two non-subsistence expenditures (cosmetics and phone recharge)[203]. We included a variable for income stability -calculated from household income sources- because it could potentially affect the preference for filters (one-time investment) versus KJ (regular small payments). Peer behavior and feelings of pride have been found to moderately affect safe water practices in low-income communities[200,201]. Variables reflecting social influence in our study were participation in a women's group, peer behavior, and recommendations about drinking water from peers or influential community members. Risk perception is often included in health behavior studies[182,204]. We defined risk perception of gastric illness as a combination of expressed complaints and self-perceived likelihood of getting gastric illness from tubewell water. Arsenic risk perception was defined as a combination of expressed complaints and factual knowledge about arsenic (e.g. visibility, health effects, treatment methods). We used dissatisfaction with iron as a proxy for iron risk perception, because there are no agreed-upon symptoms of iron ingestion. Self-efficacy, which may affect the ability to act upon one's condition[178,205], was defined as the expressed importance of personal effort (hard work, education) compared to fate[205]. Perceived taste, color, safety and convenience may influence the adoption of safe water options[178,180,193,202], and indicators for such perceptions were included. We also included a proxy for extra-household exposure to KJ, based on frequent travel to urban areas. Finally, the presence of small children, who are the most vulnerable to gastric illnesses[206], was included, as this may affect household water decisions. The derivation of each explanatory variable is detailed in the Appendix.

2.4. Statistical Data Analysis

We investigated correlations among explanatory variables using estimated covariance and PCA. For PCA, we only report principal components with an eigenvalue greater than 1. Correlations between explanatory variables and outcome variables were explored using PCA and then further analyzed with logistic regressions in hierarchical models. We did not use PCA as a variable reduction method, but rather as a preliminary approach to inform our hierarchical regression models.

In a logistic model, the probability of a binary outcome *p* for household *i* is defined by Equation 5-1, where β_0 is the intercept, β_j are the regression coefficients (log of odd ratios), EV_j are the explanatory variables, and K is the number of explanatory variables included in the regression.

$$ln\left(\frac{p_i}{1-p_i}\right) = \beta_0 + \sum_{j=1}^{K} \beta_j * EV_{j,i} \qquad \text{(Equation 5-1)}$$

In our analyses, the outcome was successively defined as the use of *any* alternatives, and then of KJ, filters, government tubewells, and piped water individually. We first regressed each outcome variable against each explanatory variable in isolation (K=1). We then built hierarchical models with a first block of explanatory variables that the PCA analysis indicated were highly correlated with the outcome (K=1-2). We progressively added blocks of variables (K=3-12) to end with the fully-adjusted model (K=13). The conceptual framework of hierarchical regressions is summarized in Figure 5-4. This step-wise approach allowed us to identify confounding variables (i.e. explanatory variables decreasing the impact of the main predictors), as well as variables with an overrated impact in the fully-adjusted models.

In addition, multinomial logistic regressions were used to compare between users of different alternatives, according to Equation 5-2, where the reference category was successively the use of no alternative, KJ and filters:

$$ln\left(\frac{p_{alternative\ x,i}}{p_{ref.category\ y,i}}\right) = \beta_{0,xy} + \sum_{j=1}^{K} \beta_{j,xy} * EV_{j,xy,i} \qquad \text{(Equation 5-2)}$$

All regressions were conducted both on the full data set and on two socioeconomic subsets (below and above median SES). Finally, to further explore the factors affecting the degree of use of KJ (Area 1) or piped water (Area 2), we compared the distributions of explanatory variables for different categories of users. PCA and binary logistic regressions were used to confirm these observations, even though their robustness may be limited due to the small sample size (n=101 and 92 respectively). All statistical analyses were conducted using R (version 3.2.0).

2.5. Ethics

This study was approved by the Committee for the Protection of Human Subjects at the University of California Berkeley (protocol number 2014-06-6433). All respondents provided informed verbal consent before participating in the survey.

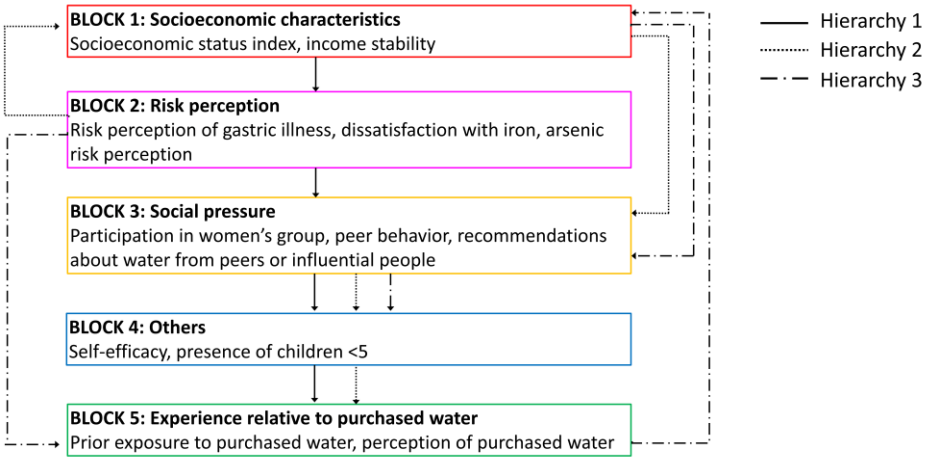

Figure 5-4: Conceptual framework for hierarchical regression models. 3 hierarchies are represented.

3. RESULTS: AREA 1

3.1. Explanatory Variables

Table 5-4 indicates that explanatory variables were generally mildly correlated (most coefficients between -0.3 and 0.3). SES and income stability (correlation coefficient = 0.5), and risk perception of gastric illness and dissatisfaction with iron (correlation coefficient = 0.4) were more strongly correlated. The first principal component (PC1) of the 13 explanatory variables was dominated by SES, income stability and arsenic risk perception, while PC2 was dominated by dissatisfaction with iron, risk perception of gastric illness and perception of KJ (Figure 5-5).

The correlation between dissatisfaction with iron and risk perception of gastric illness suggests that respondents tended to attribute GI disorders to iron, which they can see and taste. Enumerators indeed noted the widespread belief that iron causes gastric illness. The correlation between perception of KJ and iron/gastric illness variables was expected, because our survey assessed appreciation of KJ by comparison with tubewell water.

PCA indicated a significant correlation between arsenic risk perception and socioeconomic indicators (Figure 5-5). Overall, factual knowledge about arsenic was low (65% of respondents stated having no knowledge about arsenic), and significantly lower for female than for male respondents (-0.35, $p<0.001$). Only two respondents had visible arsenicosis symptoms (skin pigmentation), possibly explaining the lack of arsenic awareness in the community. In contrast to arsenic risk perception, dissatisfaction with iron and risk perception of gastric illness were largely independent of SES (Figure 5-5) and gender.

Table 5-4: Correlation table and summary statistics (mean, standard deviation and boxplot) of 13 explanatory variables in Area 1. Statistical significance: •: p<0.1; *: p<0.05; **:p<0.01; ***:p<0.001.

Variables	**1**	**2**	**3**	**4**	**5**	**6**	**7**	**8**	**9**	**10**	**11**	**12**	**13**
SES													
Income stability	0.50***												
Exposure to KJ	0.10*	0.13**											
Women's group	-0.01	0.02	0.01										
Peer behavior	0.13**	0.07	-0.06	-0.01									
External advice	0.00	-0.05	0.02	-0.02	0.04								
Doctor's advice	0.21***	0.23***	-0.03	0.08	0.04	-0.22***							
Risk perc. "gas"	0.19***	0.20***	0.02	0.08	0.14**	0.03	0.05						
Diss. with iron	0.15**	0.06	0.00	0.03	0.04	0.02	0.06	0.39***					
Arsenic risk perc.	0.27***	0.22***	-0.02	-0.10*	0.14**	0.14**	0.19***	0.12*	0.12*				
Children <5	-0.05	-0.04	-0.02	-0.13*	0.00	-0.06	0.09•	-0.09•	-0.03	0.04			
Self-efficacy	0.15**	0.09•	-0.14**	0.04	0.16**	0.05	0.08	0.11*	0.11*	0.18***	0.10*		
Perception of KJ	0.05	0.00	-0.02	-0.02	0.11*	0.14**	0.01	0.13*	0.14**	0.06	0.06	0.06	
Mean	-0.002	0.000	0.000	0.000	0.000	0.000	0.000	-0.010	0.000	0.000	0.000	0.000	0.000
St. dev.	0.54	1.00	1.00	1.00	1.00	1.00	1.00	0.70	0.81	0.74	1.00	1.00	0.69

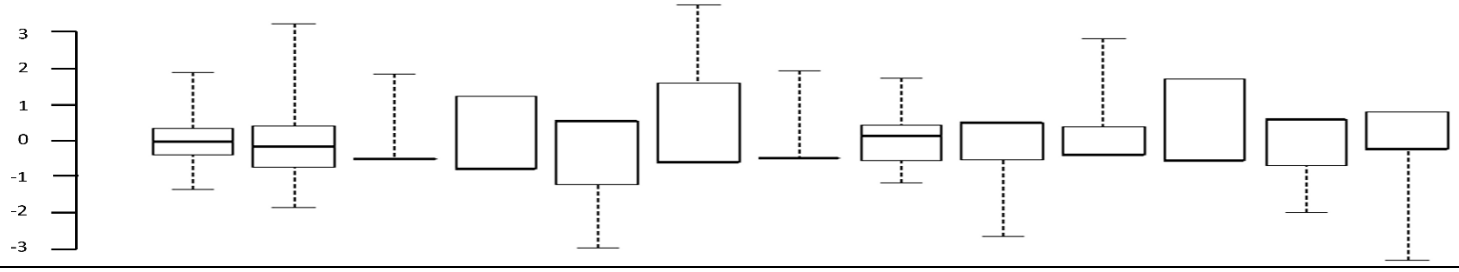

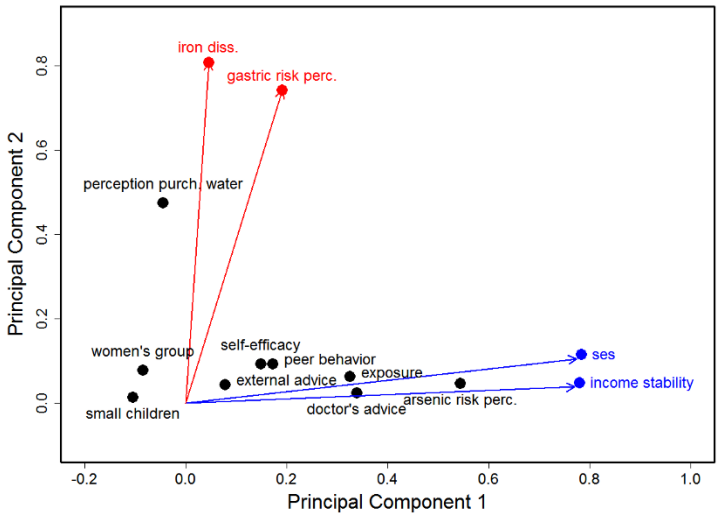

	PC1	PC2	PC3	PC4	PC5
Socioeconomic status	**0.78**	0.11	0.06	0.05	-0.04
Income stability	**0.78**	0.05	-0.05	0.15	-0.09
Exposure to purchased water	0.33	0.06	**-0.64**	-0.13	0.04
Women's group participation	-0.08	0.08	0.13	0.19	**-0.69**
Peer behavior	0.17	0.09	**0.52**	-0.15	-0.04
External advice	0.08	0.04	0.14	**-0.79**	0.03
Doctor's advice	0.34	0.02	0.17	**0.64**	0.05
Risk perception of gastric illness	0.19	**0.74**	0.06	0.02	-0.19
Dissatisfaction with iron	0.05	**0.81**	0.01	0.07	-0.02
Arsenic risk perception	**0.54**	0.05	0.34	-0.14	0.24
Presence of children <5	-0.10	0.01	0.10	0.29	**0.72**
Self-efficacy	0.15	0.09	**0.67**	0.04	0.04
Perception of purchased water	-0.04	**0.47**	0.14	-0.21	0.28
Cumulative % of variance explained	14%	26%	36%	46%	55%

Figure 5-5: Principal component analysis of 13 explanatory variables in Area 1 (rotation with 5 principal components).

3.2. Description of Household Water Practices

Figure 5-6a shows the breakdown of household drinking water sources in Area 1. Of all households, 54% used private tubewells exclusively. KJ, filters and government tubewells were used by 25%, 19% and 8% of households, respectively. Most users reported using KJ irregularly or concurrently with untreated tubewell water; only 34% reported using it exclusively (or with another alternative). Exclusive use was similar for government tubewells (31%) but significantly higher for filters (82%). The degree of use of alternatives is summarized in Figure 5-6b, which is consistent with other studies reporting non-exclusive use of safe water options[207,208]. Finally, water from filters was often used for cooking (65%), in contrast with KJ (3%) and government tubewell water (22%) (Table 5-5).

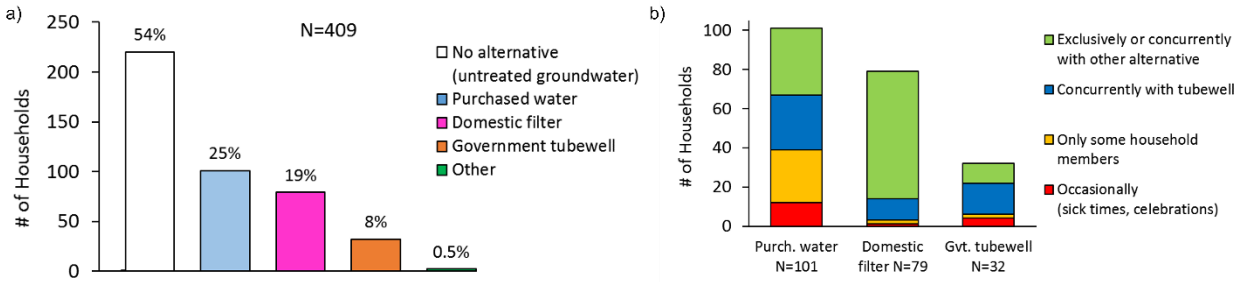

Figure 5-6: Household water practices in Area 1. a) Household drinking water sources. b) Degree of use of 3 alternatives to shallow groundwater (KJ, filters, and government tubewells).

Table 5-5: Details on use of drinking water sources in Areas 1 and 2. When applicable, averages and 90% confidence intervals (CI, 5th and 95th percentiles) are reported. *Children<5 were counted as 0.5 person. INR 61 = USD 1 in 2014.

	Study area 1 (n=409)	**Study area 2 (n=92)**
Use of tubewells		
# of collections per day *(all households)*	4.8 (2.0-11.8)	3.5 (1.0-8.1)
Use of purchased water		
Reported price *(all households)*	INR 25.9 (20-30)	INR 27.5 (20-35)
Don't know price *(all households)*	2.4%	31.5%
Volume (L) per day and per person* *(users)*	1.2 (0.2-2.9)	NA
Use purchased water for cooking *(users)*	3.0%	NA
Use of domestic filters		
Use of domestic filters for cooking *(users)*	65%	67%
Use of government tubewells		
Use of government tubewells for cooking *(users)*	22%	NA
Use of piped water		
# of collections per day *(users)*	NA	1.9 (0.3-3.5)
Use of piped water for cooking *(users)*	NA	61%

3.3. Factors Influencing the Use of Alternatives

In Table 5-6, we present logistic regressions of the regular use of alternatives (all alternatives combined) against different blocks of explanatory variables. Occasional users of alternatives (n=17, Figure 5-6b) were not included. The fully adjusted model shows that SES and risk perception of gastric illness were the primary predictors of the use of alternatives, followed by arsenic risk perception and dissatisfaction with iron. Likewise, the PCA (Figure 5-7) indicates that the use of alternatives was almost exclusively determined by PC1 (SES, income stability, arsenic risk perception) and PC2 (dissatisfaction with iron, risk perception of gastric illness, perception of KJ).

Our hierarchical models show that none of the other variables significantly modified the effect of the main predictors (Table 5-6). Controlling for SES decreased the effect of arsenic risk perception, but did not impact the effect of perceived iron or gastric illness risk. In addition, the effects of SES and risk perception of gastric illness decreased when controlling for income stability and dissatisfaction with iron respectively, consistent with the close correlations between these variables (Table 5-4 and Figure 5-5). Self-efficacy appears to be negatively correlated with the use of alternatives in the fully-adjusted model (Table 5-6, column 7). However, there is no such correlation in the non-adjusted model (Table 5-6, column 1), which indicates that the correlation in the fully-adjusted model is an artifact of controlling for variables associated with self-efficacy (arsenic knowledge, SES and risk perception of gastric illness).

Table 5-6: Regression coefficients for the use of alternatives to shallow groundwater in Area 1 (all alternatives combined) using hierarchical models. K is the number of explanatory variables in the model. 178 regular users of alternatives out of 409 households. Grey cells indicate variables not included in the model. Statistical significance: •: p<0.1; *: p<0.05; **:p<0.01; ***:p<0.001.

	K=1	**K=1**	**K=2**	**K=5**	**K=9**	**K=11**	**K=13**	**K=1**	**K=2**	**K=3**	**K=5**
Socioeconomic status	1.6***	1.6***	1.3***	1.1***	1.1***	1.2***	1.2***				1.1***
Income stability	0.6***		0.3*	0.2 •							0.2 •
Exposure to purchased water	0.1										
Women's group participation	- 0.1										
Peer behavior	0.2*										
External advice	0.0										
Doctor's advice	0.4***										
Risk perception of gastric illness	1.0***			0.8***	0.8***	0.8***	0.8***	1.0***	1.0***	0.8***	0.8***
Dissatisfaction with iron	0.7***			0.4*	0.4*	0.4*	0.4*			0.4*	0.4*
Arsenic risk perception	0.8***			0.5**	0.4*	0.5**	0.5**		0.7***	0.7***	0.5*
Presence of children <5	0.0										
Self-efficacy	0.1					- 0.2 •	- 0.2 •				
Perception of purchased water	0.4*										

The outcomes of fully-adjusted logistic regressions for the use of KJ, filters and government tubewells -individually- are given in Table 5-7 (columns 2-7). We show results of

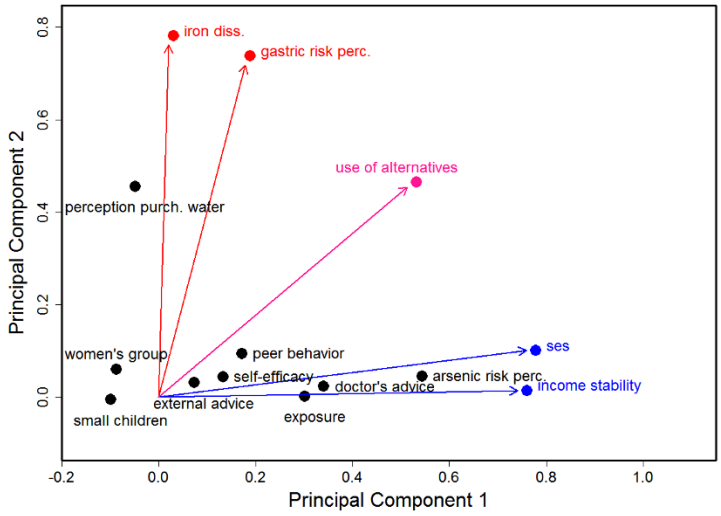

	PC1	PC2	PC3	PC4	PC5
Socioeconomic status	**0.78**	0.10	0.06	-0.04	-0.05
Income stability	**0.76**	0.01	-0.03	-0.14	-0.12
Exposure to purchased water	0.30	0.00	**-0.59**	0.14	-0.01
Women's group participation	-0.09	0.06	0.15	-0.18	**-0.71**
Peer behavior	0.17	0.09	**0.51**	0.15	-0.03
External advice	0.07	0.03	0.14	**0.80**	0.02
Doctor's advice	0.34	0.02	0.18	**-0.64**	0.05
Risk perception of gastric illness	0.19	**0.74**	0.06	-0.01	-0.20
Dissatisfaction with iron	0.03	**0.78**	0.03	-0.05	-0.04
Arsenic risk perception	**0.54**	0.04	0.33	0.15	0.24
Presence of children <5	-0.10	-0.01	0.13	-0.28	**0.70**
Self-efficacy	0.13	0.04	**0.71**	-0.03	0.00
Perception of purchased water	-0.05	**0.46**	0.16	0.21	0.27
Use of alternatives	**0.53**	**0.46**	-0.06	-0.06	0.11

Figure 5-7: Principal component analysis of the use of alternatives and 13 explanatory variables in Area 1 (rotation of 5 principal components).

both binomial regressions (where users and non-users of a given alternative are compared, columns 2-4) and multinomial regressions (where users of an alternative are compared to households not using any alternative at all, columns 5-7). Following SES, risk perception of gastric illness and dissatisfaction with iron were the primary predictors of KJ and filter use respectively. A socioeconomic comparison between users and non-users of KJ (Table 5-9) confirms higher SES for KJ users. Perception of KJ (aesthetics and safety) and doctor's advice were also significantly correlated with KJ use. The use of government tubewells, which is free, was not correlated with SES, and was only governed by risk perception of gastric illness. Regressions using hierarchical models for the individual use of KJ and filters (Tables 5-8 and 5-10, respectively) were similar to those for all alternatives combined.

We performed subset analyses for below and above median SES (Table 5-11). These analyses suggest that SES and arsenic risk perception only predicted the use of alternatives in the above-median subset, with little to no influence in the below-median subset. Dissatisfaction with iron, a strong predictor of filter use, was substantially amplified in the below-median subset. Finally, risk perception of gastric illness and perception of KJ were supplanted by doctor's advice as a predictor of KJ use in the below-median subset.

3.4. The Choice among Several Alternatives

Our multinomial regression results suggest that two variables predicted the choice of alternative among households using these (N = 178): a higher SES favored filters and KJ, and participation in a women's group favored KJ (Table 5-7, columns 8 – 10). While the role of SES in the choice between paying and free alternatives is intuitive, the link between women's groups and the preference for KJ is more difficult to interpret. A favorable perception of KJ was a secondary predictor of KJ use.

Except for dissatisfaction with iron, which favored filters, risk perception factors (gastric illness, arsenic) were not significantly different among users of different alternatives. This suggests that even though the use of alternatives is related to higher risk perceptions (Table 5-7, column 1), the choice among available alternatives is dictated by SES, social interactions and perceptions of KJ.

Table 5-7: Regression coefficients for the use of each specific alternative in Area 1 (KJ, filter and government tubewell) using fully-adjusted binomial and multinomial models. The number of households in each regression is indicated. Statistical significance: •: p<0.1; *: p<0.05; **:p<0.01; ***:p<0.001.

	Binomial logistic regressions				**Multinomial logistic regressions**					
					Ref = No alternative			**Ref = KJ**		**Ref = Filt**
	Any alt. (178:409)	**KJ (89:409)**	**Filter (78:409)**	**Gvt. tw (28:409)**	**KJ (89:231)**	**Filter (66:231)**	**Gvt. tw (21:231)**	**Filter (66:89)**	**Gvt. tw (21:89)**	**Gvt. tw (21:66)**
Socioeconomic status	1.2***	0.5 •	1.2***	- 0.9 •	1.2***	1.7***			-1.4*	-1.9**
Income stability										
Exposure to purchased water										
Women's group participation		0.2 •				-0.3 •	-0.7*	-0.4*	-0.7*	
Peer behavior										
External advice								-0.3 •		
Doctor's advice		0.3*			0.3*			-0.3 •		
Risk perception of gastric illness	0.8***	0.7**		0.9**	0.9***	0.6*	1.2***			
Dissatisfaction with iron	0.4*		0.7*			0.8*		0.7 •		
Arsenic risk perception	0.5**		0.4*		0.4*	0.6**				
Presence of children <5										
Self-efficacy	- 0.2 •				-0.3 •					
Perception of purchased water		0.5*			0.6*			- 0.5 •	- 0.7 •	

Table 5-8: Regression coefficients for the use of purchased water in Area 1 using hierarchical models. K is the number of explanatory variables in the model. 89 regular users of purchased water out of 409 households. Grey cells indicate variables not included in the model. Statistical significance: •: p<0.1; *: p<0.05; **:p<0.01; ***:p<0.001.

	K=1	**K=1**	**K=2**	**K=5**	**K=9**	**K=11**	**K=13**	**K=1**	**K=2**	**K=3**	**K=5**	**K=7**
Socioeconomic status	0.9***	0.9***	0.7**	0.5*	0.5 •	0.6*	0.5 •					0.5 •
Income stability	0.4**											
Exposure to purchased water	0.1											
Women's group participation	0.2					0.2 •	0.2 •					
Peer behavior	0.2 •											
External advice	0.1					0.2 •						
Doctor's advice	0.4***				0.3*	0.3*	0.3*					
Risk perception of gastric illness	0.8***			0.6**	0.6**	0.7**	0.7**	0.8***	0.7***	0.7***	0.7***	0.6**
Dissatisfaction with iron	0.4*											
Arsenic risk perception	0.4**								0.4*	0.4*	0.4*	
Presence of children <5	0.1											
Self-efficacy	0.0											
Perception of purchased water	0.6**						0.5*				0.5**	0.5**

Table 5-9: Comparison of socioeconomic indicators between users and non-users of purchased water in Area 1 (INR 61 = USD 1 in 2014). When applicable, averages and 90% confidence intervals (CI, 5th and 95th percentiles) are reported.

	Regular users of purchased water (n=89)	**Non-users of purchased water (n=320)**
Community problems (% times listed in top 3)		
Water	91.0	79.1
Households		
Size	4.5 (2-7)	4.1 (2-7)
Number of children	1.6 (0-4)	1.5 (0-3)
Number of rooms	3.1 (1-6)	2.7 (1-5)
Land ownership	60.7 %	58.8 %
Metered electricity connection	88.8%	81.3%
Member abroad	12.4 %	8.1 %
Member away in country	4.5 %	10.6 %
Dwelling	84.3% concrete, brick or mixed 15.7% mud or bamboo	76.9% concrete, brick or mixed 23.1% mud or bamboo
Roof	97.8% concrete or tiles 2.2% tin or hay	98.4% concrete or tiles 1.6% tin or hay
Floor	52.8% finished	34.1% finished
Refrigerator	8.9%	3.1%
Television/radio	59.6%	36.9%
Watch	42.7%	29.1%
Motorcycle	37.1%	16.3%
Van rickshaw	5.6%	4.4%
Bicycle	92.1%	84.4%
Cell phone	91.0%	80.6%
Kerosene stove	7.9%	7.8%
Gas stove	33.7%	18.1%
Fan	93.3%	83.1%
Goat/cow	77.5%	73.8%
Chicken	76.4%	69.7%
Type of income source	49.4 % cultivation 32.6 % daily labor 41.6 % business 16.9 % remittances	55.9 % cultivation 44.7 % daily labor 20.0 % business 17.8 % remittances
Monthly expenditures	Phone: INR 272 (0-720) Soap, cosmetics: INR 343 (54-1000) Cigarettes: INR 204 (0-600)	Phone: INR 187 (0-505) Soap, cosmetics: INR 236 (40-700) Cigarettes: INR 144 (0-600)

Table 5-10: Regression coefficients for the use of domestic filters in Area 1 using hierarchical models. K is the number of explanatory variables in the model. 78 regular users of domestic filters out of 409 households. Grey cells indicate variables not included in the model. Statistical significance: •: p<0.1; *: p<0.05; **:p<0.01; ***:p<0.001.

	K=1	**K=1**	**K=2**	**K=5**	**K=9**	**K=11**	**K=13**	**K=1**	**K=2**	**K=3**	**K=5**	**K=7**
Socioeconomic status	1.7***	1.7***	1.5***	1.2***	1.2***	1.2***	1.2***					1.3***
Income stability	0.6***		0.3 •									0.3 •
Exposure to purchased water	0.0											
Women's group participation	-0.2											
Peer behavior	0.2											
External advice	-0.2											
Doctor's advice	0.3**											
Risk perception of gastric illness	0.6***							0.6***	0.6**	0.4*	0.4*	
Dissatisfaction with iron	0.9***			0.6*	0.7*	0.7*	0.7*			0.7*	0.7*	0.6*
Arsenic risk perception	0.6***			0.3*	0.4*	0.4*	0.4*		0.6***	0.6***	0.6***	0.3*
Presence of children <5	0.0											
Self-efficacy	0.1											
Perception of purchased water	0.1											

3.5. Use of Purchased Water (KJ)

Figure 5-8 compares the distributions of explanatory variables between occasional users (i.e. during sickness or special occasions), households where only some members drank KJ, non-exclusive users, and exclusive users. SES, income stability, external advice, dissatisfaction with iron, and perception of KJ all trend up with higher degrees of KJ use; this is consistent with the PCA (Figure 5-9) and fully-adjusted regressions (Table 5-12). Finally, linear regressions of the volume of water purchased per person per day against the 13 explanatory variables showed that SES was the only predictor (Table 5-13a), consistent with its importance in the transition from irregular to regular use (Figure 5-8). We found that 12% of surveyed households in Area 1 had purchased water in the past but had since stopped (since up to 2 years prior to the survey). Table 5-13b suggests that interrupting KJ use was predicted by filter ownership and by lower risk perception of gastric illness, doctor's advice and KJ perception.

Table 5-11: Regression coefficients of the use of all alternatives, purchased water, domestic filters and government tubewells in Area 1 using fully-adjusted binomial and multinomial models. Regressions were conducted on 2 socioeconomic subsets (below and above median socioeconomic status). The number of households in each regression is indicated. Statistical significance: •: p<0.1; *: p<0.05; **:p<0.01; ***:p<0.001.

BINOMIAL LOGISTIC REGRESSIONS →																	
	Any alternative			Purchased water			Domestic filter			Government tubewell			Purchased water		
	All (178:409)	Low SES (63:205)	High SES (115:204)	All (89:409)	Low SES (33:205)	High SES (56:204)	All (78:409)	Low SES (17:205)	High SES (61:204)	All (28:409)	Low SES (16:205)	High SES (12:204)	All (89:231)	Low SES (33:142)	High SES (56:89)
Socioeconomic status	1.2 ***		2.2 ***	0.5 •		0.8 •	1.2 ***	3.0 •	1.0 *	- 0.9 •		- 2.6 •	1.2 ***		2.3 ***
Income stability								0.8 *							
Exposure to KJ															
Women group participation				0.2 •		0.4 •					- 0.6 •				
Peer behavior		0.4 •													
External advice									- 0.3 •						
Doctor's advice				0.3 *	0.7 **								0.3 *	0.6 **	
Risk perc. of gastric illness	0.8 ***	0.7 *	1.0 ***	0.7 **		0.8 **				0.9 **	1.0 *	1.0 *	0.9 ***		1.2 ***
Dissatisfaction with iron	0.4 *	0.5 •					0.7 *	1.8 *							
Arsenic risk perception	0.5 **		0.5 *				0.4 *		0.4 •				0.4 *	0.6 •	
Presence of children <5															
Self-efficacy	- 0.2 •	- 0.3 •											-0.3 •		
Perception of KJ				0.5 *		0.6 *							0.6 *		0.6 •

MULTINOMIAL, REF = NO ALTERNATIVE							MULTINOMIAL, REF = PURCHASED WATER						MULTIN., REF=FILTER		
	Domestic filter			Government turewell			Domestic filter			Government tubewell			Government tubewell		
	All (66:231)	Low SES (16:142)	High SES (50:89)	All (21:231)	Low SES (13:142)	High SES (8:89)	All (66:89)	Low SES (16:33)	High SES (50:56)	All (21:89)	Low SES (13:33)	High SES (8:56)	All (21:66)	Low SES (13:16)	High SES (8:50)
Socioeconomic status	1.7 ***	2.8 •	2.5 ***							-1.4 *		-4.0 *	-1.9 **		-4.2 *
Income stability		1.2 **						1.0 *						- 1.1 *	
Exposure to KJ															
Women group participation	-0.3 •	-0.6 •		-0.7 *	- 0.9 *	-0.9 •	-0.4 *	-0.7 •	-0.4 •	-0.7 *	-0.9 *	-1.1 *			
Peer behavior															
External advice			-0.4 •				-0.3 •		-0.4 •						
Doctor's advice						0.6 •	-0.3 •	-1.1 *							
Risk perc. of gastric illness	0.6 *		0.8 *	1.2 ***	1.3 **	1.7 *									
Dissatisfaction with iron	0.8 *	2.0 *					0.7 •	1.7 •							
Arsenic risk perception	0.6 **		0.6 *												
Presence of children <5						-8.6 ***						-9.0 ***			-9.3***
Self-efficacy															
Perception of KJ							- 0.5 •	-1.1 •		- 0.7 •		-1.3 *			

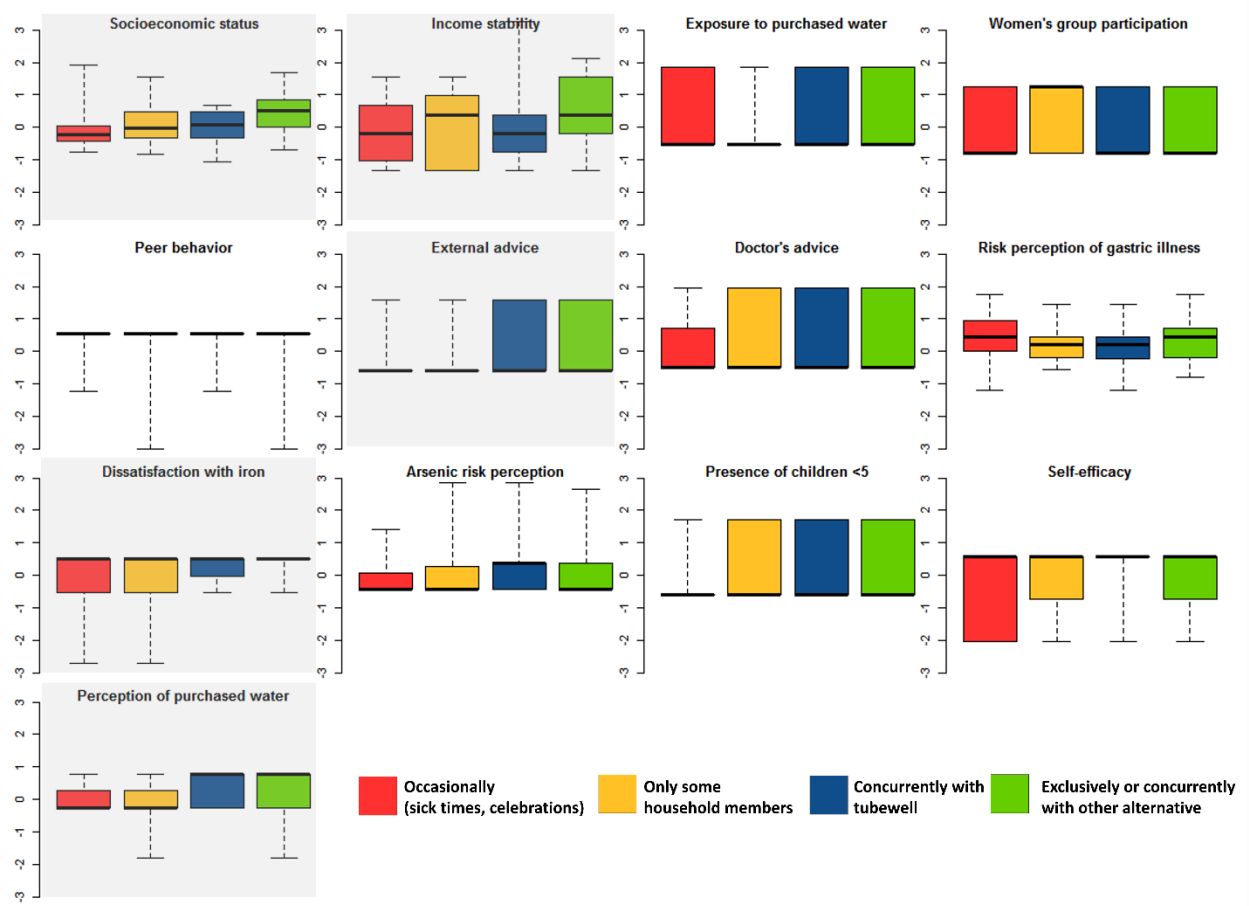

Figure 5-8: Comparison of explanatory variables between 4 categories of households using purchased water in Area 1 (n=101). Grey backgrounds indicate variables showing an upward trend as the degree of purchased water use increases.

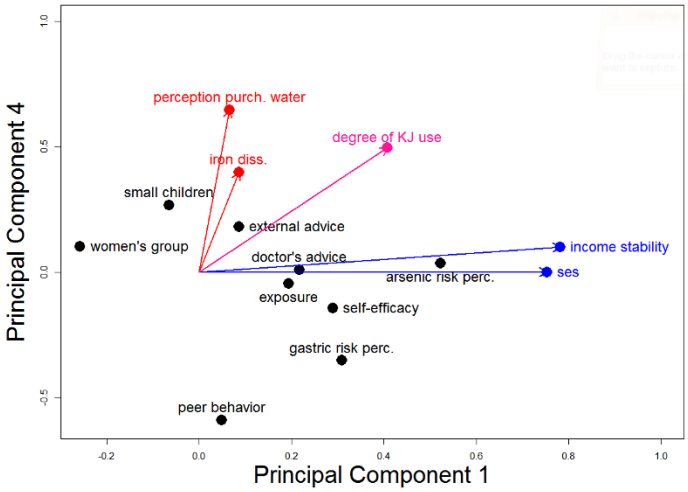

	PC1	PC2	PC3	PC4	PC5
Socioeconomic status	**0.75**	0.05	0.09	0.00	-0.18
Income stability	**0.78**	-0.22	0.08	0.10	0.05
Exposure to purchased water	0.19	0.23	-0.11	-0.05	**-0.69**
Women's group participation	-0.26	-0.13	**0.65**	0.10	0.09
Peer behavior	0.05	0.19	-0.11	-0.59	0.36
External advice	0.09	**0.82**	0.01	0.18	0.09
Doctor's advice	0.22	**-0.72**	-0.03	0.01	0.22
Risk perception of gastric illness	0.31	0.10	**0.56**	-0.35	0.16
Dissatisfaction with iron	0.09	0.03	**0.60**	**0.40**	0.05
Arsenic risk perception	**0.52**	0.01	-0.22	0.04	0.18
Presence of children <5	-0.06	-0.23	-0.55	0.27	**0.41**
Self-efficacy	0.29	0.13	0.03	-0.14	**0.68**
Perception of purchased water	0.07	0.20	-0.04	**0.65**	0.04
Degree of use of purchased water	**0.41**	**0.27**	0.06	**0.50**	0.17

Figure 5-9: Principal component analysis of the degree of purchased water use and 13 explanatory variables in Area 1 (rotation of 5 principal components).

Table 5-12: Regression coefficients for different degrees of purchased water use (fully-adjusted models). Level 1: occasional use; level 2: only some household members; level 3: non-exclusive use, level 4: exclusive use. The number of households in each regression is indicated. Statistical significance: • : p<0.1; *: p<0.05; **:p<0.01; ***:p<0.001.

	From levels 1-2 to higher levels				**From lower levels to level 4**		
	3 vs 2 (28:55)	**3-4 vs 2 (62:89)**	**3 vs 1-2 (28:67)**	**3-4 vs 1-2 (62:101)**	**4 vs 3 (34:62)**	**4 vs 2-3 (34:89)**	**4 vs 1-2-3 (34:101)**
Socioeconomic status					1.6 *	1.4 *	1.2 *
Income stability					0.9 *	0.9 *	0.8 *
Exposure to purchased water	1.0 •						
Women's group participation							
Peer behavior							
External advice	1.1 *	1.1 **	1.0 **	1.1 ***		0.5 •	0.6 •
Doctor's advice							
Risk perception of gastric illness							
Dissatisfaction with iron							
Arsenic risk perception						- 0.9 *	- 0.9 *
Presence of children <5							
Self-efficacy	1.5 *		0.9 *		- 1.0 *		
Perception of purchased water	1.6 *	1.1 *	1.2 •	0.9 *			

Table 5-13: a) Linear regression coefficients for the volume of water purchased per person per day, for all users (n=101), using unadjusted (K=1) and fully-adjusted (K=13) models. Children < 5 were counted as 0.5 person. b) Logistic regression coefficients for the interruption of purchased water use, using unadjusted (K=1) and fully-adjusted (K=13-14) models. 49 "stoppers" out of 150 current and past users of KJ. Grey cells indicate variables not included in the model. Statistical significance: •: p<0.1; *: p<0.05; **:p<0.01; ***:p<0.001.

a)

	Linear regression	
	Volume of KJ (L) per person per day	
	K=1	**K=13**
Socioeconomic status	0.9***	0.7**
Income stability	0.3*	
Exposure to purchased water	0.2	
Women's group participation	- 0.2	
Peer behavior	0.0	
External advice	0.2	
Doctor's advice	- 0.1	
Risk perception of gastric illness	0.3	
Dissatisfaction with iron	0.0	
Arsenic risk perception	0.0	
Presence of children <5	- 0.2	
Self-efficacy	0.1	
Perception of purchased water	0.3	
Domestic filter ownership		

b)

	Logistic regression		
	Interruption of KJ use		
	K=1	**K=13**	**K=14**
Socioeconomic status	-0.2		
Income stability	0.0		
Exposure to purchased water	0.0		
Women's group participation	0.0		
Peer behavior	-0.2		
External advice	0.1		
Doctor's advice	- 0.5*	-0.5*	-0.6*
Risk perception of gastric illness	-0.8**	-1.1**	-1.1**
Dissatisfaction with iron	0.0		
Arsenic risk perception	-0.4 •		
Presence of children <5	- 0.1		
Self-efficacy	0.0		
Perception of purchased water	-0.5 •	-0.7*	-0.8*
Domestic filter ownership	1.0*		1.8**

4. RESULTS: AREA 2

4.1. Explanatory Variables

A comparison of socioeconomic indicators shows that Area 2 was poorer than Area 1 (Tables 5-1 and 5-2, Figure 5-10), consistent with lower land ownership and higher prevalence of insecure daily labor as an income source in Area 2 (Table 5-2). As with Area 1, correlations among explanatory variables were generally low (most correlation coefficients > -0.2 and < 0. 4, Table 5-14), with the exception of SES and income stability (PC1, Figure 5-11), and risk perception of gastric illness and dissatisfaction with iron (PC2, Figure 5-11). Arsenic risk perception was correlated with SES (Table S5). The three components of piped water perceptions -aesthetics, safety and convenience- were independent and weighed equally in the aggregate variable (Table 5-14). Perceived safety of piped water was associated with dissatisfaction with iron, but not with risk perception of gastric illness, which suggests that households may have used iron as their criterion of water safety.

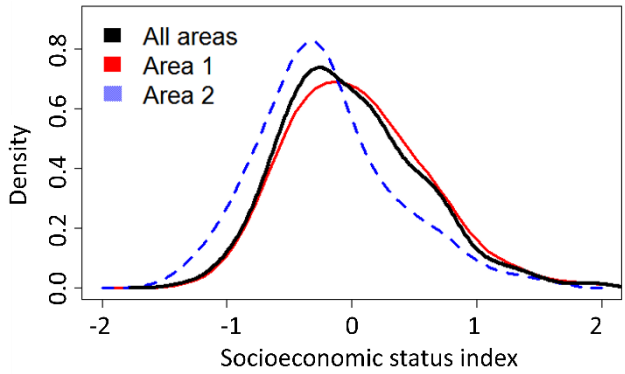

Figure 5-10: Comparison of socioeconomic status between Area 1 and Area 2. For this figure only, a socioeconomic status index was calculated using data from the entire sample (n=501) and compared between the two survey areas.

4.2. Description of Household Water Practices

The breakdown of household drinking water sources in Area 2 before and soon after (1-18 months) the installation of public taps is shown in Figure 5-12a. Before piped water became available, 66% of households exclusively used untreated groundwater, while 24% and 16% used KJ and filters respectively. By the time of the survey, 78% of Area 2 households were using piped water for drinking, without additional treatment. Figure 5-12b shows the degree of use of the three alternatives present in Area 2. 72% of households using piped water reported exclusive use (or concurrent with another alternative). Exclusive use was similarly high for filter users (89%), consistent with Area 1. KJ was only used occasionally (in sickness, for celebrations, or as a back-up in case the pipeline broke). Piped water was also used for cooking by a large proportion of users (61%) (Table 5-5).

Table 5-14: Correlation table and summary statistics (mean, standard deviation and boxplot) of 14 explanatory variables in Area 2.

Variables	**1**	**2**	**3**	**4**	**5**	**6**	**7**	**8**	**9**	**10**	**11**	**12**	**13**	**14**
SES														
Income stability	0.59***													
Women's group	0.17	0.01												
External advice	0.05	-0.08	0.13											
Doctor's advice	0.19•	0.13	0.03	-0.18•										
Risk perc. "gas"	0.04	0.08	0.05	-0.08	0.19.									
Diss. with iron	0.05	0.13	0.00	-0.02	0.16	0.54***								
Arsenic risk perc.	0.34***	0.22*	0.09	0.21*	0.14	-0.05	0.06							
Children <5	-0.01	0.06	0.10	0.04	-0.07	-0.16	-0.11	0.04						
Self-efficacy	0.29**	0.31**	0.18•	0.16	0.10	0.03	-0.04	0.12	0.06					
Piped water perc.	-0.02	0.09	0.04	0.09	0.19•	0.15	0.31**	0.00	-0.15	0.01				
Perc. aesthetics	-0.04	0.04	-0.10	0.02	0.12	0.14	0.17	0.00	-0.15	-0.01	0.62***			
Perc. safety	0.04	0.03	0.15	0.06	0.05	0.21*	0.33**	0.05	-0.10	0.04	0.54***	-0.02		
Perc. convenience	-0.03	0.09	0.02	0.08	0.16	-0.09	0.05	-0.06	-0.03	-0.02	0.63***	0.14	-0.01	
Mean	-0.007	0.000	0.000	0.000	0.000	0.000	0.000	0.000	0.000	0.000	0.000	0.000	0.000	0.000
St. dev.	0.65	1.00	1.00	1.00	1.00	0.71	0.83	0.76	1.00	1.00	0.60	1.00	1.00	1.00

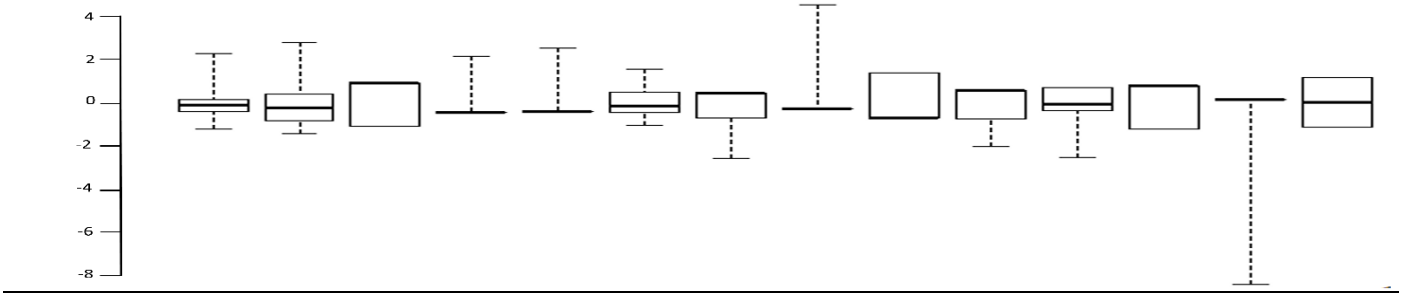

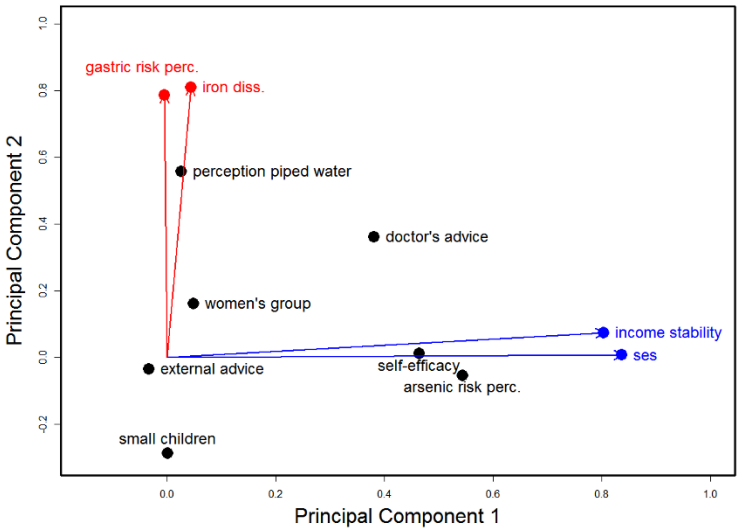

	PC1	PC2	PC3	PC4
Socioeconomic status	**0.84**	0.01	0.04	0.10
Income stability	**0.80**	0.07	-0.14	0.04
Women's group participation	0.05	0.16	0.22	**0.73**
External advice	-0.03	-0.03	**0.87**	0.15
Doctor's advice	0.38	0.36	-0.24	-0.11
Risk perception of gastric illness	0.00	**0.79**	-0.18	0.12
Dissatisfaction with iron	0.04	**0.81**	-0.01	-0.02
Arsenic risk perception	**0.54**	-0.05	**0.44**	-0.08
Presence of children <5	0.00	-0.29	-0.15	**0.60**
Self-efficacy	0.46	0.01	0.14	**0.42**
Perception of piped water	0.03	0.56	0.32	-0.21
Cumulative % of variance explained	18%	35%	46%	57%

Figure 5-11: Principal component analysis of 11 explanatory variables in Area 2 (rotation of 4 principal components).

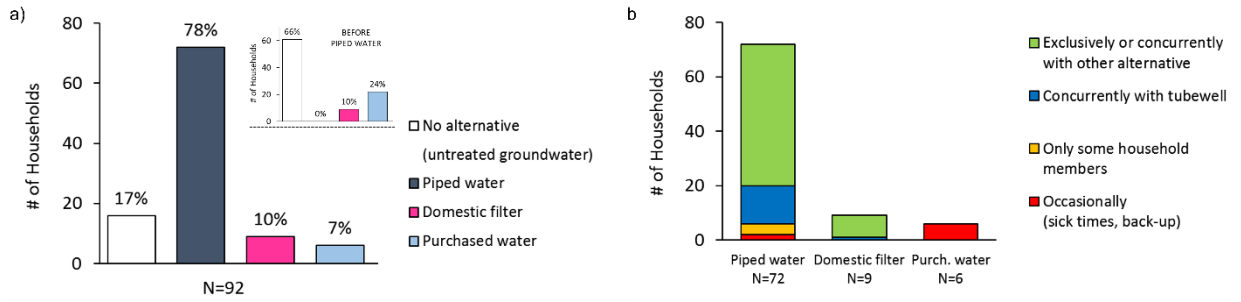

Figure 5-12: Household water practices in Area 2. a) Household drinking water sources before and after the installation of public taps. b) Degree of use of 3 alternatives to shallow groundwater: piped water, filters and KJ.

4.3. Factors Influencing Piped Water Use

The sample size for Area 2 (n=92) is small, but quantitative results are nevertheless presented as a first exploration of the factors potentially influencing piped water use. Table 5-15 shows the results of logistic regressions of piped water use against the 13 explanatory variables. Unadjusted models indicate that piped water use was significantly correlated with perceived aesthetics and convenience, and with risk perception of gastric illness. It was also negatively correlated with the presence of children under 5, possibly because households with children needing to be watched favored tubewells close to the house over safer but more distant piped water[209]. The fully-adjusted model shows that, when controlling for all variables, perceived aesthetics were the primary driver of piped water use, consistent with PCA (Figure 5-13). Risk perception of gastric illness, perceived convenience and SES may be secondary predictors (Table 5-15 and Figure 5-13). The negative effect of self-efficacy in the fully-adjusted model is an artifact of controlling for correlated variables, such as socioeconomic status (Table 5-14), as shown by the hierarchical models (Table 5-15).

Table 5-15: Regression coefficients for the use of piped water in Area 2 using hierarchical models (70 regular users of piped water out of 92 households). K is the number of explanatory variables in the model. Grey cells indicate variables not included in the model. Statistical significance: •: p<0.1; *: p<0.05; **:p<0.01; ***:p<0.001.

	K=1	**K=2**	**K=5**	**K=8**	**K=10**	**K=11**	**K=13**
Socioeconomic status	0.6						
Income stability	0.6 •				-0.7 •		
Women's group participation	-0.1						
External advice	-0.2						
Doctor's advice	0.5						
Risk perception of gastric illness	0.8*		0.8 •			1.1 •	1.1 •
Dissatisfaction with iron	0.3					-0.9 •	
Arsenic risk perception	0.1						
Presence of children <5	-0.6*	-0.5*	-0.5*	-0.5 •	-0.6*		
Self-efficacy	-0.3				-0.6 •	-0.8*	-0.9*
Perception of piped water	1.6**					1.7**	
Perceived aesthetics of piped water	1.0***						1.1**
Perceived safety of piped water	0.1						
Perceived convenience of piped water	0.5*						0.7 •

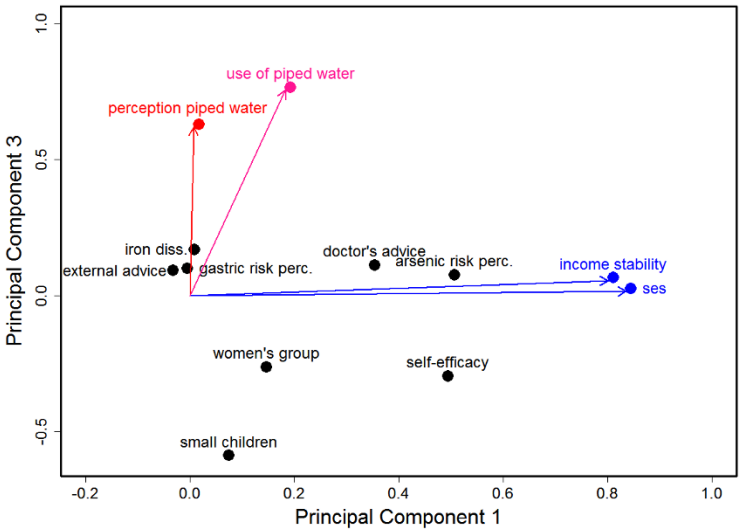

	PC1	PC2	PC3	PC4
Socioeconomic status	**0.85**	0.00	0.03	0.05
Income stability	**0.81**	0.07	0.07	-0.13
Women's group participation	0.15	0.02	-0.26	**0.49**
External advice	-0.03	-0.15	0.09	**0.85**
Doctor's advice	0.35	0.37	0.11	-0.24
Risk perception of gastric illness	-0.01	**0.83**	0.10	-0.05
Dissatisfaction with iron	0.01	**0.80**	0.17	0.07
Arsenic knowledge	**0.51**	-0.10	0.08	0.35
Presence of children <5	0.07	-0.07	**-0.59**	0.07
Self-efficacy	**0.49**	0.10	-0.30	0.29
Perception of piped water	0.02	0.30	**0.63**	0.25
Use of piped water	**0.19**	0.08	**0.77**	-0.13

Figure 5-13: Principal component analysis of piped water use and 11 explanatory variables in Area 2 (rotation of 4 principal components).

Among households using piped water (n=72), we compared the distributions of explanatory variables between exclusive users and inconsistent or occasional users (Figure 5-14). Six variables exhibited an upward trend when the degree of piped water use increased: participation in a women's group, risk perception of gastric illness, dissatisfaction with iron, perception of piped water, SES and income stability, suggesting that these factors may influence the consistency of piped water use.

5. DISCUSSION

5.1. Adoption of Alternatives to Shallow Groundwater in Rural West Bengal

The limited overall proportion of households using alternatives in our study areas (52.9% for Areas 1 and 2 combined) is consistent with results from 2009-2010 in arsenic-affected Bangladesh, where no more than 62.1% of 1,268 households were found to use alternatives to shallow tubewells[181]. We found that SES predicted the use of purchased alternatives but not the use of free alternatives. This finding suggests that SES does not affect the desire for alternatives to shallow groundwater, but only the ability to pay for them.

SES aside, we found that risk perception of gastric illness was the primary predictor of the use of alternatives to untreated groundwater in Area 1 (except in the case of filter use where it was outweighed by dissatisfaction with iron). By contrast, arsenic risk perception was either not correlated with the use of alternatives (for government tubewells and piped water), or it was not as strong a predictor as other risk perception indicators (for KJ and filters). This result suggests that households seeking alternatives to untreated groundwater primarily react to its readily

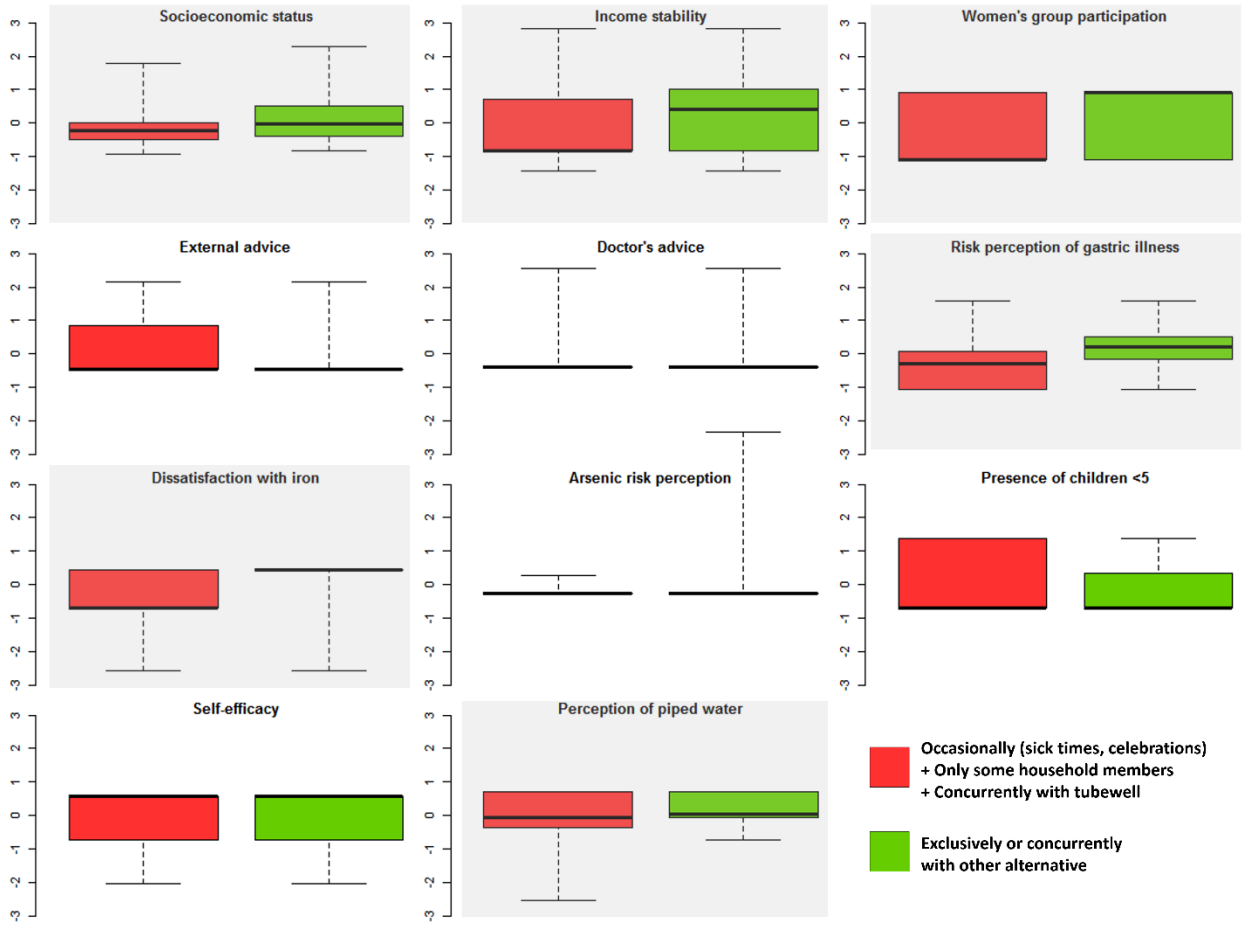

Figure 5-14: Comparison of explanatory variables between 2 categories of households using piped water in Area 2 (n=72). Grey backgrounds indicate variables showing an upward trend as the degree of use of piped water increases.

noticeable disadvantages, i.e. gastric illness and iron color and taste, rather than to an invisible carcinogen with long-term effects.

One implication of this finding is that raising awareness about arsenic, which has traditionally been the focus of interventions[210,211], may not be the most effective lever to increase the use of available alternatives. A related implication is that knowledge about arsenic is not required for households to switch water sources: when groundwater has more tangible disadvantages (e.g. taste, color, GI illness), households will switch if they can. Because GI disorders are a primary health concern for households (as opposed to arsenic poisoning, Table 5-3), 23% and 65 % of households in Area 1 and 2 respectively were using alternatives while having no knowledge about arsenic. Finally, because arsenic risk perception was significantly more correlated with SES than gastric illness risk perception and dissatisfaction with iron (Figure 5-5), our results suggest that leveraging awareness of non-arsenic contaminants may be a more inclusive strategy towards behavior change. However, microbial pathogens and iron do not always co-occur with arsenic contamination in the Bengal Basin[36,37]. For example, 33% of tubewells with arsenic concentrations above 10µg/L in the BGS dataset (n=2589) have low iron levels (< 0.3 mg/L, the

WHO MCL)[36]. Therefore, leveraging non-arsenic contaminants are a supplement to, rather than a substitute for, raising awareness about arsenic.

Our results indicate that once a household has decided to switch away from shallow groundwater, the choice amongst several alternatives is influenced by SES, social interactions (such as participation in a women's group) and households' perceptions of these alternatives (safety, convenience, and aesthetics). Specifically, we found that these choices were not influenced by risk perceptions of contaminants. This result is consistent with studies conducted in the context of microbial water contamination, which showed that preferences for safe water options are primarily driven by convenience, taste and odor[193,212]. Our findings suggest that households may perceive all alternatives as protecting health equally, which is problematic for arsenic mitigation: where filters or government tubewells are not designed to be arsenic-safe, they may nevertheless be chosen by households as an alternative to untreated shallow tubewell water. Therefore, raising awareness about arsenic-safe alternatives to shallow groundwater remains crucial to ensure that households choose alternatives that protect their health effectively.

Finally, variables pertaining to social influence were not correlated with the use of filters, government tubewells and piped water. For KJ, participation in a women's group, doctor's and external advice were correlated with uptake, sustained use and/or degree of use (Tables 5-7, 5-12 and 513, and Figure 5-9), but peer behavior had no effect. Overall, our results were consistent with previous studies showing limited influence of social networks on drinking water behaviors and preferences[213,214] .

5.2. SSIPs as a "Solution" to Arsenic-Contaminated Groundwater?

Our interview with the entrepreneur providing most of the KJ in Area 1 revealed that he had been operating for four years, and was producing approximately 150 20L containers per day at a cost of INR 5-6 each. Containers were sold for INR 8-10 to distributors in charge of delivery, who charged households INR 20-30. The survival of this business over four years suggests that SSIPs in rural West Bengal can find enough demand to be financially sustainable. In arsenic-affected areas, water from SSIPs can potentially be safer in the long run than groundwater treated at home, because commonly used domestic filters are rarely designed to remove arsenic (as per our observations), and even when they are, adequate filter maintenance by households is challenging[32,215,216]. In contrast, SSIPs have access to effective treatment technologies for arsenic removal, monitoring equipment, and maintenance services, and can, in theory, and with regulation, produce safe water consistently. Finally, this model of water provision has a direct mechanism for cost-recovery, which is important to maintain service quality and scale up. However, our study illustrates three limitations of this market-driven approach to drinking water access.

First, KJ may not provide universal access. Our results show that both the use and the degree of use of KJ are strongly associated with higher SES, leaving poorer households at greater risk than their wealthier counterparts. These results illustrate the tension between cost-recovery and universal access[217]. If SSIPs are proposed as a way to address groundwater contamination in West Bengal[218,219] and if the costs of water treatment and distribution cannot be substantially reduced with technology innovation alone, subsidies will be needed to ensure universal access.

Second, KJ is used more irregularly than other alternatives such as filters and piped water (Figures 5-6 and 5-12), and virtually never used for cooking (Table 5-5), suggesting that – at least at current prices -- it does not eliminate the ingestion of arsenic. However, we note that unlike diarrheal diseases, which can be triggered by a one-time consumption of microbiologically-contaminated water, arsenic health effects arise due to cumulative exposure[220]. Therefore even irregular use of alternatives to arsenic-contaminated groundwater is preferable to no use at all.

Third, consistent with the popularity of free piped water observed previously in rural Bengal[32,33,221], our findings in Area 2 suggest that the installation of free public taps in a community can –at least initially– decrease demand for KJ significantly, and could therefore be a business threat to water entrepreneurs. We recommend that this vulnerability be taken into account if state-level arsenic mitigation strategies are to include both public and private provision of water[219,222]. More generally, the sustainability of community-scale water treatment plants strongly depends on the popularity of the other available alternatives[223] (filters, piped water), and, in some cases, KJ may only be an interim solution to groundwater contamination until piped water provision becomes widespread.

5.3. Limitations of this Study

Our study had several limitations. First, we did not test the water quality of private tubewells and of the different alternatives because we wanted to understand household water practices through the lens of people's perceptions. However, alternatives to shallow groundwater constitute a solution to the arsenic crisis only if they provide chemically and microbiologically safe water. Therefore, the water quality of different alternatives should be tested before any action is taken to scale them up. Second, we used a systematic sampling strategy, but occasional leeway in the counting sequence possibly biased our sample towards wealthier households and may have led us to overestimate the proportion of households using alternatives. However, this would not undermine our comparative analysis between users and non-users of alternatives. Third, our results are based on *reported* household water practices, which were not always possible to verify. We do not know the direction in which reporting biases, if any, may have affected the proportion of households "using" alternatives. Fourth, in Area 2, piped water had only been available for a few months (1-18 months), and water practices prevalent at the time of survey may change in the long term. For example, dissatisfaction with piped water because it is intermittent could lead to increased demand for KJ in the future. Finally, our study areas may not be representative of villages with higher prevalence of *visible* arsenicosis symptoms[14], where arsenic risk perception may be a more important driver for the use of alternatives.

5.4. Conclusions

In this exploratory study, we investigated household drinking water practices in arsenic-affected Murshidabad, West Bengal, India. We found that despite low arsenic awareness, a substantial fraction of households (52.9% overall) used alternatives to shallow groundwater. These included KJ from SSIPs, filters (both significantly more used by higher SES households), government tubewells and piped water (both with no influence of SES). We found that risk

perception of gastric illness or dissatisfaction with iron were stronger predictors of the use of alternatives than arsenic risk perception, indicating that households primarily react to readily noticeable water disadvantages rather than to an invisible carcinogen with long-term effects. This finding should be taken into consideration in behavior change interventions and compliance studies when several water contaminants co-occur. In West Bengal, our findings suggest that interventions aiming to increase the use of alternatives to shallow groundwater should address the most tangible water problems (iron and gastric illness) in addition to arsenic awareness, which remains important to ensure that households choose arsenic-safe alternatives, and because tangible contaminants do not always co-occur with arsenic.

Finally, our results show that small-scale private water providers can be financially sustainable and can contribute to improving access to drinking water alternatives to contaminated groundwater. However, we found that exclusive use of KJ was rare, and that a large proportion of KJ users concurrently drank untreated tubewell water. In addition, without subsidies, KJ is unlikely to provide universal access to safe water. Finally, our results suggest that water provision through SSIPs may only be an interim solution to arsenic-contaminated groundwater until publicly-provided piped water becomes widespread in rural West Bengal.

CHAPTER 6. Conclusion

The motivation of my PhD work was to investigate whether the decentralized provision of treated water can solve the arsenic crisis in rural West Bengal. This objective led to two complementary research questions. First, is it possible to produce safe drinking water at low-cost in decentralized groundwater treatment plants? Second, to what extent can the purchase of water from local entrepreneurs mitigate arsenic exposure in low-income communities?

Chapters 2, 3 and 4 addressed the first question by examining arsenic and bacteria removal by iron electrocoagulation (Fe-EC). These chapters focused on the mechanisms of contaminant removal to better predict how operating conditions and groundwater chemistry may affect Fe-EC performance. Chapter 5 addressed the second question by investigating household water decisions in rural West Bengal when alternatives to contaminated groundwater are available. This final chapter provides a summary of my results followed by an overview of remaining research questions, and concludes with a personal reflection on cross-disciplinary research.

1. GROUNDWATER TREATMENT BY FE-EC

1.1. Summary of results

Two processes contribute to the removal of arsenic in Fe-EC: the oxidation of As(III) to As(V), and the adsorption of As(V) (and As(III) to a lesser extent) to Fe(III) precipitates[48,49]. When the process limiting arsenic removal is As(III) oxidation, decreasing the Fe dosage rate improves Fe-EC performance (i.e. the amount of arsenic removed for a given Fe concentration). By contrast, when the process limiting arsenic removal is As(V) adsorption, changing the Fe dosage rate has no effect on Fe-EC performance. For an operator, it is very important to understand when the Fe dosage rate can or cannot be a lever to control performance. I found that the process limiting arsenic removal in Fe-EC is determined by the pH and the O_2 concentration, which both control the longevity of Fe(II), a major competitor of As(III) for reactive oxidants. When the pH < 7.5 or when the solution is not saturated with O_2, As(III) oxidation is the limiting factor, and the Fe dosage rate can be a useful lever to improve Fe-EC performance. When the pH > 7.5 and the solution is saturated with O_2, the limiting factor is As(V) adsorption; thus lowering the Fe dosage rate does not improve arsenic removal significantly, and only results in increasing the treatment time and cost.

Fe-EC can attenuate bacterial contamination in synthetic Bengal groundwater without detriment to arsenic removal. The primary process of bacteria attenuation is encapsulation in Fe(III) flocs and removal by gravitational settling. More specifically, Fe(III) precipitates adhere to the surface of bacterial cells, mainly through interactions with bacterial phosphate groups, resulting in bacteria enmeshment in Fe(III) precipitates. Bivalent cations (e.g. Ca^{2+}, Mg^{2+}) can complex bacterial phosphate groups and therefore inhibit bacteria removal. The effect of oxyanions (e.g. Si, P) depends on their affinity for Fe(III) oxide surfaces. Weakly-sorbing Si does

not compete effectively with bacterial phosphate groups, and has therefore no significant effect on bacteria removal. In contrast, aqueous P competes with bacterial phosphate moieties for sorption on Fe(III) precipitates, and therefore inhibits removal. However, bivalent cations can bridge between sorbed P and bacterial phosphate moieties, thus canceling the inhibitory effect of aqueous P on bacteria removal. Natural organic matter (NOM) in concentrations representative of groundwater does not affect bacteria attenuation, likely because NOM's dominant functional groups, carboxyl and hydroxyl, do not compete effectively with bacterial phosphate moieties. Bacteria removal is independent of the cell wall structure, which likely results from two factors: first, Fe(III) precipitates are very small relative to bacterial cells, and presumably insensitive to large features such as the length of lipopolysaccharides; second, phosphate functional groups are equally abundant on Gram-positive and Gram-negative cells. Bacteria inactivation by germicidal reactive oxidants can also take place in Fe-EC. However, inactivation remains limited in the presence of HCO_3^-, a ubiquitous ion in natural waters. Although inactivation is amplified in conditions that extend the longevity of Fe(II), such as a low pH (< 7.0) or a low O_2 concentration, it remains a secondary process of bacteria attenuation compared to encapsulation and removal with Fe(III) flocs.

One important contribution of this dissertation is the innovative approach used to elucidate the mechanisms of bacteria encapsulation in flocs. Spectroscopic techniques (ATR-FITR, XAS) could not adequately determine bacteria-precipitate interactions taking place inside flocs and in complex groundwater-like electrolytes. Instead, building on previous spectroscopic studies conducted in more simple and controlled systems, macroscopic data of bacteria attenuation in systematically varied electrolytes were combined with ζ-potential measurements to constrain the bacterial functional groups governing removal and understand the impact of major groundwater ions. This approach provided chemically-sound results, which can more broadly be used to predict the effect of water chemistry on iron-based coagulation methods commonly used in water and wastewater treatment.

1.2. Remaining questions

While arsenic removal by Fe-EC has been demonstrated in the field[46,47], the attenuation of real enteric bacteria from real groundwater remains to be validated. Compared to laboratory strains, enteric bacteria may be associated with more extracellular polymeric substances (EPS), as a result of different growth conditions. However, Fe(III) precipitates are expected to interact with EPS similarly as with bacterial cell walls, because EPS contain phosphate functional groups that can form bonds with Fe(III) oxides[224,225]. Therefore, this difference is not expected to affect the adhesion of Fe(III) precipitates significantly. A second difference between my lab experiments and typical field conditions is the concentration and type of bacteria in influent water. My experiments used *E. coli* concentrations of $10^{6.5}$ CFU/mL to be able to detect large log attenuations of fecal indicators. By contrast, levels of fecal bacteria in shallow Bengal groundwater rarely exceed 10^2 CFU/mL[37,39,41], and other bacteria are likely to be present as well in significant concentrations. However, assuming that bacteria-precipitate collisions can be described by the Smoluchowski equation (where the number of collisions is proportional to the number of precipitates multiplied by the number of bacteria[226]), the number of collisions per cell should

remain unchanged. In addition, assuming that all bacteria have comparable affinities for Fe(III) precipitates (consistent with the results in chapter 4), collisions are equally likely to result in adhesion for fecal and non-fecal bacteria, and the likelihood for enteric pathogens to have Fe(III) precipitates adhere to their surface should not be affected. Therefore, despite these two differences, I expect that Fe-EC operated in the field will achieve sufficient bacteria attenuation to meet drinking water standards.

More work is needed to assess virus attenuation by Fe-EC. Rotavirus has been detected in shallow groundwater in rural Bengal[38], and effective virus attenuation is critical to protect public health, especially as the infective dose of enteric viruses can be as low as 1-100 microorganisms[45]. A prior study using surface-water like electrolytes showed that Fe-EC can attenuate the model virus MS2, primarily due to enmeshment in Fe(III) flocs[81]. The capsid of enteric viruses is made of proteins, which have hydroxyl, amine and carboxyl functional groups, but no phosphate moieties[227]. Therefore, virus interactions with Fe-EC precipitates cannot be easily predicted from my work on bacteria. Fe(III) oxides do not have a strong affinity for hydroxyl and amine moieties[134,135], but they can interact with carboxyl groups to form outer- or inner-sphere complexes[142,228]. However, these interactions are expected to be weaker than with phosphate moieties, and groundwater oxyanions (e.g., Si and P) may inhibit virus removal more significantly than bacteria removal. Because protein capsids do not have functional groups that strongly sorb to Fe(III) oxides, virus removal by Fe-EC may be governed primarily by electrostatic and hydrophobic –as opposed to specific– interactions. It is difficult to predict the impact of the long protein spikes on the surface of some viruses (e.g,. adenovirus, rotavirus): these spikes mediate the adhesion of viruses to host cells[229,230], but their potential to facilitate adhesion to mineral surfaces is unknown. They may also cause steric hindrance to Fe(III) precipitates, whose size is comparable to that of viruses. The type and lifetime of germicidal species generated in Fe-EC are largely governed by groundwater chemistry (e.g., pH, HCO_3^-), but the susceptibility to such species can depend on the microorganism[82,83,231]. Therefore, limited bacteria inactivation during Fe-EC cannot be extrapolated to viruses, which may have a different response to Fe(II) and reactive intermediates than bacteria[83]. Both laboratory and field experiments are needed to determine if Fe-EC can safely remove virus contamination from groundwater.

Fe-EC is already a simple and robust process adapted to resource-limited settings[47,51], but several improvements are needed for it to become a mature technology. Ways to limit the accumulation of rust on electrodes, which decreases Fe-EC performance, are currently under investigation. Transforming the current batch process into a continuous process would eliminate the down-time that occurs when water is transferred from the dosing reactor to the settling reactor, and would thus augment throughput if plug-flow conditions can be maintained. In addition, sludge containment, disposal, and/or valorization needs to be optimized based on ongoing research[232,233] to prevent the return of sludge-borne contaminants to the environment. Finally, minimizing the overall cost of water treatment should remain a priority, because this cost will be directly reflected in the price, affordability, and consumption of treated water in low-income communities. I hope that my PhD work can be used towards this crucial objective. First, avoiding the use of low Fe dosage rates when they do not improve arsenic removal would help reduce treatment time and

costs. Second, confirming effective microbial attenuation with Fe-EC would allow avoiding an additional disinfection step and the associated costs.

2. HOUSEHOLD WATER PRACTICES IN RURAL WEST BENGAL

2.1. Summary of results

In rural West Bengal, alternatives to shallow groundwater such as domestic filters, purchased water, government (deep) tubewells or piped water exist in a number of areas. These alternatives are not always arsenic-safe, but they are used by a significant fraction of households who desire avoiding private tubewells, which often have unpleasant levels of iron and are associated with gastric illness. Arsenic contamination, which is not as tangible as these readily noticeable problems, is only a secondary –if not negligible– motivator for seeking alternatives. One corollary is that different alternatives are equally valued as long as they remove iron and reduce gastric illness, even though they may not be equally arsenic-safe. As a result, small entrepreneurs selling treated water are in effect in competition with domestic filters, which are rarely designed to remove arsenic but produce iron-free water whose taste is sometimes preferred to that of purchased water. The use and degree of use of purchased water are strongly influenced by socioeconomic status, which indicates that this alternative does not provide universal access, at least at the price of INR 20-30/20L. In addition, purchased water is seldom the exclusive source of drinking water, and is virtually never used for cooking, which suggests that this form of water provision can reduce, but not eliminate, arsenic exposure. Although private entrepreneurs can certainly improve access to safe water in rural West Bengal, and have the potential of doing so durably and at scale, it is important to be aware of the limitations of this model –difficulty to outcompete domestic filters, non-exclusive use, and unequitable access. Because it can only be a partial solution to the arsenic crisis, the provision of safe water through private entrepreneurs should remain an interim approach before free piped water, which seems to overcome some of the above limitations, becomes widely available.

2.2. Remaining questions

A mid-term solution involving small private entrepreneurs runs the risk of consolidating a two-tier system, where cities receive publicly-provided (and almost free) piped water while rural areas have to rely on the private sector. In this context, it is important to emphasize that water provision through small independent providers does not eliminate, but rather redefines the role of the state. There are 3 areas in which the state retains key responsibilities: facilitation of cross-subsidies, enforcement of water quality standards, and sustainable groundwater management.

Because the use of purchased water is highly influenced by socioeconomic status, cross-subsidies may be needed to improve equity of access. While cross-subsidies are commonly used by water utilities in urban areas[234], implementing a subsidy scheme in "off-grid" areas serviced by a multitude of small independent providers is not straightforward. Should the subsidy be given to

entrepreneurs so that they can decrease tariffs and reach more customers? Or should the subsidy be targeted at the poorest households? In the first case, where would the subsidy come from, when urban water utilities are far from recovering their costs[235]? The second option is appealing because it would leverage the higher willingness to pay of a community's wealthier households to reach the very poor. Such targeted subsidies have been used for piped water supplies[234,236], but is it not clear that it can be implemented for bottled water vending. First, setting tariffs would be challenging since households start or interrupt using purchased water over time, potentially affecting the ratio of subsidizers to subsidized. Second, applying different tariffs to different customers may put water entrepreneurs in a difficult position. Overall, research and experimentation are needed to improve access of the poorest through adequate subsidies.

A second area of concern is the regulation of small water entrepreneurs to ensure that treated water meets national quality standards and to avoid unsustainable groundwater use. Such surveillance could be implemented through a licensing system, as has been done elsewhere[236]. However, the current situation in rural West Bengal, where a large fraction of small water entrepreneurs operates informally despite the existence of licensing laws, suggests that enforcement is difficult (or not a priority). Finding ways to incentivize entrepreneurs to get licensed seems to be a promising approach. One possibility would be to grant public subsidies to license holders, which would allow them to reduce their tariffs and increase their customer base. At least in theory, such a system could address the challenges of regulation and equity of access simultaneously. Generally, public policies are needed to improve state oversight of (and support to) small water businesses who are filling a service gap in rural areas.

3. PERSONAL REFLECTION ABOUT CROSS-DISCIPLINARY RESEARCH

My PhD project has given me the opportunity to explore both the engineering and social science aspects of safe water provision in a developing country. I believe that these two aspects are complementary and equally important to remediate the unacceptable persistence of inequities in access to water in the world. There is now a consensus that engineers with multidisciplinary training are better equipped to address complex real-life problems that are not purely technical. In this context, I am surprised that cross-disciplinary PhD projects are not more common (or more encouraged). Admittedly, the traditional partitioning of university departments and the widespread anxiety that diversifying happens at the expense of depth and expertise are two important reasons for the rarity of cross-disciplinary PhD projects. However, I believe that there may be a third reason. Through my interactions with engineers and socials scientists over the past four years, I have come to realize that there is a subtle but inherent difference in their mindsets, which can result in a sort of "cultural clash".

Engineers believe that they can solve problems. They are trained to think this way. Inventing solutions is their *raison d'être*. This aspiration to solve problems comes with an intrinsic optimism. Engineers know that technologies face challenges in the field, and that sound products can fail (and do fail) to achieve their purpose because of insufficient attention to cultural, institutional, and political realities. But such awareness does not alter their optimism: "the problem

is more complicated than we thought, but we can still solve it, we just need to try harder". This is what I believe the engineer's mindset is.

Social scientists are intrinsically more skeptical. They do not necessarily agree that what engineers would call a "solution" is in fact a solution. They are trained to ask who a technology really serves (and who it does not) and who bears its costs –financial, opportunity, and leisure costs. They are of course committed to improving livelihoods, but they do not believe that problems can be "solved" as confidently as engineers do. And what does it mean to solve a problem anyway? Remediating the manifestations of a problem (e.g., lack of access to safe water in poor communities) does not address its root causes (e.g., incompetent state institutions and/or lack of voice of the poor).

I believe that this subtle difference in mindset between the tireless optimist and the hardened skeptic can create a disconnection and hamper dialogue. It is not inescapable, but I think it explains that social scientists and engineers can have difficulties in finding a common ground to collaborate. I think that I now share a little bit of both mindsets. Looking back, I realize that my experience at Berkeley has been a cross-cultural journey in more ways than I expected, and I am grateful for the opportunity that my PhD project has given me to broaden my perspective.

REFERENCES

(1) Ravenscroft, P.; Brammer, H.; Richards, K. *Arsenic Pollution: A Global Synthesis*; Wiley-Blackwell: Oxford, UK, 2009.

(2) Smedley, P. .; Kinniburgh, D. . A review of the source, behaviour and distribution of arsenic in natural waters. *Appl. Geochemistry* **2002**, *17*, 517–568.

(3) Mailloux, B. J.; Trembath-Reichert, E.; Cheung, J.; Watson, M.; Stute, M.; Freyer, G. A.; Ferguson, A. S.; Ahmed, K. M.; Alam, M. J.; Buchholz, B. A.; et al. Advection of surface-derived organic carbon fuels microbial reduction in Bangladesh groundwater. *Proc. Natl. Acad. Sci. U. S. A.* **2013**, *110*, 5331–5335.

(4) Neumann, R. B.; Ashfaque, K. N.; Badruzzaman, A. B. M.; Ashraf Ali, M.; Shoemaker, J. K.; Harvey, C. F. Anthropogenic influences on groundwater arsenic concentrations in Bangladesh. *Nat. Geosci.* **2009**, *3*, 46–52.

(5) Datta, S.; Neal, A. W.; Mohajerin, T. J.; Ocheltree, T.; Rosenheim, B. E.; White, C. D.; Johannesson, K. H. Perennial ponds are not an important source of water or dissolved organic matter to groundwaters with high arsenic concentrations in West Bengal, India. *Geophys. Res. Lett.* **2011**, *38*, n/a – n/a.

(6) Amini, M.; Abbaspour, K. C.; Berg, M.; Winkel, L.; Hug, S. J.; Hoehn, E.; Yang, H.; Johnson, C. A. Statistical Modeling of Global Geogenic Arsenic Contamination in Groundwater. *Environ. Sci. Technol.* **2008**, *42*, 3669–3675.

(7) Winkel, L.; Berg, M.; Amini, M.; Hug, S. J.; Annette Johnson, C. Predicting groundwater arsenic contamination in Southeast Asia from surface parameters. *Nat. Geosci.* **2008**, *1*, 536–542.

(8) van Geen, A.; Zheng, Y.; Versteeg, R.; Stute, M.; Horneman, A.; Dhar, R.; Steckler, M.; Gelman, A.; Small, C.; Ahsan, H.; et al. Spatial variability of arsenic in 6000 tube wells in a 25 km 2 area of Bangladesh. *Water Resour. Res.* **2003**, *39*, n/a – n/a.

(9) Schaefer, M. V.; Ying, S. C.; Benner, S. G.; Duan, Y.; Wang, Y.; Fendorf, S. Aquifer Arsenic Cycling Induced by Seasonal Hydrologic Changes within the Yangtze River Basin. *Environ. Sci. Technol.* **2016**, acs.est.5b04986.

(10) Hamadani, J. D.; Tofail, F.; Nermell, B.; Gardner, R.; Shiraji, S.; Bottai, M.; Arifeen, S. E.; Huda, S. N.; Vahter, M. Critical windows of exposure for arsenic-associated impairment of cognitive function in pre-school girls and boys: a population-based cohort study. *Int. J. Epidemiol.* **2011**, *40*, 1593–1604.

(11) Rahman, M.; Sohel, N.; Hore, S. K.; Yunus, M.; Bhuiya, A.; Streatfield, P. K. Prenatal arsenic exposure and drowning among children in Bangladesh. *Glob. Health Action* **2015**, *8*, 28702.

(12) Chen, Y.; van Geen, A.; Graziano, J. H.; Pfaff, A.; Madajewicz, M.; Parvez, F.; Hussain, A. Z. M. I.; Slavkovich, V.; Islam, T.; Ahsan, H. Reduction in urinary arsenic levels in

response to arsenic mitigation efforts in Araihazar, Bangladesh. *Environ. Health Perspect.* **2007**, *115*, 917–923.

(13) Pierce, B. L.; Argos, M.; Chen, Y.; Melkonian, S.; Parvez, F.; Islam, T.; Ahmed, A.; Hasan, R.; Rathouz, P. J.; Ahsan, H. Arsenic exposure, dietary patterns, and skin lesion risk in bangladesh: a prospective study. *Am. J. Epidemiol.* **2011**, *173*, 345–354.

(14) Das, A. The economic analysis of arsenic in water: A case study of West Bengal, Kolkata:Jadavpur University, 2011.

(15) Roy, J. Economic benefits of arsenic removal from ground water — A case study from West Bengal, India. *Sci. Total Environ.* **2008**, *397*, 1–12.

(16) Smith, A. H.; Lingas, E. O.; Rahman, M. Contamination of drinking-water by arsenic in Bangladesh: a public health emergency. *Bull. World Health Organ.* **2000**, *78*.

(17) WHO/UNICEF Joint Monitoring Programme for Water Supply and Sanitation. Country Files http://www.wssinfo.org/.

(18) Census of India. Census of India http://censusindia.gov.in/ (accessed Jan 18, 2016).

(19) World Bank. *Towards a more effective operational response : arsenic contamination of groundwater in South and East Asian countries*; 2005; Vol. Volume 1,.

(20) Chakraborti, D.; Das, B.; Rahman, M. M.; Chowdhury, U. K.; Biswas, B.; Goswami, A. B.; Nayak, B.; Pal, A.; Sengupta, M. K.; Ahamed, S.; et al. Status of groundwater arsenic contamination in the state of West Bengal, India: a 20-year study report. *Mol. Nutr. Food Res.* **2009**, *53*, 542–551.

(21) Chakraborti, D.; Rahman, M. M.; Das, B.; Nayak, B.; Pal, A.; Sengupta, M. K.; Hossain, M. A.; Ahamed, S.; Sahu, M.; Saha, K. C.; et al. Groundwater arsenic contamination in Ganga–Meghna–Brahmaputra plain, its health effects and an approach for mitigation. *Environ. Earth Sci.* **2013**, *70*, 1993–2008.

(22) UNICEF. *Annual Report 1973*; 1973.

(23) Beyer, M. G. *Water and Sanitation in UNICEF 1946-1986*; 1987.

(24) Kabay, N.; Bundschuh, J.; Hendry, B.; Bryjak, M.; Yoshizuka, K.; Bhattacharya, P.; Anaç, S. *The Global Arsenic Problem: Challenges for Safe Water Production*; CRC Press, 2010.

(25) Leber, J.; Rahman, M. M.; Ahmed, K. M.; Mailloux, B.; van Geen, A. Contrasting influence of geology on E. coli and arsenic in aquifers of Bangladesh. *Ground Water* **2011**, *49*, 111–123.

(26) Levine, R. J.; Khan, M. R.; D'Souza, S.; Nalin, D. R. Failure of sanitary wells to protect against cholera and other diarrhoeas in Bangladesh. *Lancet (London, England)* **1976**, *2*, 86–89.

(27) Khan, M. U.; Mosley, W. H.; Chakraborty, J.; Majid Sarder, A.; Khan, M. R. The relationship of cholera to water source and use in rural Bangladesh. *Int. J. Epidemiol.* **1981**, *10*, 23–25.

(28) Chakraborti, D.; Rahman, M. M.; Paul, K.; Chowdhury, U. K.; Sengupta, M. K.; Lodh, D.; Chanda, C. R.; Saha, K. C.; Mukherjee, S. C. Arsenic calamity in the Indian subcontinent What lessons have been learned? *Talanta* **2002**, *58*, 3–22.

(29) Hossain, M. A.; Sengupta, M. K.; Ahamed, S.; Rahman, M. M.; Mondal, D.; Lodh, D.; Das, B.; Nayak, B.; Roy, B. K.; Mukherjee, A.; et al. Ineffectiveness and Poor Reliability of Arsenic Removal Plants in West Bengal, India. *Environ. Sci. Technol.* **2005**, *39*, 4300–4306.

(30) Das, A.; Roy, J.; Chakraborti, S. *Socio-Economic Analysis of Arsenic Contamination of Groundwater in West Bengal*; India Studies in Business and Economics; Springer Singapore: Singapore, 2016.

(31) Ahmad, J.; Goldar, B. .; Misra, S.; Jakariya, M. Willingness to Pay for Arsenic-Free, Safe Drinking Water in Bangladesh http://www.wsp.org/sites/wsp.org/files/publications/WSP_Pay_Arsenic_free.pdf (accessed Apr 29, 2014).

(32) Hoque, B. A.; Hoque, M. M.; Ahmed, T.; Islam, S.; Azad, A. K.; Ali, N.; Hossain, M.; Hossain, M. S. Demand-based water options for arsenic mitigation: an experience from rural Bangladesh. *Public Health* **2004**, *118*, 70–77.

(33) Johnston, R.; Hug, S. J.; Inauen, J.; Khan, N. I.; Mosler, H.-J.; Yang, H. Enhancing arsenic mitigation in Bangladesh: findings from institutional, psychological, and technical investigations. *Sci. Total Environ.* **2014**, *488-489*, 477–483.

(34) West Bengal Public Health Engineering Department. Achievements http://www.wbphed.gov.in/main/index.php/achievements (accessed Mar 25, 2016).

(35) National Sample Survey. *Key indicators of drinking water, sanitation, hygiene and housing condition in India*; 2012.

(36) British Geological Survey. Arsenic contamination of groundwater in Bangladesh http://www.bgs.ac.uk/research/groundwater/health/arsenic/Bangladesh/data.html (accessed May 22, 2015).

(37) van Geen, A.; Ahmed, K. M.; Akita, Y.; Alam, M. J.; Culligan, P. J.; Emch, M.; Escamilla, V.; Feighery, J.; Ferguson, A. S.; Knappett, P.; et al. Fecal contamination of shallow tubewells in bangladesh inversely related to arsenic. *Environ. Sci. Technol.* **2011**, *45*, 1199–1205.

(38) Ferguson, A. S.; Layton, A. C.; Mailloux, B. J.; Culligan, P. J.; Williams, D. E.; Smartt, A. E.; Sayler, G. S.; Feighery, J.; McKay, L. D.; Knappett, P. S. K.; et al. Comparison of fecal indicators with pathogenic bacteria and rotavirus in groundwater. *Sci. Total Environ.* **2012**, *431*, 314–322.

(39) Knappett, P. S. K.; McKay, L. D.; Layton, A.; Williams, D. E.; Alam, M. J.; Mailloux, B. J.; Ferguson, A. S.; Culligan, P. J.; Serre, M. L.; Emch, M.; et al. Unsealed tubewells lead to increased fecal contamination of drinking water. *J. Water Health* **2012**, *10*, 565–578.

(40) Escamilla, V.; Knappett, P. S. K.; Yunus, M.; Streatfield, P. K.; Emch, M. Influence of Latrine Proximity and Type on Tubewell Water Quality and Diarrheal Disease in Bangladesh. *Ann. Assoc. Am. Geogr.* **2013**, *103*, 299–308.

(41) Wu, J.; Yunus, M.; Islam, M. S.; Emch, M. Influence of Climate Extremes and Land Use on Fecal Contamination of Shallow Tubewells in Bangladesh. *Environ. Sci. Technol.* **2016**.

(42) WHO. Iron in Drinking-water. *Backgr. Doc. Dev. WHO Guidel. Drink. Qual.* **2003**.

(43) Shirk, M. B.; Thadani, U.; Zimmerman, T. J. *Drug Facts and Comparisons- Chapter on Iron*; 60th ed.; 2006.

(44) Wurzelmann, J. I.; Silver, A.; Schreinemachers, D. M.; Sandler, R. S.; Everson, R. B. Iron intake and the risk of colorectal cancer. *Cancer Epidemiol. Biomarkers Prev.* **1996**, *5*, 503–507.

(45) WHO. *WHO | Guidelines for drinking-water quality, fourth edition*; World Health Organization, 2011.

(46) Amrose, S.; Gadgil, A.; Srinivasan, V.; Kowolik, K.; Muller, M.; Huang, J.; Kostecki, R. Arsenic removal from groundwater using iron electrocoagulation: effect of charge dosage rate. *J. Environ. Sci. Health. A. Tox. Hazard. Subst. Environ. Eng.* **2013**, *48*, 1019–1030.

(47) Amrose, S. E.; Bandaru, S. R. S.; Delaire, C.; van Genuchten, C. M.; Dutta, A.; DebSarkar, A.; Orr, C.; Roy, J.; Das, A.; Gadgil, A. J. Electro-chemical arsenic remediation: field trials in West Bengal. *Sci. Total Environ.* **2014**, *488-489*, 539–546.

(48) van Genuchten, C. M.; Addy, S. E. A.; Peña, J.; Gadgil, A. J. Removing arsenic from synthetic groundwater with iron electrocoagulation: an Fe and As K-edge EXAFS study. *Environ. Sci. Technol.* **2012**, *46*, 986–994.

(49) Li, L.; van Genuchten, C. M.; Addy, S. E. A.; Yao, J.; Gao, N.; Gadgil, A. J. Modeling As(III) oxidation and removal with iron electrocoagulation in groundwater. *Environ. Sci. Technol.* **2012**, *46*, 12038–12045.

(50) van Genuchten, C. M.; Peña, J.; Amrose, S. E.; Gadgil, A. J. Structure of Fe(III) precipitates generated by the electrolytic dissolution of Fe(0) in the presence of groundwater ions. *Geochim. Cosmochim. Acta* **2014**, *127*, 285–304.

(51) Gadgil, A.; Roy, J.; Amrose, S.; Das, A.; Miller, S.; Dutta, A.; Debsarkar, A. Addressing Arsenic Poisoning in South Asia. *Solutions* **2012**, *5*, 40–45.

(52) Hug, S. J.; Leupin, O. Iron-catalyzed oxidation of arsenic(III) by oxygen and by hydrogen peroxide: pH-dependent formation of oxidants in the Fenton reaction. *Environ. Sci. Technol.* **2003**, *37*, 2734–2742.

(53) Holt, P. K.; Barton, G. W.; Mitchell, C. A. The future for electrocoagulation as a localised water treatment technology. *Chemosphere* **2005**, *59*, 355–367.

(54) Neumann, A.; Kaegi, R.; Voegelin, A.; Hussam, A.; Munir, A. K. M.; Hug, S. J. Arsenic removal with composite iron matrix filters in Bangladesh: a field and laboratory study. *Environ. Sci. Technol.* **2013**, *47*, 4544–4554.

(55) Gao, Y.; Mucci, A. Acid base reactions, phosphate and arsenate complexation, and their competitive adsorption at the surface of goethite in 0.7 M NaCl solution. *Geochim. Cosmochim. Acta* **2001**, *65*, 2361–2378.

(56) Dixit, S.; Hering, J. G. Comparison of Arsenic(V) and Arsenic(III) Sorption onto Iron Oxide Minerals: Implications for Arsenic Mobility. *Environ. Sci. Technol.* **2003**, *37*, 4182–4189.

(57) van Genuchten, C. M.; Gadgil, A. J.; Peña, J. Fe(III) nucleation in the presence of bivalent cations and oxyanions leads to subnanoscale 7 Å polymers. *Environ. Sci. Technol.* **2014**, *48*, 11828–11836.

(58) Roberts, L. C.; Hug, S. J.; Ruettimann, T.; Billah, M. M.; Khan, A. W.; Rahman, M. T. Arsenic Removal with Iron(II) and Iron(III) in Waters with High Silicate and Phosphate Concentrations. *Environ. Sci. Technol.* **2004**, *38*, 307–315.

(59) Benjamin, M. M. *Water Chemistry*; 3rd ed.; 2000.

(60) Li, L.; Li, J.; Shao, C.; Zhang, K.; Yu, S.; Gao, N.; Deng, Y.; Yin, D. Arsenic removal in synthetic ground water using iron electrolysis. *Sep. Purif. Technol.* **2014**, *122*, 225–230.

(61) Rantakari, M.; Heiskanen, J.; Mammarella, I.; Tulonen, T.; Linnaluoma, J.; Kankaala, P.; Ojala, A. Different Apparent Gas Exchange Coefficients for CO2 and CH4: Comparing a Brown-Water and a Clear-Water Lake in the Boreal Zone during the Whole Growing Season. *Environ. Sci. Technol.* **2015**, *49*, 11388–11394.

(62) Hunt, J. R. *Reader for CE 211A, Environmental Physical-Chemical Processes for Water Treatment, UC Berkeley*; 2013.

(63) King, D. W. Role of Carbonate Speciation on the Oxidation Rate of Fe(II) in Aquatic Systems. *Environ. Sci. Technol.* **1998**, *32*, 2997–3003.

(64) Emmenegger, L.; King, D. W.; Sigg, L.; Sulzberger, B. Oxidation Kinetics of Fe(II) in a Eutrophic Swiss Lake. *Environ. Sci. Technol.* **1998**, *32*, 2990–2996.

(65) Pettine, M.; Campanella, L.; Millero, F. J. Arsenite oxidation by H2O2 in aqueous solutions. *Geochim. Cosmochim. Acta* **1999**, *63*, 2727–2735.

(66) van Genuchten, C. M.; Jasquelin, P.; Amrose, S. E.; Gadgil, A. J. *Structure of Fe(III) precipitates generated by the electrolytic dissolution of Fe(0) in the presence of groundwater ions*.

(67) Voegelin, A.; Kaegi, R.; Frommer, J.; Vantelon, D.; Hug, S. J. Effect of phosphate, silicate, and Ca on Fe(III)-precipitates formed in aerated Fe(II)- and As(III)-containing water studied by X-ray absorption spectroscopy. *Geochim. Cosmochim. Acta* **2010**, *74*, 164–186.

(68) Rahman, M. M.; Naidu, R.; Bhattacharya, P. Arsenic contamination in groundwater in the Southeast Asia region. *Environ. Geochem. Health* **2009**, *31 Suppl 1*, 9–21.

(69) Islam, M. S.; Siddika, A.; Khan, M. N.; Goldar, M. M.; Sadique, M. A.; Kabir, A. N.; Huq, A.; Colwell, R. R. Microbiological analysis of tube-well water in a rural area of Bangladesh. *Appl. Environ. Microbiol.* **2001**, *67*, 3328–3330.

(70) Luby, S. P.; Gupta, S. K.; Sheikh, M. A.; Johnston, R. B.; Ram, P. K.; Islam, M. S. Tubewell water quality and predictors of contamination in three flood-prone areas in Bangladesh. *J. Appl. Microbiol.* **2008**, *105*, 1002–1008.

(71) Hira-Smith, M. M.; Yuan, Y.; Savarimuthu, X.; Liaw, J.; Hira, A.; Green, C.; Hore, T.;

Chakraborty, P.; von Ehrenstein, O. S.; Smith, A. H. Arsenic concentrations and bacterial contamination in a pilot shallow dugwell program in West Bengal, India. *J. Environ. Sci. Health. A. Tox. Hazard. Subst. Environ. Eng.* **2007**, *42*, 89–95.

(72) Sengupta, C.; Sukumaran, D.; Barui, D.; Saha, R.; Chattopadhyay, A.; Naskar, A.; Dave, S. Water Health Status in Lower Reaches of River Ganga, India. *Appl. Ecol. Environ. Sci.* **2014**, *2*, 20–24.

(73) Wu, J.; van Geen, A.; Ahmed, K. M.; Alam, Y. A. J.; Culligan, P. J.; Escamilla, V.; Feighery, J.; Ferguson, A. S.; Knappett, P.; Mailloux, B. J.; et al. Increase in diarrheal disease associated with arsenic mitigation in Bangladesh. *PLoS One* **2011**, *6*, e29593.

(74) Fortin, D.; Ferris, F. G. Precipitation of iron, silica, and sulfate on bacterial cell surfaces. *Geomicrobiol. J.* **1998**, *15*, 309–324.

(75) Ferris, F. G.; Beveridge, T. J.; Fyfe, W. S. Iron-silica crystallite nucleation by bacteria in a geothermal sediment. *Nature* **1986**, *320*, 609–611.

(76) Cowen, J. P.; Bruland, K. W. Metal deposits associated with bacteria: implications for Fe and Mn marine biogeochemistry. *Deep Sea Res. Part A. Oceanogr. Res. Pap.* **1985**, *32*, 253–272.

(77) Mohanty, S. K.; Torkelson, A. A.; Dodd, H.; Nelson, K. L.; Boehm, A. B. Engineering solutions to improve the removal of fecal indicator bacteria by bioinfiltration systems during intermittent flow of stormwater. *Environ. Sci. Technol.* **2013**, *47*, 10791–10798.

(78) Zhang, L.; Seagren, E. A.; Davis, A. P.; Karns, J. S. The capture and destruction of Escherichia coli from simulated urban runoff using conventional bioretention media and iron oxide-coated sand. *Water Environ. Res.* **2010**, *82*, 701–714.

(79) Zhuang, J.; Jin, Y. Interactions between viruses and goethite during saturated flow: effects of solution pH, carbonate, and phosphate. *J. Contam. Hydrol.* **2008**, *98*, 15–21.

(80) Zhu, B.; Clifford, D. A.; Chellam, S. Virus removal by iron coagulation–microfiltration. *Water Res.* **2005**, *39*, 5153–5161.

(81) Tanneru, C. T.; Chellam, S. Mechanisms of virus control during iron electrocoagulation--microfiltration of surface water. *Water Res.* **2012**, *46*, 2111–2120.

(82) Kim, J. Y.; Park, H.-J.; Lee, C.; Nelson, K. L.; Sedlak, D. L.; Yoon, J. Inactivation of Escherichia coli by nanoparticulate zerovalent iron and ferrous ion. *Appl. Environ. Microbiol.* **2010**, *76*, 7668–7670.

(83) Kim, J. Y.; Lee, C.; Love, D. C.; Sedlak, D. L.; Yoon, J.; Nelson, K. L. Inactivation of MS2 coliphage by ferrous ion and zero-valent iron nanoparticles. *Environ. Sci. Technol.* **2011**, *45*, 6978–6984.

(84) Ghernaout, D.; Badis, A.; Kellil, A.; Ghernaout, B. Application of electrocoagulation in Escherichia coli culture and two surface waters. *Desalination* **2008**, *219*, 118–125.

(85) Zhu, B.; Clifford, D. A.; Chellam, S. Comparison of electrocoagulation and chemical coagulation pretreatment for enhanced virus removal using microfiltration membranes.

Water Res. **2005**, *39*, 3098–3108.

(86) Tanneru, C. T.; Jothikumar, N.; Hill, V. R.; Chellam, S. Relative insignificance of virus inactivation during aluminum electrocoagulation of saline waters. *Environ. Sci. Technol.* **2014**, *48*, 14590–14598.

(87) Tanneru, C. T.; Rimer, J. D.; Chellam, S. Sweep flocculation and adsorption of viruses on aluminum flocs during electrochemical treatment prior to surface water microfiltration. *Environ. Sci. Technol.* **2013**, *47*, 4612–4618.

(88) Tareq, S. M.; Maruo, M.; Ohta, K. Characteristics and role of groundwater dissolved organic matter on arsenic mobilization and poisoning in Bangladesh. *Phys. Chem. Earth, Parts A/B/C* **2013**, *58-60*, 77–84.

(89) Fujii, S.; Dupin, D.; Araki, T.; Armes, S. P.; Ade, H. First direct imaging of electrolyte-induced deswelling behavior of pH-responsive microgels in aqueous media using scanning transmission X-ray microscopy. *Langmuir* **2009**, *25*, 2588–2592.

(90) Abudalo, R. A.; Ryan, J. N.; Harvey, R. W.; Metge, D. W.; Landkamer, L. Influence of organic matter on the transport of Cryptosporidium parvum oocysts in a ferric oxyhydroxide-coated quartz sand saturated porous medium. *Water Res.* **2010**, *44*, 1104–1113.

(91) Li, Z.; Greden, K.; Alvarez, P. J. J.; Gregory, K. B.; Lowry, G. V. Adsorbed polymer and NOM limits adhesion and toxicity of nano scale zerovalent iron to E. coli. *Environ. Sci. Technol.* **2010**, *44*, 3462–3467.

(92) Rossman, T. G.; Meyn, M. S.; Troll, W. Effects of arsenite on DNA repair in Escherichia coli. *Environ. Health Perspect.* **1977**, *19*, 229–233.

(93) Rossman, T. G.; Stone, D.; Molina, M.; Troll, W. Absence of arsenite mutagenicity in E coli and chinese hamster cells. *Environ. Mutagen.* **1980**, *2*, 371–379.

(94) Jackson, C. R.; Jackson, E. F.; Dugas, S. L.; Gamble, K.; Williams, S. E. Microbial transformations of arsenite and arsenate in natural environments. *Recent Res. Dev. Microbiol.* **2003**, *7*, 103–118.

(95) Lakshmanan, D.; Clifford, D. A.; Samanta, G. Ferrous and Ferric Ion Generation During Iron Electrocoagulation. *Environ. Sci. Technol.* **2009**, *43*, 3853–3859.

(96) Gášková, D.; Sigler, K.; Janderová, B.; Plášek, J. Effect of high-voltage electric pulses on yeast cells: factors influencing the killing efficiency. *Bioelectrochemistry Bioenerg.* **1996**, *39*, 195–202.

(97) Grahl, T.; Märkl, H. Killing of microorganisms by pulsed electric fields. *Appl. Microbiol. Biotechnol.* **1996**, *45*, 148–157.

(98) Liu, X.; Yousef, A. E.; Chism, G. W. Inactivation of Escherichia Coli O157:H7 by the combination of organic acids and pulsed electric field. *J. Food Saf.* **1997**, *16*, 287–299.

(99) Dubrawski, K. L.; van Genuchten, C. M.; Delaire, C.; Amrose, S. E.; Gadgil, A. J.; Mohseni, M. Production and transformation of mixed-valent nanoparticles generated by Fe(0)

electrocoagulation. *Environ. Sci. Technol.* **2015**, *49*, 2171–2179.

(100) Godin, M.; Bryan, A. K.; Burg, T. P.; Babcock, K.; Manalis, S. R. Measuring the mass, density, and size of particles and cells using a suspended microchannel resonator. *Appl. Phys. Lett.* **2007**, *91*, 123121.

(101) Schwertmann, U.; Cornell, R. M. *Iron Oxides in the Laboratory: Preparation and Characterization*; Wiley, 2000.

(102) Matsui, Y.; Matsushita, T.; Sakuma, S.; Gojo, T.; Mamiya, T.; Suzuoki, H.; Inoue, T. Virus Inactivation in Aluminum and Polyaluminum Coagulation. *Environ. Sci. Technol.* **2003**, *37*, 5175–5180.

(103) Biber, M. V.; dos Santos Afonso, M.; Stumm, W. The coordination chemistry of weathering: IV. Inhibition of the dissolution of oxide minerals. *Geochim. Cosmochim. Acta* **1994**, *58*, 1999–2010.

(104) Small, P.; Blankenhorn, D.; Welty, D.; Zinser, E.; Slonczewski, J. L. Acid and base resistance in Escherichia coli and Shigella flexneri: role of rpoS and growth pH. *J. Bacteriol.* **1994**, *176*, 1729–1737.

(105) WHO | Evaluating household water treatment options. **2011**.

(106) Rijnaarts, H. H. M.; Norde, W.; Lyklema, J.; Zehnder, A. J. B. The isoelectric point of bacteria as an indicator for the presence of cell surface polymers that inhibit adhesion. *Colloids Surfaces B Biointerfaces* **1995**, *4*, 191–197.

(107) Walker, S. L.; Redman, J. A.; Elimelech, M. Role of Cell Surface Lipopolysaccharides in Escherichia coli K12 adhesion and transport. *Langmuir* **2004**, *20*, 7736–7746.

(108) Fowle, D. A.; Fein, J. B. Competitive adsorption of metal cations onto two gram positive bacteria: testing the chemical equilibrium model. *Geochim. Cosmochim. Acta* **1999**, *63*, 3059–3067.

(109) Kosmulski, M. The pH-dependent surface charging and the points of zero charge. *J. Colloid Interface Sci.* **2002**, *253*, 77–87.

(110) Appenzeller, B. M. R.; Duval, Y. B.; Thomas, F.; Block, J.-C. Influence of Phosphate on Bacterial Adhesion onto Iron Oxyhydroxide in Drinking Water. *Environ. Sci. Technol.* **2002**, *36*, 646–652.

(111) Hamid, R. D.; Swedlund, P. J.; Song, Y.; Miskelly, G. M. Ionic strength effects on silicic acid (H4SiO4) sorption and oligomerization on an iron oxide surface: an interesting interplay between electrostatic and chemical forces. *Langmuir* **2011**, *27*, 12930–12937.

(112) Wan, W.; Pepping, T. J.; Banerji, T.; Chaudhari, S.; Giammar, D. E. Effects of water chemistry on arsenic removal from drinking water by electrocoagulation. *Water Res.* **2011**, *45*, 384–392.

(113) Kim, J. Y.; Park, H.-J.; Lee, C.; Nelson, K. L.; Sedlak, D. L.; Yoon, J. Inactivation of Escherichia coli by nanoparticulate zerovalent iron and ferrous ion. *Appl. Environ. Microbiol.* **2010**, *76*, 7668–7670.

(114) Joux, F.; Lebaron, P. Use of fluorescent probes to assess physiological functions of bacteriaat single-cell level. *Microbes Infect.* **2000**, *2*, 1523–1535.

(115) Parikh, S. J.; Chorover, J. ATR-FTIR spectroscopy reveals bond formation during bacterial adhesion to iron oxide. *Langmuir* **2006**, *22*, 8492–8500.

(116) Gu, B.; Schmitt, J.; Chen, Z.; Liang, L.; McCarthy, J. F. Adsorption and desorption of natural organic matter on iron oxide: mechanisms and models. *Environ. Sci. Technol.* **1994**, *28*, 38–46.

(117) Ghernaout, D.; Ghernaout, B.; Kellil, A. Natural organic matter removal and enhanced coagulation as a link between coagulation and electrocoagulation. *Desalin. Water Treat.* **2012**, *2*, 203–222.

(118) Giasuddin, A. B. M.; Kanel, S. R.; Choi, H. Adsorption of Humic Acid onto Nanoscale Zerovalent Iron and Its Effect on Arsenic Removal. *Environ. Sci. Technol.* **2007**, *41*, 2022–2027.

(119) Jiang, L.; Zhu, J.; Wang, H.; Fu, Q.; Hu, H.; Huang, Q.; Violante, A.; Huang, L. Sorption of humic acid on Fe oxides, bacteria, and Fe oxide-bacteria composites. *J. Soils Sediments* **2014**, *14*, 1378–1384.

(120) Feachem, R. G. *Bradley. D. J. *Garelick. H. D. D. Sanitation and disease : health aspects of excreta and wastewater management. **1983**, 1–534.

(121) Delaire, C.; van Genuchten, C. M.; Nelson, K. L.; Amrose, S. E.; Gadgil, A. J. Escherichia coli Attenuation by Fe Electrocoagulation in Synthetic Bengal Groundwater: Effect of pH and Natural Organic Matter. *Environ. Sci. Technol.* **2015**, *49*, 9945–9953.

(122) Barrera-Díaz, C.; Ureña-Nuñez, F.; Campos, E.; Palomar-Pardavé, M.; Romero-Romo, M. A combined electrochemical-irradiation treatment of highly colored and polluted industrial wastewater. *Radiat. Phys. Chem.* **2003**, *67*, 657–663.

(123) Keenan, C. R.; Sedlak, D. L. Factors Affecting the Yield of Oxidants from the Reaction of Nanoparticulate Zero-Valent Iron and Oxygen. *Environ. Sci. Technol.* **2008**, *42*, 1262–1267.

(124) Ikawa, S.; Kitano, K.; Hamaguchi, S. Effects of pH on Bacterial Inactivation in Aqueous Solutions due to Low-Temperature Atmospheric Pressure Plasma Application. *Plasma Process. Polym.* **2010**, *7*, 33–42.

(125) Korshunov, S. S.; Imlay, J. A. A potential role for periplasmic superoxide dismutase in blocking the penetration of external superoxide into the cytosol of Gram-negative bacteria. *Mol. Microbiol.* **2002**, *43*, 95–106.

(126) Alt, E.; Leipold, F.; Milatovic, D.; Lehmann, G.; Heinz, S.; Schömig, A. Hydrogen peroxide for prevention of bacterial growth on polymer biomaterials. *Ann. Thorac. Surg.* **1999**, *68*, 2123–2128.

(127) Pericone, C. D.; Overweg, K.; Hermans, P. W.; Weiser, J. N. Inhibitory and bactericidal effects of hydrogen peroxide production by Streptococcus pneumoniae on other inhabitants of the upper respiratory tract. *Infect. Immun.* **2000**, *68*, 3990–3997.

(128) Borrok, D.; Turner, B. F.; Fein, J. B. A universal surface complexation framework for modeling proton binding onto bacterial surfaces in geologic settings. *Am. J. Sci.* **2005**, *305*, 826–853.

(129) Fein, J. B.; Daughney, C. J.; Yee, N.; Davis, T. A. A chemical equilibrium model for metal adsorption onto bacterial surfaces. *Geochim. Cosmochim. Acta* **1997**, *61*, 3319–3328.

(130) Johnson, K. J.; Szymanowski, J. E. S.; Borrok, D.; Huynh, T. Q.; Fein, J. B. Proton and metal adsorption onto bacterial consortia: Stability constants for metal–bacterial surface complexes. *Chem. Geol.* **2007**, *239*, 13–26.

(131) Ngwenya, B. T.; Sutherland, I. W.; Kennedy, L. Comparison of the acid-base behaviour and metal adsorption characteristics of a gram-negative bacterium with other strains. *Appl. Geochemistry* **2003**, *18*, 527–538.

(132) Yee, N.; Fein, J. B. Quantifying Metal Adsorption onto Bacteria Mixtures: A Test and Application of the Surface Complexation Model. *Geomicrobiol. J.* **2003**, *20*, 43–60.

(133) Yee, N.; Fowle, D. A.; Ferris, F. G. A Donnan potential model for metal sorption onto Bacillus subtilis. *Geochim. Cosmochim. Acta* **2004**, *68*, 3657–3664.

(134) McBride, M. B.; Kung, K.-H. Adsorption of phenol and substituted phenols by iron oxides. *Environ. Toxicol. Chem.* **1991**, *10*, 441–448.

(135) Norén, K.; Loring, J. S.; Persson, P. Adsorption of alpha amino acids at the water/goethite interface. *J. Colloid Interface Sci.* **2008**, *319*, 416–428.

(136) Elzinga, E. J.; Huang, J.-H.; Chorover, J.; Kretzschmar, R. ATR-FTIR spectroscopy study of the influence of pH and contact time on the adhesion of Shewanella putrefaciens bacterial cells to the surface of hematite. *Environ. Sci. Technol.* **2012**, *46*, 12848–12855.

(137) Arai, Y.; Sparks, D. L. ATR–FTIR Spectroscopic Investigation on Phosphate Adsorption Mechanisms at the Ferrihydrite–Water Interface. *J. Colloid Interface Sci.* **2001**, *241*, 317–326.

(138) PARFITT, R. L.; FARMER, V. C.; RUSSELL, J. D. ADSORPTION ON HYDROUS OXIDES I. OXALATE AND BENZOATE ON GOETHITE. *J. Soil Sci.* **1977**, *28*, 29–39.

(139) Filius, J. D.; Lumsdon, D. G.; Meeussen, J. C. L.; Hiemstra, T.; Van Riemsdijk, W. H. Adsorption of fulvic acid on goethite. *Geochim. Cosmochim. Acta* **2000**, *64*, 51–60.

(140) Filius, J. D.; Meeussen, J. C. L.; Lumsdon, D. G.; Hiemstra, T.; van Riemsdijk, W. H. Modeling the binding of fulvic acid by goethite: the speciation of adsorbed FA molecules. *Geochim. Cosmochim. Acta* **2003**, *67*, 1463–1474.

(141) Chassé, A. W.; Ohno, T.; Higgins, S. R.; Amirbahman, A.; Yildirim, N.; Parr, T. B. Chemical Force Spectroscopy Evidence Supporting the Layer-by-Layer Model of Organic Matter Binding to Iron (oxy)Hydroxide Mineral Surfaces. *Environ. Sci. Technol.* **2015**, *49*, 9733–9741.

(142) Parikh, S. J.; Mukome, F. N. D.; Zhang, X. ATR-FTIR spectroscopic evidence for biomolecular phosphorus and carboxyl groups facilitating bacterial adhesion to iron oxides.

Colloids Surf. B. Biointerfaces **2014**, *119*, 38–46.

(143) Beveridge, T. J.; Murray, R. G. Uptake and retention of metals by cell walls of Bacillus subtilis. *J. Bacteriol.* **1976**, *127*, 1502–1518.

(144) Beveridge, T. J.; Koval, S. F. Binding of metals to cell envelopes of Escherichia coli K-12. *Appl. Environ. Microbiol.* **1981**, *42*, 325–335.

(145) Truesdail, S. .; Lukasik, J.; Farrah, S. .; Shah, D. .; Dickinson, R. . Analysis of Bacterial Deposition on Metal (Hydr)oxide-Coated Sand Filter Media. *J. Colloid Interface Sci.* **1998**, *203*, 369–378.

(146) Chen, G.; Walker, S. L. Fecal indicator bacteria transport and deposition in saturated and unsaturated porous media. *Environ. Sci. Technol.* **2012**, *46*, 8782–8790.

(147) Jacobson, K. H.; Gunsolus, I. L.; Kuech, T. R.; Troiano, J. M.; Melby, E. S.; Lohse, S. E.; Hu, D.; Chrisler, W. B.; Murphy, C. J.; Orr, G.; et al. Lipopolysaccharide Density and Structure Govern the Extent and Distance of Nanoparticle Interaction with Actual and Model Bacterial Outer Membranes. *Environ. Sci. Technol.* **2015**, *49*, 10642–10650.

(148) Miot, J.; Benzerara, K.; Morin, G.; Kappler, A.; Bernard, S.; Obst, M.; Férard, C.; Skouri-Panet, F.; Guigner, J.-M.; Posth, N.; et al. Iron biomineralization by anaerobic neutrophilic iron-oxidizing bacteria. *Geochim. Cosmochim. Acta* **2009**, *73*, 696–711.

(149) Chan, C. S.; Fakra, S. C.; Edwards, D. C.; Emerson, D.; Banfield, J. F. Iron oxyhydroxide mineralization on microbial extracellular polysaccharides. *Geochim. Cosmochim. Acta* **2009**, *73*, 3807–3818.

(150) Miot, J.; Benzerara, K.; Obst, M.; Kappler, A.; Hegler, F.; Schädler, S.; Bouchez, C.; Guyot, F.; Morin, G. Extracellular iron biomineralization by photoautotrophic iron-oxidizing bacteria. *Appl. Environ. Microbiol.* **2009**, *75*, 5586–5591.

(151) STEC center. STEC center website http://shigatox.net/new/reference-strains/ecor.html (accessed Jan 1, 2016).

(152) Mazel, D.; Dychinco, B.; Webb, V. A.; Davies, J. Antibiotic resistance in the ECOR collection: integrons and identification of a novel aad gene. *Antimicrob. Agents Chemother.* **2000**, *44*, 1568–1574.

(153) Stevenson, G.; Neal, B.; Liu, D.; Hobbs, M.; Packer, N. H.; Batley, M.; Redmond, J. W.; Lindquist, L.; Reeves, P. Structure of the O antigen of Escherichia coli K-12 and the sequence of its rfb gene cluster. *J. Bacteriol.* **1994**, *176*, 4144–4156.

(154) Shock, E. L.; Koretsky, C. M. Metal-organic complexes in geochemical processes: Calculation of standard partial molal thermodynamic properties of aqueous acetate complexes at high pressures and temperatures. *Geochim. Cosmochim. Acta* **1993**, *57*, 4899–4922.

(155) Bratbak, G.; Dundas, I. Bacterial dry matter content and biomass estimations. *Appl. Envir. Microbiol.* **1984**, *48*, 755–757.

(156) Hug, S. J.; Leupin, O. Iron-Catalyzed Oxidation of Arsenic(III) by Oxygen and by

Hydrogen Peroxide: pH-Dependent Formation of Oxidants in the Fenton Reaction. *Environ. Sci. Technol.* **2003**, *37*, 2734–2742.

(157) Medinas, D. B.; Cerchiaro, G.; Trindade, D. F.; Augusto, O. The carbonate radical and related oxidants derived from bicarbonate buffer. *IUBMB Life* **2007**, *59*, 255–262.

(158) Augusto, O.; Miyamoto, S. Oxygen Radicals and Related Species | Ohara Augusto - Academia.edu. In *Principles of Free Radical Biomedicine. Volume 1*; Pantopoulos, H. M., Ed.; Nova Science Publishers, Inc., 2011.

(159) Stumm, W.; Morgan, J. J. *Aquatic Chemistry: Chemical Equilibria and Rates in Natural Waters*; Wiley-Interscience, 1996.

(160) René, A.; Abasq, M.-L.; Hauchard, D.; Hapiot, P. How Do Phenolic Compounds React toward Superoxide Ion? A Simple Electrochemical Method for Evaluating Antioxidant Capacity. *Anal. Chem.* **2010**, *82*, 8703–8710.

(161) Shafirovich, V.; Dourandin, A.; Huang, W.; Geacintov, N. E. The carbonate radical is a site-selective oxidizing agent of guanine in double-stranded oligonucleotides. *J. Biol. Chem.* **2001**, *276*, 24621–24626.

(162) Neta, P.; Huie, R. E.; Ross, A. B. Rate Constants for Reactions of Inorganic Radicals in Aqueous Solution. *J. Phys. Chem. Ref. Data* **1988**, *17*, 1027.

(163) Jacobsen, F.; Holcman, J.; Sehested, K. Reactions of the ferryl ion with some compounds found in cloud water. *Int. J. Chem. Kinet.* **1998**, *30*, 215–221.

(164) Koppenol, W. H.; Liebman, J. F. The oxidizing nature of the hydroxyl radical. A comparison with the ferryl ion (FeO2+). *J. Phys. Chem.* **1984**, *88*, 99–101.

(165) Stachowicz, M.; Hiemstra, T.; van Riemsdijk, W. H. Multi-competitive interaction of As(III) and As(V) oxyanions with Ca(2+), Mg(2+), PO(3-)(4), and CO(2-)(3) ions on goethite. *J. Colloid Interface Sci.* **2008**, *320*, 400–414.

(166) Kanematsu, M.; Young, T. M.; Fukushi, K.; Green, P. G.; Darby, J. L. Arsenic(III, V) adsorption on a goethite-based adsorbent in the presence of major co-existing ions: Modeling competitive adsorption consistent with spectroscopic and molecular evidence. *Geochim. Cosmochim. Acta* **2013**, *106*, 404–428.

(167) Senn, A.-C.; Kaegi, R.; Hug, S. J.; Hering, J. G.; Mangold, S.; Voegelin, A. Composition and structure of Fe(III)-precipitates formed by Fe(II) oxidation in water at near-neutral pH: Interdependent effects of phosphate, silicate and Ca. *Geochim. Cosmochim. Acta* **2015**, *162*, 220–246.

(168) Madigan, M. T.; Martinko, J. M.; Parker, J. *Brock biology of microorganisms*; Prentice Hall: Upper Saddle River NJ, 2000.

(169) Jiang, W.; Saxena, A.; Song, B.; Ward, B. B.; Beveridge, T. J.; Myneni, S. C. B. Elucidation of functional groups on gram-positive and gram-negative bacterial surfaces using infrared spectroscopy. *Langmuir* **2004**, *20*, 11433–11442.

(170) Felix, A.; Pitt, R. M. Virulence and Immunogenic Activities of B. typhosus in Relation to

its Antigenic Constituents. *J. Hyg. (Lond).* **1935**, *35*, 428–436.

(171) United States Geologival Survey. Water Hardness and Alkalinity http://water.usgs.gov/owq/hardness-alkalinity.html (accessed May 9, 2016).

(172) Driver, S. J.; Perdue, E. M. *Advances in the Physicochemical Characterization of Dissolved Organic Matter: Impact on Natural and Engineered Systems*; Rosario-Ortiz, F., Ed.; ACS Symposium Series; American Chemical Society: Washington, DC, 2014; Vol. 1160.

(173) Chen, J.; Gu, B.; Leboeuf, E. J.; Pan, H.; Dai, S. Spectroscopic characterization of the structural and functional properties of natural organic matter fractions. *Chemosphere* **2002**, *48*, 59–68.

(174) Spiegel, S. J.; Farmer, J. K.; Garver, S. R. Heavy metal concentrations in municipal wastewater treatment plant sludge. *Bull. Environ. Contam. Toxicol.* **1985**, *35*, 38–43.

(175) Kurniawan, T. A.; Chan, G. Y. S.; Lo, W.-H.; Babel, S. Physico–chemical treatment techniques for wastewater laden with heavy metals. *Chem. Eng. J.* **2006**, *118*, 83–98.

(176) Madajewicz, M.; Pfaff, A.; van Geen, A.; Graziano, J.; Hussein, I.; Momotaj, H.; Sylvi, R.; Ahsan, H. Can information alone change behavior? Response to arsenic contamination of groundwater in Bangladesh. *J. Dev. Econ.* **2007**, *84*, 731–754.

(177) Lucas, P. J.; Cabral, C.; Colford, J. M. Dissemination of drinking water contamination data to consumers: a systematic review of impact on consumer behaviors. *PLoS One* **2011**, *6*, e21098.

(178) Huber, A. C.; Mosler, H.-J. Determining behavioral factors for interventions to increase safe water consumption: a cross-sectional field study in rural Ethiopia. *Int. J. Environ. Health Res.* **2013**, *23*, 96–107.

(179) Inauen, J.; Mosler, H.-J. Mechanisms of behavioural maintenance: Long-term effects of theory-based interventions to promote safe water consumption. *Psychol. Health* **2015**.

(180) Mosler, H.-J.; Blöchliger, O. R.; Inauen, J. Personal, social, and situational factors influencing the consumption of drinking water from arsenic-safe deep tubewells in Bangladesh. *J. Environ. Manage.* **2010**, *91*, 1316–1323.

(181) Inauen, J.; Hossain, M. M.; Johnston, R. B.; Mosler, H.-J. Acceptance and use of eight arsenic-safe drinking water options in Bangladesh. *PLoS One* **2013**, *8*, e53640.

(182) Mosler, H.-J. A systematic approach to behavior change interventions for the water and sanitation sector in developing countries: a conceptual model, a review, and a guideline. *Int. J. Environ. Health Res.* **2012**, *22*, 431–449.

(183) Rosa, G.; Clasen, T. Estimating the scope of household water treatment in low- and medium-income countries. *Am. J. Trop. Med. Hyg.* **2010**, *82*, 289–300.

(184) Kariuki, M.; Schwartz, J. Small-scale Private Service Providers of Water Supply and Electricity: A Review of Incidence, Structure, Pricing, and Operating Characteristics. *World Bank Policy Res. Work. Pap.* **2005**, 37.

(185) Solo, T. M. Small-scale entrepreneurs in the urban water and sanitation market. *Environ.*

Urban. **1999**, *11*, 117–132.

(186) Kjellen, M.; McGranahan, G. Informal water vendors and the urban poor. *Int. Inst. Environ. Dev.* **2006**, 26.

(187) Schaub-Jones, D. Harnessing entrepreneurship in the water sector: expanding water services through independent network operators. *Waterlines* **2008**, *27*.

(188) World Bank. Water resources sector strategy : strategic directions for World Bank engagement. **2004**, 1–88.

(189) Government of India. *HANDBOOK OF SERVICE LEVEL BENCHMARKING, Ministry of Urban Development*; 2008.

(190) Delaire, C. Personal communication. Expert interview in Behrampore City, 2014.

(191) Bakker, K. The Business of Water: Market Environmentalism in the Water Sector. *Annu. Rev. Environ. Resour.* **2014**, *39*, 469–494.

(192) Davis, J. PRIVATE-SECTOR PARTICIPATION IN THE WATER AND SANITATION SECTOR. *Annu. Rev. Environ. Resour.* **2005**, *30*, 145–183.

(193) Amrose, S.; Burt, Z.; Ray, I. Safe Drinking Water for Low-Income Regions. *Annu. Rev. Environ. Resour.* **2015**, *40*, 203–231.

(194) Orgill, J.; Shaheed, A.; Brown, J.; Jeuland, M. Water quality perceptions and willingness to pay for clean water in peri-urban Cambodian communities. *J. Water Health* **2013**, *11*, 489–506.

(195) Government of India-Planning Commission. *West Bengal Development Report*; 2010.

(196) West Bengal Public Health Engineering Department. Water Quality Survey During 2002-2006 under the Joint Plan of Action with UNICEF http://www.wbphed.gov.in/main/index.php/component/content/category/95-water-quality (accessed Apr 1, 2016).

(197) National Rural Drinking Water Program. Water Sample Testing-Habitation Wise (E3) http://indiawater.gov.in/IMISReports/Reports/WaterQuality/rpt_WQM_HabitationWiseLabTesting_S.aspx?Rep=0&RP=Y (accessed Apr 1, 2016).

(198) Telecom Regulatory Authority fo India. *Highlights of Telecom Subscription Data as on 31st October, 2015*; 2015.

(199) Gruber, J. S.; Arnold, B. F.; Reygadas, F.; Hubbard, A. E.; Colford, J. M. Estimation of treatment efficacy with complier average causal effects (CACE) in a randomized stepped wedge trial. *Am. J. Epidemiol.* **2014**, *179*, 1134–1142.

(200) Kremer, M.; Miguel, E.; Null, C.; Peterson Zwane, A. Trickle down: Diffusion of chlorine for drinking water treatment in Kenya. *Work. Pap.* **2008**.

(201) Huber, A. C.; Bhend, S.; Mosler, H.-J. Determinants of exclusive consumption of fluoride-free water: a cross-sectional household study in rural Ethiopia. *J. Public Health (Bangkok).* **2011**, *20*, 269–278.

(202) Etmannski, T. R.; Darton, R. C. A methodology for the sustainability assessment of arsenic mitigation technology for drinking water. *Sci. Total Environ.* **2014**, *488-489*, 505–511.

(203) Filmer, D.; Pritchett, L. H. Estimating Wealth Effects without Expenditure Data-or Tears: An Application to Educational Enrollments in States of India. *Demography* **2001**, *38*, 115–132.

(204) Weinstein, N. Conceptualizing and Measuring Risk Perceptions http://cancercontrol.cancer.gov/brp/presentations/weinstein.pdf (accessed Apr 29, 2014).

(205) Bernard, T.; Dercon, S.; Taffesse, A. . Beyond fatalism. An empirical exploration of self-efficacy and aspirations failure in Ethiopia http://www.ifpri.org/publication/beyond-fatalism (accessed Apr 29, 2014).

(206) WHO. Water-related diseases http://www.who.int/water_sanitation_health/diseases/diarrhoea/en/ (accessed Mar 7, 2016).

(207) Rosa, G.; Kelly, P.; Clasen, T. Consistency of Use and Effectiveness of Household Water Treatment Practices Among Urban and Rural Populations Claiming to Treat Their Drinking Water at Home: A Case Study in Zambia. *Am. J. Trop. Med. Hyg.* **2016**, *94*, 445–455.

(208) Reygadas, F. User Compliance, Field Efficacy, and Greenhouse Gas Emissions of an Ultraviolet Water Disinfection System and other Drinking Water Treatment Alternatives for Rural Households in Mexico, 2014.

(209) Kremer, M.; Leino, J.; Miguel, E.; Zwane, A. P. Spring Cleaning: Rural Water Impacts, Valuation and Property Rights Institutions. **2009**.

(210) Bangladesh Department of Public Health Engineering. Arsenic Contamination and Mitigation in Bangladesh http://www.dphe.gov.bd/index.php?option=com_content&view=article&id=96&Itemid=104 (accessed May 2, 2016).

(211) Johnston, R. B.; Sarker, M. H. Arsenic mitigation in Bangladesh: national screening data and case studies in three upazilas. *J. Environ. Sci. Health. A. Tox. Hazard. Subst. Environ. Eng.* **2007**, *42*, 1889–1896.

(212) Albert, J.; Luoto, J.; Levine, D. End-user preferences for and performance of competing POU water treatment technologies among the rural poor of Kenya. *Environ. Sci. Technol.* **2010**, *44*, 4426–4432.

(213) Kremer, M.; Miguel, E.; Mullainathan, S.; Null, C.; Peterson Zwane, A. *Social engineering: Evidence from a Suite of Take-Up Experiments in Kenya*; 2011.

(214) Luoto, J.; Mahmud, M.; Albert, J.; Luby, S.; Najnin, N.; Unicomb, L.; Levine, D. I. Learning to dislike safe water products: results from a randomized controlled trial of the effects of direct and peer experience on willingness to pay. *Environ. Sci. Technol.* **2012**, *46*, 6244–6251.

(215) Johnston, R. B.; Hanchett, S.; Khan, M. H. The socio-economics of arsenic removal. *Nat. Geosci.* **2010**, *3*, 2–3.

(216) Ahmad, J.; Goldar, B. .; Misra, S.; Jakariya, M. *Willingness to Pay for Arsenic-Free, Safe Drinking Water in Bangladesh*; 2003.

(217) Jaglin, S. The right to water versus cost recovery: participation, urban water supply and the poor in sub-Saharan Africa. *Environ. Urban.* **2002**, *14*, 231–245.

(218) Times of India. West Bengal: "Sulabh Drinking Water" project to provide villages arsenic-free water http://articles.economictimes.indiatimes.com/2014-11-24/news/56421204_1_ground-water-purification-pond-water (accessed Jan 19, 2016).

(219) News - India Today. Government allots Rs 1,000 crore for toxic water zones : Mail Today http://indiatoday.intoday.in/story/govt-allots-rs-1-000-crore-for-toxic-water-zones/1/563439.html (accessed Jan 19, 2016).

(220) Ahsan, H.; Chen, Y.; Parvez, F.; Zablotska, L.; Argos, M.; Hussain, I.; Momotaj, H.; Levy, D.; Cheng, Z.; Slavkovich, V.; et al. Arsenic exposure from drinking water and risk of premalignant skin lesions in Bangladesh: baseline results from the Health Effects of Arsenic Longitudinal Study. *Am. J. Epidemiol.* **2006**, *163*, 1138–1148.

(221) Ahmad, J. K. G. B. N. J. M. M. S. Fighting arsenic, listening to rural communities - findings from a study on willingness to pay for arsenic-free, safe drinking water in rural Bangladesh. **2002**, 1–14.

(222) West Bengal Public Health Engineering Department. Vision 2020 http://www.wbphed.gov.in/main/index.php/vision-2020 (accessed Apr 1, 2016).

(223) deWilde, C. K.; Milman, A.; Flores, Y.; Salmerón, J.; Ray, I. An integrated method for evaluating community-based safe water programmes and an application in rural Mexico. *Health Policy Plan.* **2008**, *23*, 452–464.

(224) Omoike, A.; Chorover, J.; Kwon, K. D.; Kubicki, J. D. Adhesion of bacterial exopolymers to alpha-FeOOH: inner-sphere complexation of phosphodiester groups. *Langmuir* **2004**, *20*, 11108–11114.

(225) Fang, L.; Cao, Y.; Huang, Q.; Walker, S. L.; Cai, P. Reactions between bacterial exopolymers and goethite: A combined macroscopic and spectroscopic investigation. *Water Res.* **2012**, *46*, 5613–5620.

(226) Benjamin, M. M.; Lawler, D. F. *Water Quality Engineering: Physical / Chemical Treatment Processes*; John Wiley & Sons, 2013.

(227) Slonczewski, J. L.; Foster, J. W. *Microbiology: An Evolving Science, 1st Edition*; 2008.

(228) Gao, X.; Metge, D. W.; Ray, C.; Harvey, R. W.; Chorover, J. Surface Complexation of Carboxylate Adheres Cryptosporidium parvum Öocysts to the Hematite−Water Interface. *Environ. Sci. Technol.* **2009**, *43*, 7423–7429.

(229) Nicklin, S. A.; Wu, E.; Nemerow, G. R.; Baker, A. H. The influence of adenovirus fiber structure and function on vector development for gene therapy. *Mol. Ther.* **2005**, *12*, 384–393.

(230) Ludert, J.; Feng, N.; Yu, J.; Broome, R.; Hoshino, Y.; Greenberg, H. Genetic mapping

indicates that VP4 is the rotavirus cell attachment protein in vitro and in vivo. *J. Virol.* **1996**, *70*, 487–493.

(231) Mattle, M. J.; Vione, D.; Kohn, T. Conceptual model and experimental framework to determine the contributions of direct and indirect photoreactions to the solar disinfection of MS2, phiX174, and adenovirus. *Environ. Sci. Technol.* **2015**, *49*, 334–342.

(232) Clancy, T. M.; Hayes, K. F.; Raskin, L. Arsenic waste management: a critical review of testing and disposal of arsenic-bearing solid wastes generated during arsenic removal from drinking water. *Environ. Sci. Technol.* **2013**, *47*, 10799–10812.

(233) Clancy, T. M.; Snyder, K. V; Reddy, R.; Lanzirotti, A.; Amrose, S. E.; Raskin, L.; Hayes, K. F. Evaluating the cement stabilization of arsenic-bearing iron wastes from drinking water treatment. *J. Hazard. Mater.* **2015**, *300*, 522–529.

(234) Komives, K.; Foster, V.; Halpern, J.; Wodon, Q. *Water, Electricity, and the Poor. Who Benefits from Utility Subsidies?*; 2005.

(235) Singh, M. R.; Upadhyay, V.; Mittal, A. K. Urban water tariff structure and cost recovery opportunities in India. *Water Sci. Technol.* **2005**, *52*, 43–51.

(236) Collignon, B. *Urban Water Supply Innovations in Côte d'Ivoire: How Cross-Subsidies Help the Poor*; 2002.

APPENDIX: Definition of Explanatory Variables from Household Survey Data (in Chapter 5)

Socioeconomic status

The following assets and expenditures were included in the socioeconomic index. When necessary, assets were scored as indicated below.

- Dwelling type: bamboo =0, mud (kancha)=1, mixed=2, concrete/brick (pacca)=3
- Floor: unfinished=0, finished=1
- Roof: hay=0, tin=1, tile=2, built roof (concrete)=3
- Ownership of electric meter, fridge, TV/radio, table, kerosene stove, gas stove, fan, goat/cow, chicken, land, mobile phone, watch, bicycle, motorcycle, van rickshaw: (1/0)
- Number of rooms per family member
- Cosmetics expenditures (soap, shampoo) per family member
- Phone credit expenditures per adult member

A PCA of the 21 normalized variables was performed. In Area 1, the first PC was dominated by floor and roof type, ownership of motorcycle, ownership of TV/radio, dwelling type and ownership of gas stove. In Area 2, the first PC was dominated by the number of rooms per person, floor type, cosmetics expenditures, ownership of gas stove and ownership of motorcycle. The socioeconomic index was defined as the weighted average of the 21 normalized variables, where the weights were the loadings of the normalized variables on the 1st PC.

Income stability

All household income sources were scored according to the metric below, which based on our understanding of income stability in the region, and added up. The resulting scores were normalized to create the income stability index.

- Agriculture from own land (criteria is land ownership only), business, service = 3
- Pension = 2
- Daily labor, remittances = 1
- Charity = 0

Exposure to purchased water

A dummy variable was computed with value 1 if a household member had a service job (likely in the nearby city) or if a household member worked/studied away from the village (abroad or somewhere else in India). The rationale is that people who work in the city, abroad, or have travelled are likely to have been exposed (and perhaps used) to bottled water, which is much more common in urban areas. This dummy variable was normalized to create the exposure index.

Women's group participation

A dummy variable (1 if a woman in the household participated in a women's group, gram-panchayat group or self-help group) was normalized to create the women's group participation index.

Peer behavior

The peer behavior index was created by normalizing the following scores:

- 0 = respondent did not know anybody purchasing water
- 1 = respondent knew a few or many people purchasing water
- 2 = respondent knew a few or many people purchasing water and had relatives purchasing water (was probably interpreted as relatives in the same village)

Doctor's advice

The doctor's advice index was created by normalizing the following scores:

- 1 = respondent had received some type of advice from a health professional regarding water (not necessarily about purchased water in particular, but generally about "good water").
- 0 = otherwise

External advice index

Similarly, dummy variables were created to score whether the respondent had received advice about "good water" from relatives, the school, women's group, political leaders and NGO members respectively. The dummy variables were added up and normalized to create an external advice index. Note that we did not average normalized variables because it would have increased the weight of unusual types of advice.

Risk perception of gastric illness

3 variables were calculated, normalized and averaged (all weights =1) to create the index for risk perception of gastric illness:

- Complaints about gastric problems #1 = 1 if respondent mentioned gastric illness or diarrhea at least once when asked about problems with the private tubewell or about reasons for using alternative to private tubwell (=0 otherwise). This question was asked towards the beginning of the interview and possible answers were not prompted.
- Perceived (stated) likelihood of getting gastric illness from drinking private tubewell water: high=3, medium=2, low=1, none=0. Note that this variable was NA for the first week of the survey. This question was asked after all household sources of drinking water had been listed.

- Complaints about gastric problems #2 = 1 if respondent mentioned any type of gastric illness or diarrhea problem in commenting why he/she thought that his/her private tubewell was unsafe. This question was asked at the very end of the interview and possible answers were not prompted.

Dissatisfaction with iron

2 variables were calculated, normalized and averaged (all weights =1) to create the index for dissatisfaction with iron:

- Complaints about iron #1 = 1 if respondent mentioned iron at least once when asked about problems with the private tubewell or about reasons for using alternative to private tubwell (=0 otherwise). This question was asked towards the beginning of the interview and possible answers were not prompted.
- Complaints about iron #2 = 1 if respondent mentioned any type of iron problem in commenting why he/she thought that his/her private tubewell was unsafe. This question was asked at the very end of the interview and possible answers were not prompted.

Arsenic risk perception

3 variables were calculated, normalized and averaged (all weights =1) to create the arsenic risk perception index:

- Complaints about arsenic #1 = 1 if respondent mentioned arsenic at least once when asked about problems with the private tubewell or about reasons for using alternative to private tubwell (=0 otherwise). This question was asked towards the beginning of the interview (before the section testing specific knowledge about arsenic) and possible answers were not prompted.
- Specific knowledge about arsenic was scored as follows:
    - -4 if respondent had never heard about arsenic and confirmed that she/he had no information about it.
    - Otherwise, starting from a score of 0: +1 if answer to question contained correct elements, -1 if answer to question did not contain any correct element (the respondent was not penalized for listing wrong answers if he/she listed correct answers too).
        - Can arsenic be detected visually? Correct answer = no
        - When is arsenic a problem? Correct answer = when drinking
        - Consequences of arsenic poisoning? Correct answer = lesions/burns, gangrene, cancer, death.
        - Solution to arsenic in water? Correct answer = filter, purchased water, new tubewell, deep tubewell, piped water, rainwater (even though some of these solutions only provide arsenic-safe water if properly designed).

Maximum score = +4, minimum score = -4

- Complaints about arsenic #2 = 1 if respondent mentioned arsenic in commenting why he/she thought that his/her private tubewell was unsafe. This question was asked at the very end of the interview and possible answers were not prompted. We note that because this question came after the section testing arsenic knowledge, respondents may have overstated their complaints about arsenic. However, only 23 respondents (out of 409 in Area 1) mentioned arsenic in this last question, and we checked that the arsenic knowledge index was not significantly different with and without this variable (correlation coefficient of 0.9 in Area 1).

Note: arsenic knowledge was generally very low. In Area 1, 65% of respondents had no arsenic knowledge at all, only 26% knew at least one health effect, and only 1% knew all the 4 health effects mentioned above. In Area 2, these proportions were 83%, 14% and 0%, respectively. Questions about perceived likelihood of getting arsenicosis were not asked to respondents who stated not having any information/knowledge about arsenic. We therefore don't have a "perceived likelihood" score for the majority of our respondents, and we decided not to include this metric in our overall arsenic risk perception index.

Presence of children under 5

A dummy variable for the presence of at least one child under 5 was normalized to create the index for the presence of young children.

Self-efficacy

Answers to the survey question assessing self-efficacy were scored as follows. Scores were then normalized to create the self-efficacy index.

- 0: respondent ranked fate first before work/education OR respondent did not answer the question
- 1: respondent ranked fate first together with work or education
- 2: respondent ranked work or education first

Perception of purchased water

2 variables were calculated, normalized and averaged (weights=1 after checking that weights did not alter regressions significantly) to create the index for the perception of purchased water:

- Perceived aesthetics were scored as follows:
    - -1 if color, taste or smell of purchased water was perceived as worse than those of the tubewell water
    - 0 if color, taste and smell of purchased water were perceived as similar to those of the tubewell water
    - +1 if color, taste and smell of purchased water were perceived as similar or better than those of the tubewell water

Note: “don’t know” answers were scored like “similar”, i.e. with 0.

- Perceived safety was scored as follows:
    - -1 if safety of purchased water was perceived as worse than that of the tubewell water
    - 0 if safety of purchased water was perceived as similar as that of the tubewell water or if respondent did not know
    - +1 if safety of purchased water was perceived as better than that of the tubewell water

We note that the survey section assessing perceptions of purchased water came before the section testing arsenic knowledge (i.e. before the surveyor mentioned arsenic).

Perception of piped water

3 variables were calculated, normalized and averaged (all weights=1) to create the index for the perception of piped water:

- Perceived aesthetics were scored as follows:
    - -1 if color, taste or smell of piped water was perceived as worse than those of the tubewell water
    - 0 if color, taste and smell of piped water were perceived as similar to those of the tubewell water
    - +1 if color, taste and smell of piped water were perceived as similar or better than those of the tubewell water

Note: “don’t know” answers were scored like “similar”, i.e. with 0.

- Perceived safety was scored as follows:
    - -1 if safety of piped water was perceived as worse than that of the tubewell water
    - 0 if safety of piped water was perceived as similar as that of the tubewell water or if respondent did not know
    - +1 if safety of piped water was perceived as better than that of the tubewell water

- Perceived convenience was scored as follows:
    - -1 if convenience of piped water was perceived as worse than that of the tubewell water
    - 0 if convenience of piped water was perceived as similar as that of the tubewell water or if respondent did not know
    - +1 if convenience of piped water was perceived as better than that of the tubewell water

We note that the survey section assessing perceptions of piped water came before the section testing arsenic knowledge (i.e. before the surveyor mentioned arsenic).